SynMuv B Proteins Regulate Chromatin Compaction during Development

Meghan Elizabeth Costello
Marquette University

SYNMUV B PROTEINS REGULATE CHROMATIN COMPACTION DURING DEVELOPMENT

by

Meghan E Costello

A Dissertation submitted to the Faculty of the Graduate School,
Marquette University,
in Partial Fulfillment of the Requirements for the
Degree of Doctor of Philosophy

Milwaukee, Wisconsin

May 2019

ABSTRACT

SYNMUV B PROTEINS REGULATE CHROMATIN COMPACTION DURING DEVELOPMENT

Meghan E Costello, B.S.

Marquette University, 2019

Tissue-specific establishment of repressive chromatin through creation of compact chromatin domains during development is necessary to ensure proper gene expression and cell fate. *C. elegans* synMuv B proteins are important for the soma/germline fate decision and mutants demonstrate ectopic germline gene expression in somatic tissue, especially at high temperature.

To study chromatin compaction during development we visualized chromatin using both nuclear-spot assays and FISH of native synMuv B regulated loci. We showed that *C. elegans* synMuv B proteins regulate developmental chromatin compaction and that timing of chromatin compaction was temperature sensitive in both wild-type and synMuv B mutants. Chromatin compaction in mutants was delayed into developmental time-periods when zygotic gene expression is upregulated and demonstrates an anterior-to-posterior pattern. Loss of this patterned compaction coincided with the developmental time-period of ectopic germline gene expression that leads to a developmental arrest in synMuv B mutants. Thus, chromatin organization throughout development is regulated both spatially and temporally by synMuv B proteins to establish repressive chromatin in a tissue-specific manner to ensure proper gene expression.

Furthermore, we showed that global loss of H3K9me2, but not H3K9me3 results in phenotypes similar to synMuv B mutants. This suggests that repression of germline genes in somatic tissue is at least in part due to establishment of H3K9me2 at synMuv B regulated promoters. Specific loss of H3K9me2 at synMuv B regulated promoters in *lin-15B* mutants suggests that LIN-15B establishes or maintains H3K9me2 for germline gene pression at promoters.

Finally, we analyzed the genetic interactions of *lin-15B* with genes involved in methylation of H3 lysine 9. We found that there is no enhancement of any phenotypes when the DREAM complex or H3K9me2 are disrupted in a *lin-15B* background. This suggests that H3K9me2, the DREAM complex, and LIN-15B work in series to repress germline gene expression at in the soma. From this work we propose that LIN-15B driven enrichment of H3K9me2 on promoters of germline genes contributes to repression of those genes in somatic tissues.

ACKNOWLEDGMENTS

Meghan E. Costello, B.S.

First, I would like to thank my advisor, Dr. Lisa Petrella, for her mentorship and guidance throughout my PhD. Lisa has given me the perfect amount of space to become an independent scientist, undergraduate mentor, and teacher while still providing support and guidance. She has created an environment within the lab that allows autonomous exploration of concepts and supports debate and discussion of good science. I have learned many lessons from her, including how to be a thorough and clever scientist, and a respected member of the scientific community.

Many thanks to my committee: Dr. Allison Abbott, Dr. Edward Blumenthal, Dr. Michael Schläppi, and Dr. Pinfen Yang for both stimulating conversation and thoughtful advice throughout the years.

I would also like to thank Dr. Anita Manogaran for her input and advice throughout the submission of my manuscript as well as being an exceptional mentor in the classroom.

Many thanks to Dr. Jim McGhee for the anti-ELT-2 antibody and worm strains that were the heart of my project.

I would like to thank our funding sources at the NIGMS and the Marquette University Fellowship for two years of support.

I would like to thank the staff in the Biological Sciences department at Marquette University, especially Deb Weaver, Kirsten Boeh, Stacia Peiffer, Tom Dunk, and Dan Holbus.

Thanks to Dr. Paul Ebner at Purdue University for kindling my love for research and teaching as an undergraduate. In good humor, Dr. Ebner has continued to challenge and support me throughout my PhD.

I would like to thank my lab-mates throughout the past 7 years. I have had the privilege of working alongside the most amazing people. Thanks to Jerrin Roy Cherian for hours of banter, both science and non-science in nature, and for becoming family over the past five years. I would also like to acknowledge Nicholas Sepúlveda for being my number one supporter and best friend. When I lack confidence, he is there to build me up, and I have too much confidence, he's there to knock me down. Nicholas keeps me grounded and gives me perspective every day. I have never experienced a bond with someone quite like ours and I am so grateful that the Petrella lab brought us together. Franki Compere has been an amazing supporter these last few years and I've enjoyed watching her become equally enamored with worms as I am. I have also had the privilege to mentor and work alongside many talented undergraduates. Many thanks to Ethan Doeger for help with the demethylase RNAi screen. I'd also like to acknowledge other undergraduate researchers: Kevin Sanchez, Emily Nett,

Jaime Lisack, Carlos Gonzalez, and Eve Proedehl for making me a better mentor and making science fun.

Lastly, I would like to thank my friends and family for their continued support throughout this long process. I have found so many friendships in other graduate students in this department, and for that I am thankful. I have found a community of people and support in Milwaukee that I will always be grateful for. Thanks to Patrick Fealey, Jenn Wigh for Netflix marathons when experiments fail, and Brad Wigh for all the adventures. Most thanks to my mother and father for always pushing me to be my best and my brother and sister for always challenging and encouraging me.

TABLE OF CONTENTS

LIST OF TABLES

LIST OF FIGURES

CHAPTER I. INTRODUCTION

Multicellular organisms establish many different cell types from one single cell and maintain these fates once established throughout the lifespan of the animal. Failure to do so causes lethality, developmental defects, and cancer (Al-Amin et al., 2016; Janic et al., 2010; Petrella et al., 2011; Whitehurst, 2014). Each zygote is totipotent, meaning that the single cell has the most differentiation potential and can give rise to all cell lineages. As cells in the developing embryos replicate and migrate, they become less potent and specialize into their individual cell identities. Establishment of cell fates is coupled with changes in gene expression specific to that cell lineage (Levin et al., 2012; Robertson and Lin, 2015; Spencer et al., 2011). As cells become more specialized, gene expression does as well. In general, genes not needed for that cell's function are repressed, whereas genes needed for that lineage will be activated, or primed for expression later in development (Perino and Veenstra, 2016; Yuzyuk et al., 2009). There are many mechanisms that regulate gene expression throughout development, including transcription factor binding and regulation of chromatin structure, to ensure proper cell fate is achieved and maintained.

ESTABLISHMENT OF CHROMATIN DOMAINS DURING DEVELOPMENT

DNA is wrapped around 8 histones to form the basic unit of chromatin

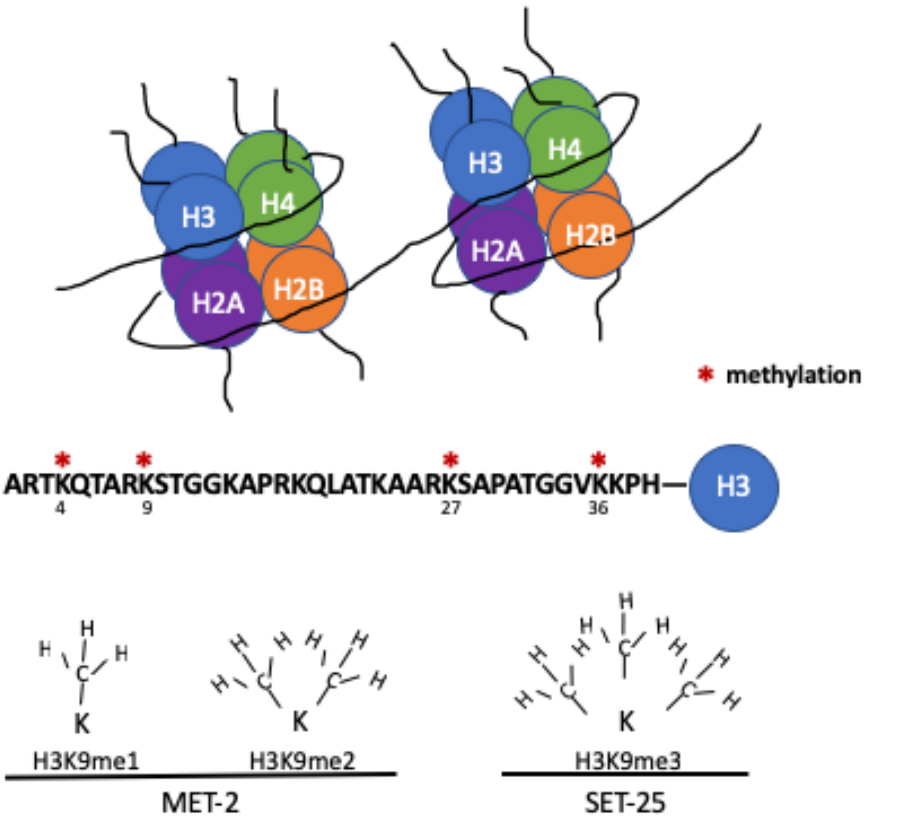

Figure 1.1 The nucleosome consists of an octamer of histone proteins. The octamer consists of dimer pairs of the four major histones, H2A, H2B, H3 and H4. Histone tails can be post-translationally modified to alter the interaction between DNA and the nucleosome. Methylation of lysines on hisone H3 tails is a common modification in both heterochromatin associated and euchromatin associated histones. Mono- and di-methylation of H3K9 is catalyzed by the methyltransferase MET-2 and tri-methylation of H3K9 is catalyzed by the methyltransferase SET-25.

Generating proper chromatin organization during development is required for fate specification (Yuzyuk et al., 2009). Chromatin is DNA and its associated proteins. These DNA associated proteins range from histones and histone readers to transcription factors, which altogether affect and regulate DNA organization. DNA is organized into chromatin so that the genome can be arranged and packaged within the nucleus (Kornberg, 1974; Olins and Olins, 1974). The most basic unit of chromatin is DNA wrapped around eight histone proteins to form the nucleosome (Figure 1.1). Approximately 146 base pairs of DNA wrap around 8 histone proteins to form the histone octamer. The histone octamer includes 2 copies of each of the core histones H2A, H2B, H3 and H4 (Figure 1.1)(Kornberg, 1974; Olins and Olins, 1974). Nucleosomes are connected by stretches of linker DNA and further levels of chromatin packaging can be achieved in response to many factors. One of these factors is the covalent modification of histone tails. Histone tails are long, unstructured, poly-peptide extensions that protrude from the octamer core (Figure 1.1). The N-terminal tails of histones H3 and H2B protrude through the minor grooves of the DNA wrapped around the octamer core (Kornberg, 1974; Olins and Olins, 1974). Covalent modifications of specific amino acids in the tail affect the interaction between the histone octamer and DNA. Specific covalent modifications can strengthen or weaken the wrapping of DNA around the core octamer, which overall affects how accessible or inaccessible the DNA is (Bannister and Kouzarides, 2011; Carrozza et al., 2005; Corona et al., 2002; Deuring et al.,

2000; Jenuwein and Allis, 2001) Alternatively, specific histone modifications can create binding sites for histone “readers.” These reader proteins bind specific histone modifications and can change the chromatin compaction state or recruit other proteins that regulate chromatin or transcription (Carrozza et al., 2005; Corona et al., 2002; Deuring et al., 2000).

Chromatin is organized into more complex structures of heterochromatin and euchromatin

Chromatin can form more complex structures through interaction of nucleosomes and other proteins to form areas of compact or open domains. Compacted chromatin, canonically called heterochromatin, is thought to make DNA inaccessible to binding of transcription factors and RNA polymerase and is associated with repressed regions of the genome (Elgin and Reuter, 2013; Simon and Kingston, 2013). Due to its density, biologists have been able to visualize compacted heterochromatin using transmission electron microscopy for decades (Figure 1.2) (Mutlu et al., 2018). Uncompacted or accessible DNA, canonically called euchromatin, is available to be bound by transcription factors that can promote expression of genes in that region. In organisms with chromosomes with point centromeres, such as mammals, heterochromatin domains are found in the middle regions of chromosomes and at the telomeric regions at chromosome tips, whereas, regions of euchromatin are enriched along chromosome arms (Figure 1.3) (Wang et al., 2016). In contrast, *C. elegans* chromosomes are holocentric, meaning centromere activity is located along the entire length of the chromosome (Albertson and Thomson, 1982; Maddox et al.,

2004). Unlike mammals, *C. elegans* chromosomes have regions of euchromatin and highly expressed genes in the chromosome centers and the arms largely contain repressed regions of heterochromatin (Figure 1.3)(Liu et al., 2011; McMurchy et al., 2017; Zeller et al., 2016). The telomere is found at the ends of the chromosomes and is enriched for heterochromatin in both organisms with centromeres and those without (Figure 1.3). Thus, chromatin modifications, are distributed in this pattern (Liu et al., 2011; McMurchy et al., 2017).

Methylation of histone H3K9 is associated with repressed genes

Because histone-tail modifications affect accessibility of genes to be bound by transcription factors and RNA polymerase, specific modifications are correlated with either expressed or repressed genes and areas of the genome (Ahringer and Gasser, 2018; Liu et al., 2011; McMurchy et al., 2017). Regions of the genome associated with compacted repressed genes are called heterochromatin, whereas highly expressed, uncompacted regions of the genome are called euchromatin. Heterochromatin and euchromatin are enriched for specific histone modifications that either make chromatin less or more accessible, respectively (Ahringer and Gasser, 2018). For example, methylation of histone H3 lysine 9 (H3K9me) is associated with heterochromatin and repressed genes in organisms from yeast to humans (Figure 1.1) (Elgin and Reuter, 2013; Simon and Kingston, 2013; Towbin et al., 2012). In *C. elegans*, histone methyltransferases, MET-2 and SET-25, target H3K9 for methylation

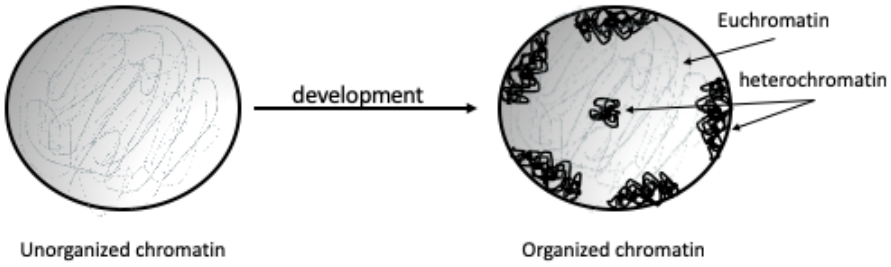

Figure 1.2 Dense domains of heterochromatin are created early in development. As development occurs, chromatin transitions from highly dynamic and unorganized into dense domains of heterochromatin that can be visualized by transmission electron microscopy.

(Figure 1.1) (Towbin et al., 2012). Both MET-2 and SET-25 have a conserved catalytic SET domain, which contains an S-adenosylmethionine binding site and a catalytic center (Yeates, 2002). MET-2 is a homolog of the mammalian H3K9 methyltransferase SETDB1, and functions to deposit mono- and dimethyl groups at H3K9 (Figure 1.1) (Ahringer and Gasser, 2018; Andersen and Horvitz, 2007; Towbin et al., 2012; Yeates, 2002; Zeller et al., 2016). SET-25 is the ortholog of the mammalian G9a and SUV39 H3K9 methyltransferase, which trimethylates the same residue (Figure 1.1) (Ahringer and Gasser, 2018; Towbin et al., 2012; Yeates, 2002; Zeller et al., 2016). Methylation of H3K9 by MET-2 and SET-25 establishes compacted, heterochromatin regions of the genome to ensure gene repression (Gonzalez-Sandoval et al., 2015; Towbin et al., 2012; Zeller et al., 2016). Because lysine methylation adds a bulky residue but does not change the charge of the side chain, this modification is thought to compact and repress chromatin through recruitment of specific reader proteins (Clark and Elgin, 1992; Nielsen et al., 2002)

Methylated H3K9 and its associated proteins are enriched on heterochromatin-rich distal chromosome arms (Liu et al., 2011, McMurchy et al., 2017). Histone readers are proteins that bind methylated histone tails and are also found distributed throughout the genome in a pattern that resembles to modification they associate with (McMurchy et al., 2017). The most well understood and studied H3K9me reader, HP1 (heterochromatin protein 1), was

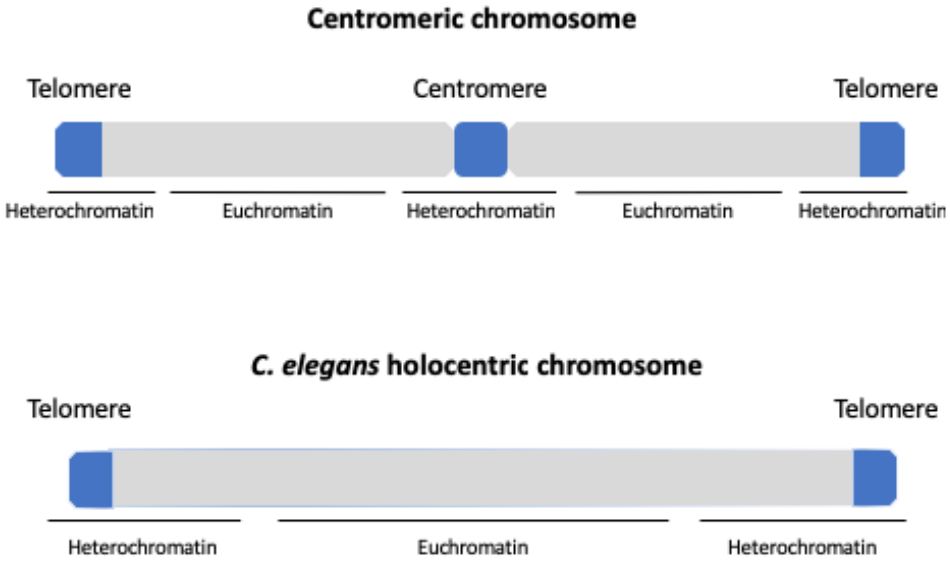

Figure 1.3: Centromeric and holocentric chromosomes have distinct domains of heterochromatin and euchromatin. Orgnanisms that have centromeric chromosomes have regions of heterochromatin close to the centromere in the middle of the chromosome, flanked by regions of euchromatin on both sides. *C. elegans* have holocentric chromosomes and no centromere. In contrast, the centers of *C. elegans* are highly euchromatic, whereas the chromosome arms are heterochromatic. Telomeric regions are heterochromatic both centromeric and holocentric chromosomes. Methyalted H3K9 colocalizes with areas of heterochromatin in both centromeric and holocentric chromosomes.

discovered in *Drosophila* and binds H3K9me through its chromodomain (Clark and Elgin, 1992; Nielsen et al., 2002). HP1 is necessary for heterochromatin compaction and has homologues in almost all eukaryotes ranging from *Schizosaccharomyces pombe* to mammals and higher plants (Lachner et al., 2001; Nakayama et al., 2001; Nielsen et al., 2002). HP1 is enriched at compacted, repressed regions of chromatin (Lachner et al., 2001; Nakayama et al., 2001; Nielsen et al., 2002, 2002). Although HP1 is enriched at heterochromatic centromeric (centers of chromosomes) and telomeric regions (ends of chromosomes) of the genome, it can also be found at euchromatic sites, as a means of tissue specific gene repression (Nakayama et al., 2001). HP1 induces chromatin compaction by its ability to dimerize with other HP1 proteins via its chromoshadow domain (Brasher et al., 2000). HP1 dimers oligomerize, which brings HP1 bound methylated histone tails close together and thus compacts chromatin. There are two HP-1 orthologs in *C. elegans. "*HP-1 Like" proteins HPL-1 and HPL-2 and three other known *C. elegans* proteins that have been shown to bind methylated H3K9: CEC-3, CEC-4, and LIN-61(Ahringer and Gasser, 2018; Garrigues et al., 2015; Gonzalez-Sandoval et al., 2015; Greer et al., 2014; Koester-Eiserfunke and Fischle, 2011). HPL-1 and HPL-2 both have the conserved HP1 chromodomain and the conserved HP1 chromoshadow domain (Couteau et al., 2002). Although HPL-2 has been shown to be associated with expressed genes in addition to repressed genes, HPL-1 and HPL-2 associate with H3K9-methylated histones and compacted chromatin in *C. elegans* (Garrigues et al., 2015).

In *C. elegans* di-methylation and tri-methylation of H3K9 have distinct distributions and generally do not overlap (citations). Di-methyaltion of H3K9 is more associated with DNA transposons and satellite repeats, whereas tri-methylation of H3K9 is associated with retrotransposon family regions (McMurchy et al., 2017; Zeller et al., 2016). Although highly associated with repetitive elements, H3K9me2 and H3K9me3 can be found at promoters (~8% of H3K9me2 associated DNA and ~10% of H3K9me3 associated DNA), exons (~18% of H3K9me2 associated DNA and ~25% of H3K9me3 associated DNA), and introns (~10% of H3K9me2 associated DNA and ~11% of H3K9me3 associated DNA), ((Zeller et al., 2016). Repetitive elements make up ~35% of H3K9me2 associated DNA and ~25% of H3K9me3 associated DNA. Repetitive DNA, including tandem repeats and sequences derived from DNA or RNA transposons, makes up approximately 20% of the *C. elegans* genome (Hillier et al., 2009; Hubley et al., 2016). These repetitive regions of the genome, along with the H3K9 methyltransferases and their reader proteins, are concentrated on the distal arm regions of the autosomes (McMurchy et al., 2017; Zeller et al., 2016). The binding and co-association of many proteins, including proteins found at the repressed nuclear lamina, at these regions suggest a role for regulation of repression of these sequences.

Nuclear localization of genes is associated with their expression

Lamin associated domains (LADs) are regions of the genome that associate with regions of the nuclear lamina. These regions have been identified

in *C. elegans, Drosophila melanogaster,* and mammals. The nuclear lamina is a stable meshwork underlying the nucleoplasmic side of the nuclear lamina. Genes in LADs are expressed at very low levels. In *C. elegans,* LADs are enriched at the distal arms of autosomes (Gonzalez-Sandoval et al., 2015; Ikegami et al., 2010; Towbin et al., 2012). LADs are associated with H3K9-methylated histones and in *C. elegans* this modification is necessary for their perinuclear anchoring (Towbin et al, 2012). A nuclear envelope associated H3K9me reader CEC-4 anchors methylated histones and their associated regions of the genome to the nuclear periphery (Gonzalez-Sandoval et al., 2015). The correlation of LADs and repressed genes suggest that the 3D topography of the genome affects overall expression of the genome.

The 3D organization of the nucleus can further be categorized into regions of repression and expression. Topologically associated domains (TADs) are areas within the genome that are more likely to interact with each other than other regions of the genome (Dixon et al., 2012; Nora et al., 2012). TADs can include genes found on the same chromosome and/or genes found on other chromosomes. The nucleus includes TADs that are highly enriched with H3K9 methylation, chromatin compaction, and gene repression (Dixon et al., 2012, Nora et al., 2012). There are also TADs that are highly enriched for expression-associated histone modifications, uncompacted chromatin, and Pol II. Although the mechanisms underlying TAD formation and the function of TADs are not well understood, disruption of TADs causes changes in gene expression due to changes in the 3D organization of the genome (Nora et al., 2012). Formation of

TADs are thought to be important in many cellular processes including cell division and differentiation (Dixon et al., 2012; Nora et al., 2012).

Chromatin is compacted and organized throughout development

Establishment and organization of expressed and repressed chromatin is necessary to achieve proper development. Cellular differentiation occurs as cells gain their fate and lose potency to achieve other fates. As cells go from a totipotent one-cell zygote to a multicellular differentiated organism, chromatin transitions from being highly dynamic and non-ordered to more static, with clear euchromatic and heterochromatic domains within the nucleus (Figure 1.2 and Figure 1.4) (Mutlu et al., 2018; Politz et al., 2013; Yuzyuk et al., 2009). Chromatin organization and condensation occurs as cell fate decisions and differentiation is achieved. As chromatin is compacted and cell lineages are defined, gene expression potential and cell potency of that lineage is reduced. Repressive chromatin domains, such as LADs and TADs, are formed during early embryogenesis. (Gonzalez-Sandoval, et al., 2015; Mutlu et al, 2018; Politz et al., 2013; Yuzyuk et al., 2009). These changes in chromatin compaction occur during a concurrent developmental transition from no/very low zygotic gene expression to zygotic, fate-specific gene expression (Figure 1.4). Formation of H3K9me2 associated electron dense heterochromatic domains precedes the maternal to zygotic switch when zygotic, fate-specific gene expression is upregulated (Mutlu et al., 2018). Thus, it is thought that proper organization of chromatin must

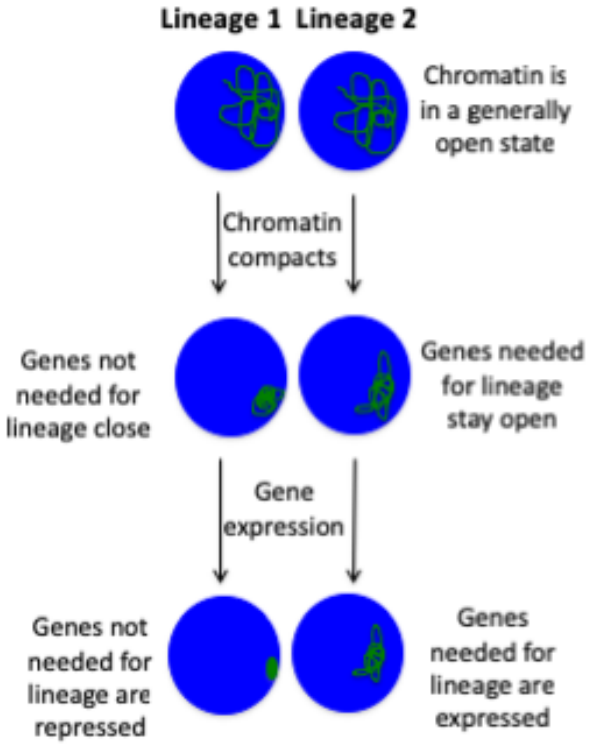

Figure 1.4 Chromatin is compacted and organized throughout development. As development progresses, chromatin transitions from unorganized and uncompacted to compacted domains. Genes not needed for a certain lineage become compacted and sequestered to the nuclear periphery where they are repressed. Genes needed of that lineage are less compacted and organized into domains that are easily accessible to binding of transcription factors and RNA Pol II.

precede zygotic expression in order to ensure proper gene expression and cell fate decisions (Levin et al., 2012; Robertson and Lin, 2015; Spencer et al., 2011).

Establishment of proper chromatin compaction throughout development involves many different mechanisms and protein players. The zygote that gives rise to all cell lineages arises from two fully differentiated cells, the egg and sperm. Thus, it is thought that in order to gain full potency, the epigenome must be erased and re-established during development (Furuhashi et al., 2010; Tabuchi et al., 2018). In *C. elegans, e*stablishment of di- and tri-methylation of H3K9 occurs early in development at the onset of gastrulation (21-100 cell embryo) just as zygotic fate-specific gene expression begins (Mutlu et al., 2018; Towbin et al., 2012). Establishment of H3K9me2 concurs with nuclear accumulation of MET-2 from the cytoplasm. Shortly after nuclear accumulation of MET-2, heterochromatin formation can be visualized by transmission electron microscopy (Mutlu et al., 2018). Loss of MET-2 results in delays in heterochromatin formation into later developmental stages (Mutlu et al., 2018). After di-methylation of H3K9me2 by MET-2, SET-25 deposits H3K9me3. SET-25 colocalizes with H3K9me3 at the nuclear periphery and is necessary for anchoring of H3K9me3 associated chromatin to the nuclear lamina to stabilize repression (Towbin et al., 2012). HPL-2 and other proteins known to promote gene repression co-localize with SET-25 and H3K9-methylated histones at the nuclear periphery to establish, regulate, and maintain gene repression.

Although H3K9-methylated histones are primarily found at heterochromatic regions of the genome that are gene-poor and repeat rich, repressive chromatin can be established in euchromatic regions of the genome. This is called facultative heterochromatin (Ahringer and Gasser, 2018). H3K9-methylated histones localize to repressed genes in euchromatic regions of the genome by tissue specific mechanisms (Smolko et al., 2018). Although histone modifications such as H3K9 methylation have been known to associate with repressed genes, many regulators and establishers of facultative heterochromatin remain unknown (Liu et al., 2011; McMurchy et al., 2017; Smolko et al., 2018; Zeller et al., 2016). Although all players involved in facultative heterochromatin formation have yet to be elucidated, it's known that facultative heterochromatin must be established in a tissue specific manner during certain developmental windows in order to achieve proper fate specification (Gaertner et al., 2012; Smolko et al., 2018). As zygotic, tissue-specific expression is achieved, mechanisms of gene repression must be in place in order to prevent improper gene expression (Gaertner et al., 2012; Smolko et al., 2018)

SYNMUV B PROTEINS REGULATE FATE DECISIONS DURING DEVELOPMENT

synMuv B mutants ectopically express germline genes and arrest during development at high temperature

In *C. elegans* many genes with presumed roles in regulating gene repression by chromatin, including the H3K9me1/2 methyltransferase and

proteins that bind methylated H3K9, were originally identified based on their synthetic multivulval (synMuv) phenotype (Andersen and Horvitz, 2007; Fay and Yochem, 2007). Single mutants of synMuv genes do not have extra ectopic vulvas (multivulva), but double mutants between synMuv class A genes and synMuv class B genes have a multivulva phenotype (Andersen and Horvitz, 2007). Although synMuv genes were first identified based on their roles in repression of vulval fate development, most are widely expressed, and single mutants show pleiotropic phenotypes and genetic interactions in non-vulval processes.

The *C. elegans* synMuv B proteins are important in the tissue specific repression of large set of germline genes in somatic tissue. A subset of synMuv B proteins, including members of the DREAM complex (EFL-1, DPL-1, LIN-9, LIN-37, LIN-52, LIN-53, LIN-54, LIN-35), LIN-15B, and MET-2 bind in the promoter region of germline genes and repress their expression in somatic tissue (Figure 1.5) (Fay and Yochem, 2007; Harrison et al., 2006). The DREAM complex is comprised of the conserved MuvB core (LIN-54, LIN-37, LIN-52, LIN-53, and LIN-9), the E2F/DP complex (EFL-1, DPL-1), and the pocket protein (LIN-35) (Figure 1.5)(Fay and Yochem, 2007; Goetsch et al., 2017). The DNA binding protein, LIN-54, facilitates MuvB binding in promoter regions of germline

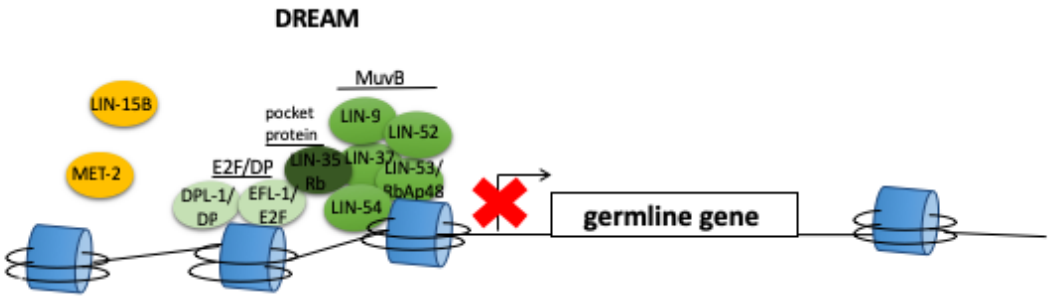

Figure 1.5 The DREAM complex, LIN-15B, and MET-2 associate at germline gene promoters to repress their expression. The DREAM complex, LIN-15B and MET-2 are found at the promoters of germline genes. The DREAM complex consists of the repressive MuvB complex that includes the DNA binding protein LIN-54, LIN-37, LIN-53, LIN-52 and LIN-9. The E2F/DP complex also makes up the DREAM complex and the Muv B repressive core and the E2F/DP complex is held together by the pocket protein LIN-35.

genes (Tabuchi et al., 2011). In mammals, flies, and worms, the MuvB core is responsible for the repressive activity of the DREAM complex. The E2F/DP complex binds DNA by EFL-1's DNA binding domain. The pocket protein LIN-35 stabilizes the interaction of the MuvB core with the E2F/DP complex in germline gene promoters and help maintain germline gene repression (Goetsch et al., 2017).

Loss of the DREAM complex, LIN-15B, or MET-2 results in the ectopic expression of germline genes in the somatic intestine (Figure 1.6) (Andersen and Horvitz, 2007; Petrella et al., 2011; Wang et al., 2005). Ectopic germline gene expression is exacerbated at 26°C compared to 20°C (Petrella et al., 2011). Proteins such as PGL-1, PGL-2, HTP-3 and REC-8 are proteins found only in germ cells in wild-type embryos and larva. However, in synMuv B mutants, antibody staining reveals that PGL-1, PGL-2, HTP-3, and REC-8 are found in the two primordial germ cells, but are also enriched in the somatic intestine in especially at high temperature (Figure 1.6) (Petrella et al., 2011). Ectopic germline gene expression in the intestine leads to loss of cell fate and High Temperature L1 larval Arrest (HTA) in DREAM complex, *lin-15B,* and *met-2* mutants (Figure 1.6) (Petrella et al., 2011; Rechtsteiner et al., 2018). The HTA phenotype is due to the inability of the intestine to properly function and mutants arrest at the L1 stage due to starvation (Petrella et al., 2011). Larval arrest demonstrated by synMuv B mutants is a marker of ectopic germline gene expression in the somatic intestine. The HTA phenotype can be rescued by

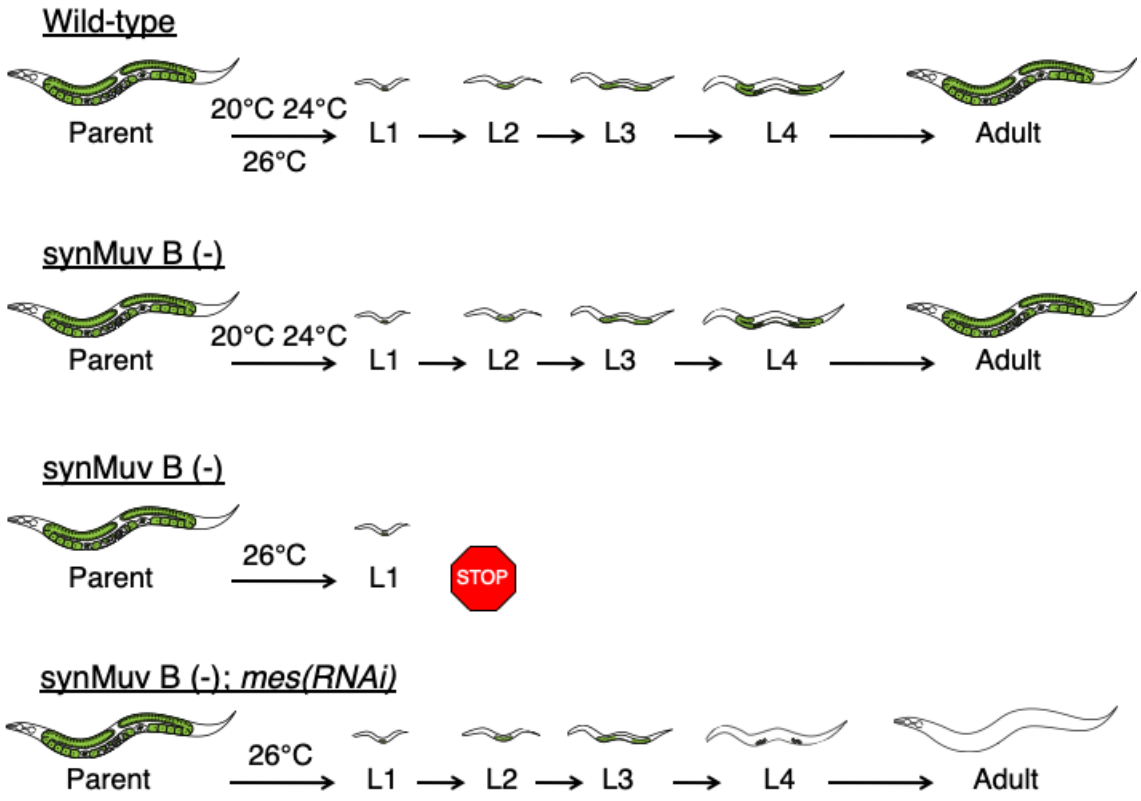

Figure 1.6: Loss of synMuv B proteins causes high temperature larval arrest (HTA) at 26°C. synMuv B mutants arrest at the Larval L1 stage at 26°C but not 24°C or 20°C. Knockdown of chromatin modifiers such as *mes* suppress the HTA phenotype.

subsequent knock-down of chromatin modifiers, suggesting that synMuv B proteins regulate gene expression at the chromatin level.

synMuv B proteins associate at germline genes to repress their expression

The most studied DREAM complex member, LIN-35, is the single worm pocket protein homolog. LIN-35 functionally resembles mammalian proteins p130/p107, which in mammals promotes assembly of the DREAM complex at promoters. p130/p107 bind to both the core MuvB portion of DREAM and the transactivation domain of repressive E2F-DP complex through different binding interfaces, completing the assembly of DREAM (Guiley et al., 2015; Takahashi et al., 2000). In *C. elegans,* the DREAM complex acts similarly to the mammalian DREAM complex as LIN-35 mediates the interaction of EFL-1-DPL-1 (E2F-DP homologs) and the MuvB core of the DREAM (Figure 1.5)(Goetsch et al., 2017; Harrison et al., 2006). In *C. elegans,* LIN-35 works to assemble DREAM complex at DREAM target genes in somatic tissue in order to repress their expression. In the absence of LIN-35, the DREAM complex has highly reduced binding and repression capabilities (Goetsch et al., 2017). Reduced binding and repression causes *lin-35* mutants to ectopically express germline genes in somatic tissue and show high temperature L1 arrest at 26°C (Figure 1.6).

The Muv B core is responsible for repression of gene expression by the DREAM complex and is bound to Cell cycle gene Homology Region (CHR) DNA elements by LIN-54 in both mammals and in *C. elegans* (Guiley et al., 2015; Tabuchi et al., 2011). CHR is a conserved DNA element that was named due to

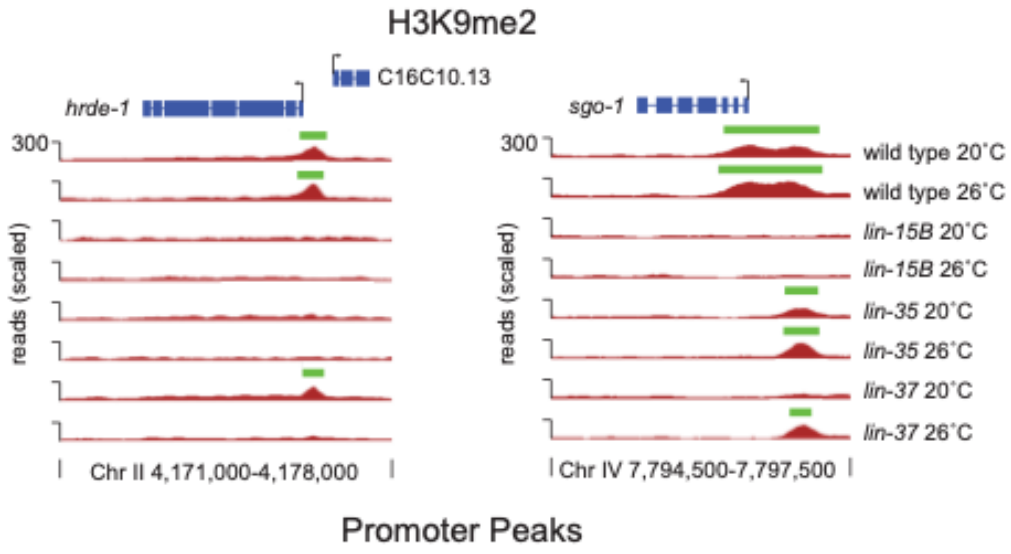

Figure 1.7: germline gene promoter enriched H3K9me2 is lost in *lin-15B* mutants. Enrichment of H3K9me2 is found at the promoter of germline genes in somatic tissues in *C. elegans*. *lin-15B* mutants lose promoter enrichment at both 20C and 26C at synMuv B regulated genes. DREAM complex mutants sometimes lose promoter enrichment as shown here with loss at *hrde-1* but not at *sgo-1* in *lin-35* mutants and loss at 26C at *hrde-1* promoters and at 20C at *sgo-1* promoters in *lin-37* mutants.

the association of LIN-54 and MuvB in the mammalian cell cycle. In *C. elegans* LIN-54 binds to gene promoters through its DNA binding domain and in *lin-54* mutnats, the DREAM complex is lost from 80-90% of target loci (Figure 1.5) (Tabuchi et al*.,* 2011). Loss of DREAM complex binding in *lin-54* mutants results in ectopic expression of germline genes and high temperature L1 arrest at 26°C (Figure 1.6) (Petrella et al., 2011).

LIN-15B is a synMuv B protein that has not been shown to be part of the DREAM complex, but has overlapping binding sites in the genome as DREAM complex members (Figure 1.5)(Rechtsteiner et al., 2018). Furthermore, *lin-15B* mutants demonstrate the same phenotypes as seen in DREAM complex mutants, including ectopic germline gene expression and HTA (Figure 1.6) (Petrella et al*.,* 2011). Other data suggest LIN-15B might be a separate entity to the DREAM complex. Although LIN-15B binds to many of the same genes as the DREAM complex, LIN-15B also binds to genes where DREAM binding is not observed (Rechtsteiner et al., 2018). LIN-15B has predicted DNA binding activity through a THAP or AT hook domain (Wormbase). LIN-15B has no known homologs outside of the genus *Caenorhabditis,* but is very important for the soma-to-germline fate decision. Differences in repressive roles of LIN-15B and the DREAM complex must be elucidated in order to fully understand how germline genes are repressed in somatic tissue.

MET-2 is the *C. elegans* homolog of mammalian SETDB1 which catalyzes mono- and di-methylation of histone H3 lysine 9 (H3K9me1 and H3K9me2), a histone modification associated with repressive chromatin (Andersen and

Horvitz, 2007; Towbin et al., 2012). In *C. elegans, met-2* mutants lose ~80% of H3K9me2 (Andersen and Horvitz, 2007; Towbin et al., 2012). Although canonical H3K9me2 deposited by MET-2 is enriched at DNA transposons and satellite repeats found on autosomal distal arms, MET-2 associated H3K9me2 is found at promoters of synMuv B regulated germline genes (Figure 1.7). These germline genes are broadly found along the length of autosomes, are enriched in the euchromatic centers, and are bound by the DREAM complex and LIN-15B (Rechtsteiner et al., 2018). Loss of H3K9me2 in *met-2* mutants causes phenotypes similar to DREAM and *lin-15B* mutants, such as HTA and ectopic germline gene expression, suggesting di-methylation of H3K9 is an important repressive mechanism at synMuv B regulated loci (Rechtsteiner et al., 2018). Interestingly, H3K9me2 promoter enrichment is lost in *lin-15B* mutants and in DREAM complex mutants, but to a much lesser extent (Figure 1.7) (Rechtsteiner et al., 2018). This suggests LIN-15B may have a separate function than the DREAM complex and acts to promote or maintain di-methylation of H3K9me2 at germline gene promoters in somatic tissue. Although loss of the DREAM complex, LIN-15B, and H3K9me2 catalyzed by MET-2 all lead to ectopic expression of germline genes, the role and order of each of these proteins at germline genes during development remains unknown.

synMuv B phenotypes are temperature sensitive

Almost all of the phenotypes displayed by synMuv B mutants are temperature sensitive. The multivulval phenotype for which they were named is

enhanced at elevated temperatures of 25°C (Andersen and Horvitz, 2007). Ectopic germline gene expression is also enhanced in synMuv B mutants at 26°C compared to 20°C. Finally, the high temperature arrest phenotype causes L1 arrest at 26°C but not 24°C or 20°C (Petrella, et al., 2011). The mechanisms that underlie these temperature sensitive phenotypes remains unknown. *lin-35, lin-15B,* and *met-2* mutants are null alleles that result in no protein at any temperature and *lin-54* mutants, although not nulls, lose 80% of DREAM complex binding at all temperatures (Andersen and Horvitz, 2007; Petrella et al., 2011; Tabuchi et al., 2011). Interestingly, chromatin formation is temperature sensitive. Previous studies have reported that *Arabidopsis thaliana* can change chromatin dynamics to modify gene expression in response to changes in temperature (Zografos and Sung, 2012). In addition to being temperature respondent, chromatin is also temperature sensitive. Early studies in *Drosophila* revealed that high temperature causes incomplete heterochromatin formation (Hartmann-Goldstein, 1967). In *C. elegans*, chromatin associated mutants, including *met-2* and *set-25* show temperature sensitive phenotypes (Gonzalez-Sandoval et al., 2015; McMurchy et al., 2017; Towbin et al., 2012). This study describes a potential connection between the temperature sensitivity of chromatin and synMuv B mutant temperature sensitive phenotypes.

C. elegans intestinal development

The *C. elegans* embryo is a powerful system to study development as the entirety of development can be tracked with single-cell resolution (Sulston et al.,

1983). The timing and orientation of every cell division, apoptotic event, and cell migration has been documented, and the exact lineal relationship of any cell to any other is known (Sulston et al., 1983). Each division is invariant and because the worm is transparent, fluorescent markers allow easy visualization of cell lineages, protein, and DNA in real time.

The entire intestinal lineage descends from a single cell, the E blastomere that arises in the eight-cell embryo. The first division of the E blastomere is an anterior to posterior division that creates 2E (Figure 1.8)(McGhee, 2007; Sulston et al., 1983). The second cell division establishes 4E and is a left-right division that establishes the bilateral symmetry of the intestine. The left-right sister cells divide together for the rest of the intestinal lineage. The third division is an anterior-posterior division that is slightly skewed in the dorsal-ventral plane to establish 8E (Figure 1.7)(McGhee, 2007; Sulston et al., 1983). The fourth division is another anterior-posterior division that establishes 16E cells lying in two tiers: ten cells in the dorsal tier and six cells in the ventral tier. At 16E, the cells become polarized, intracellular components shift, and the cells change their shape (McGhee, 2007; Sulston et al., 1983). The intestinal cells begin to migrate and the anterior pair of cells (labelled “a” in Figure 1.8) divide in the dorsal-ventral direction and the posterior pair of cells (labelled “h” in Figure 1.8) divide in an anterior-posterior direction, resulting in the final arrangement of 20E cells within the developing intestine (McGhee, 2007; Sulston et al., 1983). Cell polarizations and migrations form a series of 9 rings referred to as “ints.” “Ints”

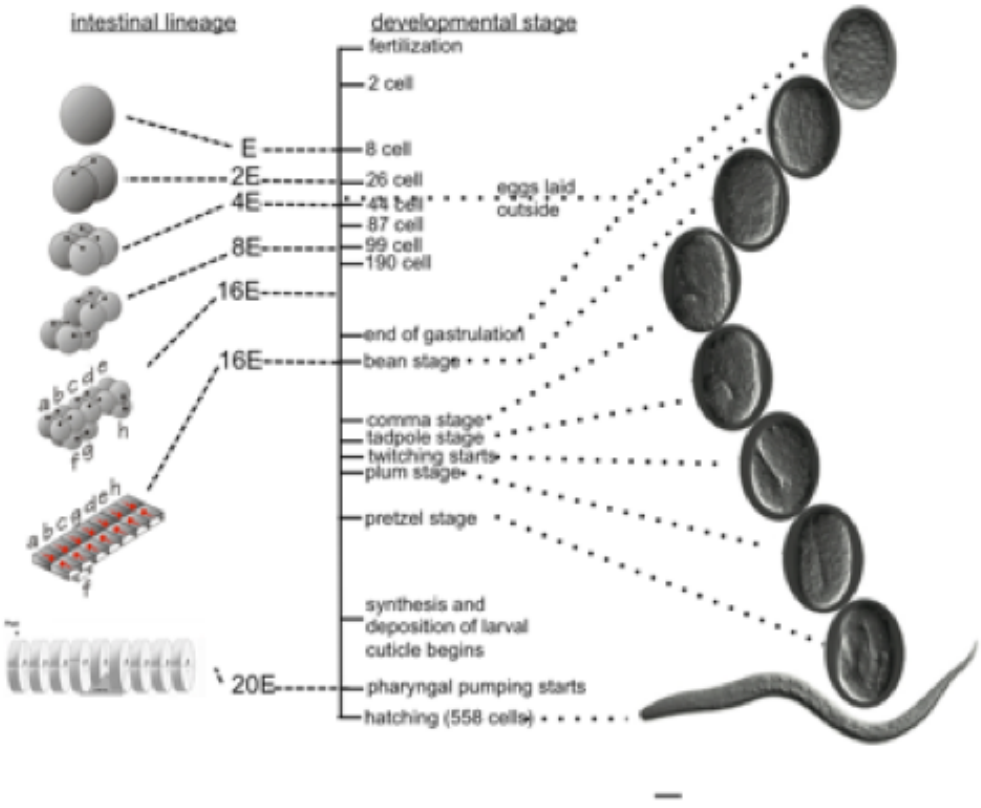

Figure 1.8 The *C. elegans* intestinal lineage. The intestinal lineage, E, arises in the 8 cell embryo. The first division of the E blastomere is an anterior to posterior division that creates 2E in the 28 cell embryo. 2E divides left-right to establish 4E. 4E divides in an anterior-posterior direction that is slightly skewed in the dorsal-ventral plane to establish 8E in the 100 cell embryo. 8E divides anterior to posterior to create 16E. At 16E, the cells become polarized and begin to migrate and the anterior pair of cells, labelled “a”, divide in the dorsal-ventral direction and the posterior pair of cells, labelled “h”, divide in an anterior-posterior direction, resulting in the final arrangement of 20E cells within the developing intestine

are the basic unit of the intestine, each “int” ring includes 2 cells except the most anterior ring (int1) has four cells (McGhee, 2007; Sulston et al., 1983).

The anterior-posterior patterning of gene expression is autonomous within the intestine lineage and reflects zygotic expression of the Wnt pathway (Schroeder and McGhee, 1998). There are a significant number of genes that are expressed in specific non-uniform patterns along the anterior-posterior axis of the intestine (Dal Santo et al., 1999). Although *C. elegans* intestinal development has been described and highly studied, factors that regulate gene expression and the mechanisms they employ during intestinal development have yet to be fully explained.

Transcriptional activation in the intestine occurs early at the 1E stage and includes some of the earliest fate-specific zygotically expressed genes. Maternally loaded proteins activate WNT signaling transcription factors that regulate target genes *end-1* and *end-3.* Expression of *end-1* and *end-3* can be detected at the 1E stage but END-1 and END-3 protein have largely decayed by 8E (Baugh et al., 2005; Zhu et al., 1997). END-1 and END-3 subsequently activate the master regulator of the intestine, the zinc-finger GATA-type transcription factor, ELT-2 (McGhee et al., 2007). ELT-2 expression begins in the 2E stage and persists throughout the lifespan of the worm. ELT-2 expression is the predominant transcription factor of the *C. elegans* intestine and *elt-2* mutants are embryonic lethal due to the inability of the intestine to develop (Fukushige et al., 1998).

synMuv B proteins regulate temporal and spatial chromatin compaction during development.

Altogether, the mechanisms by which organisms achieve and maintain their cell fates throughout development is not fully understood. It is not known how repressive chromatin is formed throughout development in order to achieve proper cell fates. Loss of a conserved class of transcriptional repressors, synMuv B proteins, causes loss of cell fate in the intestine. We hypothesize that synMuv B proteins regulate chromatin in order to repress germline genes in the somatic intestine. Prior to this study, developmental chromatin compaction had not been observed in synMuv B mutants. We set out to determine if synMuv B proteins regulate chromatin organization throughout development by observing chromatin compaction in synMuv B mutants at both 20°C and 26°C. Chromatin compaction at high temperature had not previously been observed in *C. elegans,* especially in a developmental context. We wanted to know if there was a link in chromatin and the temperature sensitive phenotypes we observe in synMuv B mutants. Overall, we found that *C. elegans* synMuv B mutants regulate spatial and temporal chromatin compaction at crucial developmental time periods in order to achieve proper germline gene repression in somatic tissues.

CHAPTER 2: MATERIALS AND METHODS

Strains and nematode culture

C. elegans were cultured on NGM plates seeded with *E. coli* strain AMA1004 at 20°C unless otherwise noted. N2 (Bristol) was used as wild-type. Strain LNP0050 containing the transgene bnEx80(68xlacO+myo-3::mCherry+worm genomic DNA); gwIs39[baf-1p::GFP::lacI::let-8583\'UTR;vit-5::GFP];caIs79(elt-2p::dTomato;pRF4)) was created for this study and crossed into mutant worms. Mutant alleles used were *lin-15B(n744), lin-35(n745), lin-54(n2231), met-2(n4256), lin-37(n758), hpl-2(tm1489), set-25(n5032), jmjd-1.1(hc184).* The complete strain list can be found in table 1.

Nuclear Spot Assay

Wildtype and mutant embryos and L1s with gwIs39[baf-1p::GFP::lacI;;let-858 3'UTR; vit-5::GFP]; bnEx85 (68xlacO+myo-3::mcherry+genomic C05C10.7+worm genomic DNA)and caIs79[elt-2p::dTomato, pRF4 (rol-6+)] arrays were collected and fixed with methanol and acetone and mounted using Gelutol (Petrella et al., 2011). Each genotype was scored at 8E, 16E, comma, and L1. High temperature samples were collected by upshifting L4 P0 worms to 26°C before collecting F1 embryos or L1s. Embryos were collected by two methods: large batch collection generally for later stage or mixed stage embryos or small batch collection by dissection of gravid adults generally for early stage embryos. In large batch collection, plates with gravid adults were washed from

plates using ~1mL of 1X M9 media per plate, collected in a 15mL falcon tube and centrifuged in a large swinging bucket centrifuge at 4.4x1000RPM for 4 minutes. Excess liquid was removed, leaving a pellet of worms. A solution containing, 2mL of bleach, 8mL of water, and 400ul of NaOH was added to the pellet. The tube was shaken and/or vortexed for 4 minutes to break up the cuticles of adult worms. The tube was again centrifuged at 4.4x1000RPM for 2 minutes. Excess liquid was removed and the pellet, now containing only embryos, was washed two times with 1XM9. Embryos were resuspended in ~200ul of 1X M9 and pipetted onto polylysine coated slides. For dissection, gravid adults were picked into 20ul bubbles of 1X M9 on hydrophobic polylysine covered slides. Adults were dissected in half at the vulva site to release embryos from inside the worm. L1 larvae were obtained by hatching embryos in the absence of food in M9 buffer. In all collection forms, a coverslip was placed over the sample, excess liquid was wicked away, and the slides was immersed in liquid nitrogen for at least 5 minutes. Slides were removed from liquid nitrogen, the coverslip was removed, and the samples were fixed in methanol at 4°C for 10 minutes and acetone at 4°C for 10 minutes. Slides were removed acetone, air dried, and labeled. Slides were washed four times for 10 minutes each in 1X PBS at room temperature and then DAPI at a 1:500 dilution was added to a coplin jar with 50mL of 1X PBS for an incubation of 10 minutes at room temperature. Slides were washed 4 more times in 1X PBS at room temperature and were then mounted in Gelutol mounting media. Images were acquired with Nikon A1R laser scanning confocal controlled by NIS-Elements fitted on a Nikon software

nverted Eclipse T*i*-E microscope with a Nikon DS-Qi1Mc camera and Plan Apo 100X/1.2 numerical aperture oil objective. For chromatin compaction analysis, each intestinal cell's GFP-labeled extra-chromosomal array was scored by eye as either open if it looked diffuse or closed if it looked punctate as described in Yuzyuk *et al,* 2009. Nuclear volumetric array compaction analysis was performed using the isosurface function in Metamporph V7.8.8.0. Specifically the volume of both the nucleus and GFP+ LacO arrays of each individual intestinal cell was measured and used to determine the percentage of the nucleus that the array represented. Statistical analysis was performed by 2-way ANOVA using Prism Graph Pad.

Anterior-to-posterior Chromatin Compaction Analysis

Embryos scored for chromatin compaction analysis were also scored for the number of cells with scored "open" extrachromosomal arrays (described above) within an embryo and a percentage was determined. The intestinal cells at each developmental stage were labeled anterior-to-posterior as in WormBook (McGhee, 2007) so that chromatin compactions in each specific intestinal cell could be compared between embryos. The exact intestinal cells along the A-P axis with open arrays in each embryo were recorded and the percentages of open intestinal cells were calculated. The percentage of each cell as open was calculated to determine the location of open cells within the embryo intestine. Statistical analysis was performed by 2-way ANOVA using Prism Graph Pad.

DNA Fluorescence In Situ Hybridization

Fluorescent probes were made by PCR labeling as described in Meister *et al*., 2013 using fluorescent 568-5-dUPT (Thermo Fisher C11399) and ULYSIS Nucleic Acid Labeling Kits using Alexa Fluor 488 (molecular probes life technologies U21650). Worm genomic DNA was used as the template to create five ~500bp probes ~50kbp upstream and downstream of *pha-4* and *myo-3* as controls and *ekl-1*, *coh-3*, and C05C10.7 experimental loci. High temperature samples were collected by upshifting L4 P0 worms to 26°C before collecting F1 embryos. Embryos were dissected in 1X M9 on slides and then frozen in liquid nitrogen. After freeze-cracking, slides were fixed in methanol (on ice, 2 minutes) followed by 4% formaldehyde (4°C, 10 minutes) and then washed two times in 1X PBS (room temperature, 2 minutes). Embryos were permeabilized in 0.5% PBS-Triton X-100 (room temperature, 5 minutes), washed two times in 1XPBS (room temperature, 2 minutes), rinsed in 0.01 N HCl, and incubated in 0.1 N HCl (room temperature, 2 minutes). Slides were then washed once with 1X PBS (room temperature, 3 minutes), once with 2X SSC (room temperature, 3 minutes) and then treated with 50 ug/mL of RNase A (VWR 1247C393) in 2X SSC for 45 minutes at 37°C by overlaying the sample with 500ul of RNAse solution and incubating in a humidified chamber. Slides were then washed once with 2X SSC (room temperature, 2 minutes) and than incubated in 2X SSC/50% formamide for 2 hours at room temperature. The probe containing sample was diluted to a concentration of 2-5 ng/ul in 100% deionized formamide and an equal volume of hybridization buffer was added. 25 ul of the probe solution was added to the

sample and overlayed with a glass chamber sealed with cement glue. The slides were pre-hybridized overnight at 37°C in a humidified chamber. FISH probe and sample were denatured at 76°C by placing the slides on a heat block and then incubated for hybridization for 3 days at 37°C. Hybridization was followed by three washes of 2X SSC (37°C, 5 minutes) and two times in 0.2X SSC (55°C, 5 minutes). Images were acquired with Nikon A1R laser scanning confocal controlled by NIS-Elements fitted on a Nikon inverted Eclipse T*i*-E microscope with a Nikon DS-Qi1Mc camera and Plan Apo 100X/1.2 numerical aperture oil objective. Images were analyzed using Metamorph isosurface function to determine the 3-D distance between the two centroids as described in Yuzyuk et al*.,* 2009. Statistical analysis was performed by 2-way ANOVA using Prism Graph Pad.

Developmental Embryo Shift HTA Assays

For downshifting experiments: P0 L4 wildtype and mutant strains expressing *caIs79[elt-2p::dTomato, pRF4 (rol-6+)]* worms were upshifted to 26°C. The next day, 2-cell embryos were dissected out of adults in 1X M9, plated on NGM, and the plate was returned to 26°C. Developmental stages were determined based on the number of intestinal cells in which *elt-2p::dTomato* expression was detected. Embryos were downshifted to 20°C when the majority of embryos on the plate were at 4E (~2 hours), 8E (~3 hours), 16E (~5 hours), comma (~7 hours), pretzel ~(9 hours), and L1 (~14 hours). The HTA phenotype was scored two days after shifting as described in Petrella et al., 2011. Each downshift

experiment was done 4-6 times with 10-20 embryos plated per replicate. For upshifting experiments a similar protocol was used: 2-cell embryos were dissected out of adults and maintained continually at 20°C. After dissection embryos were plated and kept at 20°C until being upshifted to 26°C at 4E, 8E, 16E, comma, pretzel, and L1 stage. Plates were scored for HTA two days after shifting.

PGL expression analysis

P0 L4 wildtype and mutant strains expressing *caIs79[elt-2p::dTomato, pRF4 (rol-6+)]* and *pgl-1(sam33[pgl-1::gfp::3xFlag])* worms were upshifted to 26°C. The next day, adults were dissected in 1X M9 and 2-cell embryos placed in 1X M9 on polylysine coated slides in humid chambers and returned to 26°C. Embryos were downshifted on slides to 20°C at 8E, 16E, and comma stage. Arrested L1 larva in 1XM9 were covered with a coverslip, excess liquid was wicked away, and the slide was immersed in liquid nitrogen for at least 5 minutes. Slides were removed from liquid nitrogen, the coverslip was removed, and the samples were fixed in methanol at 4°C for 10 minutes and acetone at 4°C for 10 minutes. Slides were removed acetone, air dried, and labeled. Slides were washed four times for 10 minutes each in 1X PBS at room temperature and then DAPI at a 1:500 dilution was added to a coplin jar with 50mL of 1X PBS for an incubation of 10 minutes at room Temperature. Slides were washed 4 more times in 1X PBS at room temperature and were then mounted in Gelutol mounting media. Images were acquired with Nikon A1R laser scanning confocal controlled by NIS-

Elements fitted on a Nikon inverted Eclipse T*i*-E microscope with a Nikon DS-Qi1Mc camera and Plan Apo 60X/1.2 numerical aperture oil objective. Mean fluorescent intensity of PGL-1:GFP was determined using ImageJ. After the image was opened, "set measurements" was selected from the analyze menu. Area integrated intensity and mean grey value were selected. "Measure" was then selected from the analyze menu and a popup box with mean fluorescent intensity was produced. Statistical analysis was performed by 2-way ANOVA using Prism Graph Pad.

IMMUNOSTAINING

PGL-1 Staining

Immunostaining of L1 larvae was adapted from Strome and Wood 1983). L4 worms were placed at 26°C overnight and then moved into drops of M9 buffer as gravid adults. L1 larvae were obtained from the hatching of embryos in the absence of food in the M9 buffer. L1 animals were placed on a polylysine-coated slide, a coverslip was placed over the sample, excess liquid was wicked away, and the slide was immersed in liquid nitrogen for at least 5 minutes. Slides were removed from liquid nitrogen, the coverslip was removed, and the samples were fixed in methanol at 4°C for 10 minutes and acetone at 4°C for 10 minutes. Slides were air dried, and blocked for 30 minutes at room temperature. Slides were incubated with primary antibody for ~18 hours at 4°C, anti-PGL-1 primary at 1:30,000 (Kawasaki et al. 1998). Slides were washed two times in PBS for 10 minutes, blocked for 15 minutes at room temperature, and incubated with Alexa

Fluor 488 (Invitrogen) secondary antibody at a 1:500 dilution for 2 hours at room temperature. Slides were washed four times for 10 minutes each in PBS at room temperature and were mounted in Gelutol mounting media. Images were acquired with Nikon A1R laser scanning confocal controlled by NIS-Elements fitted on a Nikon inverted Eclipse T*i*-E microscope with a Nikon DS-Qi1Mc camera and Plan Apo 60X/1.2 numerical aperture oil objective.

MET-2 Nuclear Localization anti-FLAG M2 staining

Immunostaining of embryos was adapted from Strome and Wood 1983. Embryos were collected by picking gravid adults were into 20ul bubbles of 1X M9 on hydrophobic polylysine covered slides and dissecting out embryos. Adults were dissected in half at the vulva site to release embryos from inside the worm. 2-cell embryos were moved via mouth pipet to a clean hydrophobic polylysine covered slides, placed at 20°C, and allowed to develop until 4E (~3 hours), 8E (~4 hours), 16E (~6 hours). Samples were then overlaid with a coverslip, excess liquid was wicked away, and the slide was immersed in liquid nitrogen for at least 5 minutes. Slides were removed from liquid nitrogen, the coverslip was removed, and the samples were fixed in methanol at 4°C for 10 minutes and acetone at 4°C for 10 minutes. Slides were air dried and blocked for 30 minutes at room temperature. Slides were incubated with primary antibody for ~18 hours at 4°C, anti-FLAG M2 primary at a 1:100 dilution (Mutlu et al., 2018). Slides were washed two times in PBS for 10 minutes, blocked for 15 minutes at room temperature, and incubated with Alexa Fluor 488 (Invitrogen) secondary antibody

at a 1:500 dilution and DAPI at a 1:500 dilution for 2 hours at room temperature. Slides were washed four times for 10 minutes each in PBS at room temperature and were mounted in Gelutol mounting media. Images were acquired with Nikon A1R laser scanning confocal controlled by NIS-Elements fitted on a Nikon inverted Eclipse T*i*-E microscope with a Nikon DS-Qi1Mc camera and Plan Apo 100X/1.2 numerical aperture oil objective.

smFISH

smFISH staining of embryos was adapted from Ji and van Oudenaarden (Ji and van Oudenaarden, 2012). Stellaris FISH probes (Biosearch Technologies) were created for *pgl-1* and *elt-2* with Quasar 570 and Quasar 670. L1 worms were collected by upshifting P0 L4 wildtype and mutant worms to 26°C. The next day, adults were dissected in 1X M9 and 2-cell embryos placed in 1X M9 on hydrophobic slides in humid chambers and returned to 26°C. Embryos were downshifted on slides to 20°C at 8E, ~4 hours , 16E, ~6 hours, and comma stage, ~8 hours,. Arrested L1 larva were mouth pipetted and moved into 1mL of fixation solution (5mL formaldehyde, 5mL 10X PBS, and ddiH20 up to 50mL) on a clean hydrophobic slide and incubated for 30 minutes. Excess fixation solution was removed via mouth pipet and worms were washed 2X with 1mL of 1X PBS. Worms were resuspended in 1mL of 70% EtOH at 4°C for ~24 hours. 70% EtOH was removed and worms with resuspended in 1mL of wash buffer (5mL 20X SSC, 5mL formamide, ddiH_2O to 50mL) and incubated for 10 minutes. Excess wash was removed and 100ul of hybridization buffer (1g dextran sulfate, 1mL

20X SSC, 1mL formamide, ddiH_2O to 10mL) + probe was added to the sample and incubated at 37°C for 4 hours. Probe solution was removed and worms were washed with 2X SSC and incubated at 30°C for 30 minutes. Wash buffer was removed and worms were resuspended in 1mL of wash and 1.5 ul of DAPI and incubated at 30°C for 30 minutes. DAPI solution was removed, worms were resuspended washed once with 2X SSC and then 15-40ul of 2X SSC was added to the slide. The sample was overlayed with a coverslip and imaged with a Nikon A1R laser scanning confocal controlled by NIS-Elements fitted on a Nikon inverted Eclipse T*i*-E microscope with a Nikon DS-Qi1Mc camera and Plan Apo 60X/1.2 numerical aperture oil objective.

Motif analysis

To predict motifs enriched in LIN-15B associated promoters, 169 genes with peaks called for LIN-15B, LIN-35, LIN-54 and H3K9me2 promoter enrichment were identified (Rechtsteiner et al., 2019). The 500 bp window of upstream flank of each of the 169 genes was acquired using ParaSite BioMart and analyzed using the MEME Suite 5.0.4. MEME-ChIP motif analysis of large nucleotide datasets was used and we searched for motifs with a minimum width of 7bp and a maximum width of 30bp. We confirmed the motifs lie within the ChIP peaks by individually searching five synMuv B regulated genes.

HTA larval arrest assays

L4 larvae were placed at 26°C or 24°C for ~18 hours and then moved to new plates and allowed to lay embryos for 8 hours. Progeny were scored for larval arrest as described in Petrella *et al.,* 2011 approximately 48 hours later and then again at approximately 72 hours. Worms that arrested before the L4 stage were scored as arrested and worms that were able to grow past the L4 stage were scored as not arrested.

RNAi

RNAi was carried out by feeding using clones from the Ahringer library. Feeding experiments were carried out on NGM plates containing 0.2% lactose and ampicillin. P0 L4 animals were exposed to RNAi at 26°C for HTA experiments before they were moved to fresh RNAi plates to lay embryos for 8 hours.

Table 2.1 Strain List

Strain Name	Genotype	Source
BA1083	*jmjd-1.1(hc184) II*	CGC
DUP0075	*pgl-1(sam33[pgl-1::gfp::3xFlag])*	Dustin Updike
GW638	*met-2(n4256) set-25(n5032) III*	Susan Strome
JM163	caIs79[elt-2p::dTomato, pRF4 (rol-6+)]	Jim McGhee
LNP0024	*lin-35(n745);* bnEx80(68XlacO +myo-3::mCherry+ worm genomic DNA); gwIs39[baf-1p::GFP::lacI::let-858 3\'UTR; vit-5::GFP]	This Study
LNP0026	*lin-54(n2231);* bnEx80(68XlacO +myo-3::mCherry+ worm genomic DNA); gwIs39[baf-1p::GFP::lacI::let-858 3\'UTR; vit-5::GFP]	This Study
LNP0027	*met-2(n4256);* bnEx80(68XlacO +myo-3::mCherry+ worm genomic DNA); gwIs39[baf-1p::GFP::lacI::let-858 3\'UTR; vit-5::GFP]	This Study
LNP0034	*met-2(n4256) III; lin-15B(n744) X*	This Study
LNP0035	*set-25(n5032) III; lin-15B(n744) X*	This Study
LNP0038	caIs79(elt-2p::dTomato;pRF4); *pgl-1(sam33[pgl-1::gfp::3xFlag])*	This Study
LNP0039	*met-2(n4256) set-25(n5032) III; lin-15B(n744) X*	This Study
LNP0040	*lin-15B(n744)* bnEx80(68XlacO +myo-3::mCherry+ worm genomic DNA); gwIs39[baf-1p::GFP::lacI::let-858 3\'UTR; vit-5::GFP]; (caIs79(elt-2p::dTomato;pRF4))	This Study
LNP0041	*lin-15B(n744)* caIs79(elt-2p::dTomato;pRF4); *pgl-1(sam33[pgl-1::gfp::3xFlag])*	This Study
LNP0048	*lin-35(n745) I; lin-15B(n744) X*	
LNP0049	*lin-54(n2231)* caIs79(elt-2p::dTomato;pRF4); *pgl-1(sam33[pgl-1::gfp::3xFlag])*	This Study
LNP0050	bnEx80(68xlacO+myo-3::mCherry+worm genomic DNA); gwIs39[baf-1p::GFP::lacI::let-8583\'UTR;vit-5::GFP];caIs79(elt-2p::dTomato;pRF4))	This Study
LNP0073	*lin-54(n2231) IV; lin-15B(n744) X*	This Study
LNP0074	*lin-37(n758) III; lin-15B(n744) X*	This Study
LNP0092	*jmjd-1.1(hc184) II; lin-15B(n744) X*	This Study
MT13293	*met-2(n4256) III*	Susan Strome
MT7463	*set-25(n5032) III*	Susan Strome
MT10430	*lin-35(n745) I*	Susan Strome
MT5470	*lin-37(n758) III*	Susan Strome
MT2495	*lin-15B(n744) X*	Susan Strome
MT8841	*lin-54(n2231) IV*	Susan Strome
SS1110	*hpl-2(tm1489)*	Susan Strome

CHAPTER 3: SYNMUV B PROTEINS REGULATE CHROMATIN COMPACTION

Background

Generating proper chromatin organization during development is required for fate specification. As cells go from a totipotent one-cell zygote to a multicellular differentiated organism, chromatin transitions from being highly dynamic and non-ordered to more static, with clear euchromatic and heterochromatic domains within the nucleus (Mutlu et al., 2018; Politz et al., 2013; Yuzyuk et al., 2009). These changes in chromatin occur during a concurrent developmental transition from no/very low zygotic gene expression to zygotic, fate-specific gene expression (Levin et al., 2012; Robertson and Lin, 2015; Spencer et al., 2011). Chromatin compaction and accessibility are thought to have a large influence on the level of gene expression by regulating the ability of transcription factors and polymerase to have access to genes (Elgin and Reuter, 2013; Simon and Kingston, 2013)

In early development, when chromatin is very dynamic and unorganized, somatic blastomers are developmentally plastic. It is not until the onset of gastrulation (2E stage), that cells lose plasticity and gain tissue specific characteristics. Three cell divisions later, between 8E and 16E (100-200 cell embryo), cells are more restricted in their fate potential and usually give rise to cells of a single tissue type (Sulston et al., 1983). Loss of plasticity at the 8E-16E stage is further supported by many studies that ubiquitously expressed transcription factors in the embryo using a Cell Fate Challenge Assay (Fukushige and Krause, 2005; Gilleard and McGhee, 2001). In these studies, a somatic blastomere fated for one cell type, can give rise to another, if transcription factors

are ectopically and ubiquitously expressed. This response is lost, and cells fail to adopt alternative states at the 8E-16E stage. Additionally, physically changing the location of a somatic blastomere within the embryo can also change its cell fate until the 8E-16E stage (Priess and Thomson, 1987; Wood, 1991). Changes in cell fate due to location changes within the embryo is thought to occur by intercellular signaling, including Notch and Wnt pathways which play important roles in early development (Priess, 2005). Combined, these observations suggest that *C. elegans* embryonic blastomeres are developmentally potent and plastic until the onset of gastrulation, specifically at the 8E-16E stage when tissue specific zygotic expression is upregulated.

Early development, until the onset of gastrulation, takes place in the absence of zygotic transcription. Maternally loaded proteins and mRNAs are sufficient to direct development prior to gastrulation. Specifically, in the intestinal lineage, zygotic gene expression is rapidly increased between the 8E-16E stage (McGhee et al., 2007). At this time, an intestinal master regulator, ELT-2, first expressed at the 2E stage, up-regulates a set of intestine specific genes. These genes are highly expressed from the zygotic genome and are expressed exclusively or preferentially in the embryonic intestine or the intestine of L1s (McGhee et al., 2007). It is thought that tissue specific mechanisms for gene repression must be in place before zygotic gene expression is upregulated, including chromatin-regulated gene repression (Levin et al., 2012; Robertson et al., 2015; Spencer et al., 2011)

In early development, chromatin is highly dynamic. As development proceeds, chromatin is compacted and organized as cell lineages are defined. Repressive chromatin domains are formed during early embryogenesis (Gonzalez-Sandoval, et al., 2015; Mutlu et al, 2018; Politz et al., 2013; Yuzyuk et al., 2009). Establishment of proper chromatin compaction throughout development involves many different mechanisms and protein players. MET-2 directed establishment of H3K9 methylation is necessary for timely chromatin compaction during development (Mutlu et al, 2018). Establishment of H3K9me2 concurs with nuclear accumulation of MET-2 from the cytoplasm. Shortly after nuclear accumulation of MET-2, heterochromatin formation can be visualized by transmission electron microscopy (Mutlu et al., 2018). Loss of MET-2 results in delays in heterochromatin formation into later developmental stages (Mutlu et al., 2018). Chromatin condensation by MET-2 and H3K9 methylation occurs early in development at the onset of gastrulation (21-100 cell embryo) just as zygotic fate-specific gene expression begins (Mutlu et al., 2018). Chromatin compaction by other heterochromatin promoter complexes, such as Polycomb Repressive Complex-2 (PRC2), is occurring simultaneously in developmental time (Yuzyuk et al., 2009). Together, many tissue specific mechanisms establish repressive chromatin during crucial developmental windows for proper fate specification, many of which have players and regulators yet to be elucidated.

synMuv B proteins are a group of conserved transcriptional repressors important in the tissue specific repression of a large set of genes. Loss of a subset of synMuv B proteins, including members of the DREAM complex, LIN-

15B, and MET-2, results in the ectopic expression of germline genes in the somatic intestine (Andersen and Horvitz, 2007; Petrella et al., 2011; Wang et al., 2005; Wu et al., 2012). Ectopic germline gene expression in the intestine leads to High Temperature L1 larval Arrest (HTA) in DREAM complex and *lin-15B* mutants (Petrella et al*.,* 2011). The DREAM complex and LIN-15B bind to the promoter region of target genes throughout the genome where they are thought to repress their expression. The highly conserved DREAM complex has eight known subunits including LIN-35 and LIN-54 (Fay and Yochem, 2007; Harrison et al., 2006). LIN-35, the single worm homolog of the mammalian pocket protein retinoblastoma, mediates the interaction of the subcomplex portions of the DREAM complex and in it its absence the DREAM complex has highly reduced binding and repression capabilities (Goetsch et al., 2017). LIN-54 acts as one of the DNA binding subunits of the DREAM complex and in its absence the DREAM complex is lost from 80-90% of target loci (Tabuchi et al*.,* 2011). LIN-15B has not been shown to be part of the DREAM complex, but demonstrates the same phenotypes as seen in DREAM complex mutants, including ectopic germline gene expression and HTA (Petrella et al*.,* 2011). MET-2 catalyzes mono- and di-methylation of histone H3 lysine 9 (H3K9me1 and H3K9me2), a histone modification associated with repressive chromatin (Andersen and Horvitz, 2007; Towbin et al*.,* 2012). *met-2* mutants lose ~80% of H3K9me2 (Andersen and Horvitz, 2007; Towbin et al*.,* 2012). Although loss of the DREAM complex, LIN-15B, and H3K9me2 catalyzed by MET-2 all lead to ectopic expression of

germline genes, the role and order of each of these proteins during development remains unknown.

Interestingly, H3K9me2 is found at the promoter of synMuv B regulated germline genes. The majority of methylated H3K9 is enriched across entire gene bodies of repressed genes in *C. elegans* and in other organisms including mammals. In *C. elegans,* promoter enrichment of H3K9me2 is found at germline genes along the entire length of autosomes (Rechtsteiner et al., 2019). This suggests promoter enriched H3K9me2 could be a potential tissue specific mechanism for gene repression in euchromatic regions of the genome. Further mining into the mammalian genome revealed that promoter H3K9me2 enrichment is conserved at germline gene promoters and is necessary for developmental gene repression (Dixon et al., 2012; Ebata et al., 2017)). Interestingly, H3K9me2 promoter enrichment is lost at synMuv B regulated germline genes in *lin-15B* mutants, but not in DREAM complex mutants. Canonical gene body enriched H3K9me2 is not affected by loss of LIN-15B. Loss of promoter enriched H3K9me2 in *lin-15B* mutants is not temperature sensitive (Rechtsteiner et al., 2018). Depletion of promoter H3K9me2 occurs at both 20°C and 26°C, suggesting the mechanism that underlies the temperature sensitive phenotypes displayed by synMuv B mutants remains unidentified.

The phenotypes demonstrated by synMuv B mutants are temperature sensitive. Larval arrest only happens at high temperature and ectopic germline gene expression is more extensive at high temperatures. Chromatin has been shown to be affected by changes in temperature in other organisms. For

example, early studies in *Drosophila* revealed that high temperature causes incomplete polytene heterochromatin formation (Hartmann-Goldstein, 1967). Additionally, work in plants has shown that flowering time is linked to changes in chromatin that occur in response to increased temperature (Zografos and Sung, 2012). Therefore, the temperature sensitivity of synMuv B mutants may be associated with temperature sensitivity of chromatin. We hypothesized that synMuv B proteins regulate gene expression at the chromatin level throughout development and are particularly necessary for the proper chromatin regulation and buffering of gene expression during temperature stress.

This chapter uncovers how the loss of synMuv B proteins affects chromatin compaction and accessibility during development and during times of temperature stress. The temperature sensitivity of chromatin in *C. elegans*, and its regulating proteins, has never been examined in a developmental context before this study. The timing of chromatin compaction during embryogenesis is delayed at high temperatures, even in wild-type embryos. Furthermore, synMuv B mutants have an increased amount of open chromatin, both in general chromatin assays and at specific germline gene loci, especially at high temperature. We find the delay in chromatin compaction in synMuv B mutants occurs in an anterior posterior pattern. This data supports a mechanism that synMuv B proteins are necessary to regulate the proper spatial and temporal formation of repressive chromatin throughout development.

Results

synMuv B proteins regulate developmental chromatin compaction

To determine if chromatin compaction is compromised in synMuv B mutants, we utilized the Nuclear Spot Assay to visualize chromatin compaction during development (Yuzyuk et al*.,* 2009). The Nuclear Spot Assay uses an extrachromosomal array containing numerous *lacO* sites that are bound by a ubiquitously expressed GFP-LacI protein. This assay has been previously utilized in *C. elegans* to visualize chromatin compaction throughout development as differentiation is achieved (Gonzalez-Sandoval *et al,* 2015; Yuzyuk *et al,* 2009). We predicted that if synMuv B proteins are important for establishing chromatin compaction during development, we would see more open chromatin in mutants at a later stage of development as compared to wild-type worms.

We visualized chromatin compaction in intestinal cells in wild-type, *lin-15B, lin-35, lin-54,* and *met-2* mutants at three embryonic stages and in L1 larvae at 20°C and 26°C. These specific embryonic stages were chosen based on the state of zygotic gene expression and ease of staging: 1) 8E embryos with eight intestinal cells (~100 cell embryo), representing an early embryonic stage where the zygotic gene expression program has yet to be fully activated, 2) 16E embryos with sixteen intestinal cells (~200 cell embryo), representing an early-to-mid embryonic stage when zygotic gene expression is starting to be upregulated, and 3) comma stage embryos with twenty intestinal cells, representing a mid-to-late embryonic stage when zygotic gene expression is fully underway (Fig 3.1A). We scored intestinal cells as having either open or closed arrays to determine

differences between synMuv B mutants and temperatures (Fig. 3.1B) (Yuzyuk et al., 2009). In wild-type embryos we observed that at 20°C by the 8E stage, chromatin was already in a primarily compact state in intestinal cells and stayed compacted throughout the rest of development (Fig. 3.1B). However, in wild-type embryos at 26°C at the 8E and 16E stages, we saw that there were significantly more intestinal nuclei that displayed open arrays, but that by comma stage and later the arrays were closed (Fig. 3.1B). This suggests that temperature causes a delay in developmental chromatin compaction even in a wild-type state.

In all four synMuv B mutants at 20°C at the 8E stage, we saw that there were significantly more intestinal nuclei with open arrays compared to wild-type embryos at 20°C (Fig. 3.1B). However, for all synMuv B mutants at 20°C by the 16E stage, there were very few intestinal cells with open arrays, and only in *lin-35* mutants was the number of cells with open arrays significantly higher than wild-type at 20°C (Fig. 3.1B). In mutants at 20°C a small number of intestinal cells did have open arrays into comma stage but it is not significantly more than was seen in wild-type (Fig. 3.1B). At 26°C, mutants show a more drastic delay in chromatin compaction displaying open arrays through all stages. In all four synMuv B mutants at 26°C at all stages we saw that there were significantly more intestinal nuclei with open arrays compared to wild-type embryos, with the exception of *lin-54* and *met-2* mutants at the L1 stage (Fig. 3.1B). Furthermore, we saw that within an individual mutant background at 26°C compared to 20°C, there were significantly more intestinal nuclei with open arrays at each stage of development, with the exception of *met-2* mutants at the L1 stage (Fig. 3.1B).

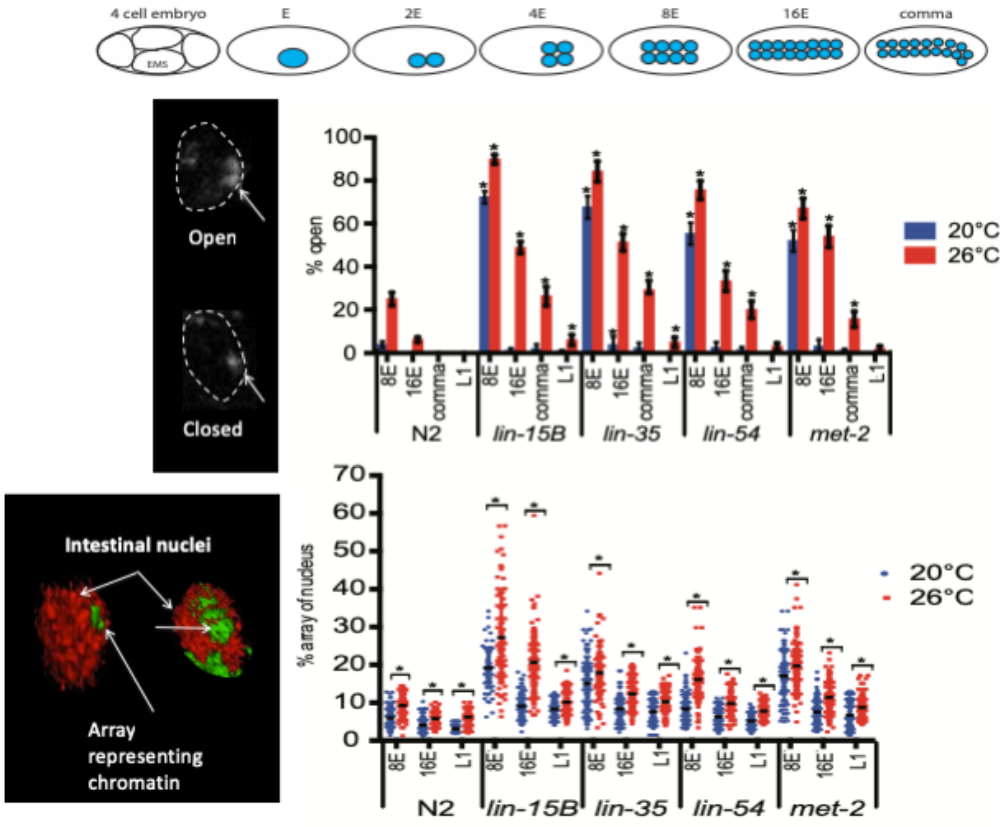

Figure 3.1: Loss of synMuv B proteins causes a delay in chromatin compaction in the intestinal lineage during development (A) A cartoon representing the number of intestinal cells and the approximate number of total cells in the stages scored throughout this study. (B) Large extrachromosomal arrays containing numerous *lacO* sites represents a pseudo chromosome that when bound by LacI::GFP is used to visualize chromatin morphology. Intestinal nuclei were scored as open or closed based on array morphology (Yuzyuk et al*.,* 2009). L4 hermaphrodites were placed at 20°C or 26°C and mixed stage F1 embryos were collected and percentage of intestinal nuclei with open arrays at the 8E, 16E, comma, and L1 stage at 20°C and 26°C were scored. 2-way ANOVA was used to determine significance: Asterisks represent significant difference between the wild-type population at that stage and temperature ($p<0.01$). Error bars indicate standard error of the proportion. n>100 cells (C) 3-D volumetric chromatin compaction analysis was performed using the isosurface function in Metamorph. The volume of the nucleus and the array were measured and used to calculate the percentage of the nucleus that the array encompassed. The percentage of the nucleus contained by the array was plotted at 8E, 16E, and comma at 20°C and 26°C. Each dot represents a single intestinal cell and the line represents the median. Asterisk represents a significant difference between 20°C and 26°C (2-way Anova $p<0.01$).

Therefore, synMuv B mutant intestinal cells showed a developmental delay in compaction at 26°C compared to 20°C, similar to wild-type intestinal cells. Additionally, mutants showed a higher percentage of cells with open arrays at each stage; and therefore, in synMuv B mutants at high temperature, compaction is delayed into developmental stages where zygotic gene expression has started.

To confirm our scoring method, we performed 3-D volumetric analysis of the intestinal nucleus measuring the volume of an array compared to the volume of the nucleus. Open arrays take up more volumetric space; and therefore, have a larger array to nucleus volumetric percentage. 3-D volumetric data showed similar trends to those described above; cells had a larger nuclear percentage of arrays in mutants vs. wild-type, and at 26°C vs. 20°C (Fig. 3.1C). In contrast to the open/closed scoring in wild-type at 26°C compared to 20°C, even at stages where we scored most or all of the arrays as closed, we saw a small but significant increase in the nuclear percentage of the array (Fig. 3.1C). This indicated that there is some variation in the nuclear volume that arrays take up even when they appear compacted. In mutants, there was a striking increase in not only the nuclear percentage that the arrays took up when compared to wild-type, but also an increase in the variance of the array volume within the same genotype, especially at 26°C. In general, as development proceeded, the volume of the extrachromosomal array within the nucleus and the variance of array volume within a genotype decreased (Fig. 3.1C). Overall, the 3-D volumetric analysis supports our open/closed analysis as we see a temperature

sensitive chromatin compaction phenotype throughout development, predominantly in synMuv B mutants.

Individual embryos contain both nuclei with open chromatin and closed chromatin

While scoring array compaction we observed that population wide, the number of intestinal cells with open arrays decreases gradually through development in mutants. For example, in pooled *lin-15B* mutant intestinal cells at 26°C at the 16E stage about 50% of the cells contain open arrays (Fig. 3.1B). We wanted to determine if, at a particular stage of development, the partial compaction seen in the population of intestinal cells was due primarily to variance in compaction of individual intestinal cells within an embryo (Fig. 3.2A: Model 1) or variance in compaction of intestinal cells between different embryos (Fig. 3.2B: Model 2). If model 1 is supported, we would expect to see a population of embryos with a mosaic of open and closed cells within each embryo. If model 2 is supported, we would expect to see a population of embryos with a binary distribution of embryos containing all intestinal cells open or all intestinal cells closed. We found that in a population of embryos, each embryo contained a mix of intestinal cells with both open and closed arrays that was close to the population mean (Fig. 3.2C). For example, in *lin-15B* mutants at 26°C at 8E, when about 90% of intestinal cells were scored as open (Fig 3.1B), embryos have a range of 6/8 to

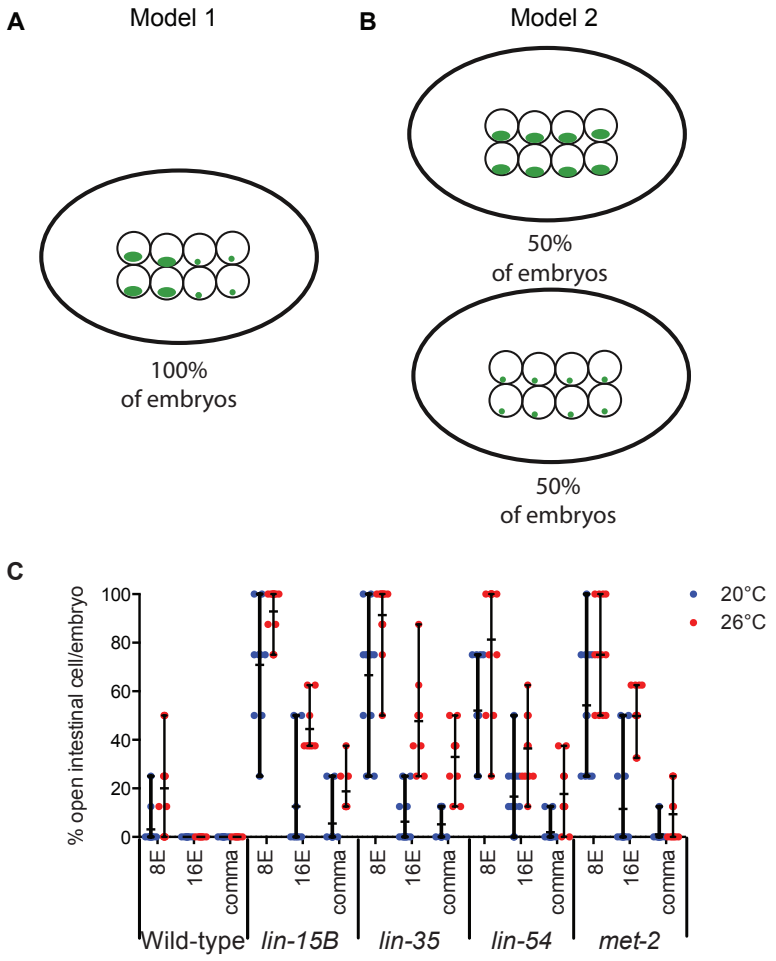

Figure 3.2: The number of intestinal cells with open chromatin varies within a single embryo. Models that explain (A) a variance in compaction of intestinal cells within an embryo or (B) a variance in compaction of intestinal cells between different embryos. (C) The percentage of intestinal cells with an array in an open configuration per embryo was determined for 8E, 16E and comma stage embryos at 20°C and 26°C. Each dot represents an embryo and the line represents the mean percentage of open cells per embryo.

8/8 cells with open arrays. While at 16E, when about 50% of intestinal cells were scored as open (Fig 3.1B), *lin-15B* mutant embryos have between 6/16 and 10/16 cells with open arrays. By comma stage, *lin-15B* mutants show decreased numbers of open cells with a range of 2/20 and 6/20 cells scored with open arrays (Fig 3.2C). We did not find any genotype or temperature with a bimodal distribution where the embryos within a population fell into a mix of 100% closed and 100% open arrays. These data support model 1. As development proceeds and chromatin compaction is achieved, the number of open cells within an embryo decreases. The pattern of compaction within an embryo is similar between mutant genotypes at the same stage and temperature (Fig 3.2C). Mutants do display differences in mean number of open cells, but all embryos have nuclei with both open and closed arrays. This suggests that chromatin compaction throughout development is regulated on a cell-by-cell basis and synMuv B proteins are necessary in establishing closed chromatin.

synMuv B proteins regulate chromatin compaction spatially in an anterior-to-posterior direction

While scoring the number of open cells within an embryo, we observed an anterior-to-posterior pattern of chromatin compaction. The intestinal cell lineage descends from a single cell, E. The first cell division is an anterior-posterior division in which E becomes 2E. These two intestinal cells divide in a left-right division (2E to 4E) to establish the bilateral symmetry of the intestine. The resulting cells are designated as sister cells with a set consisting of a left and

Figure 3

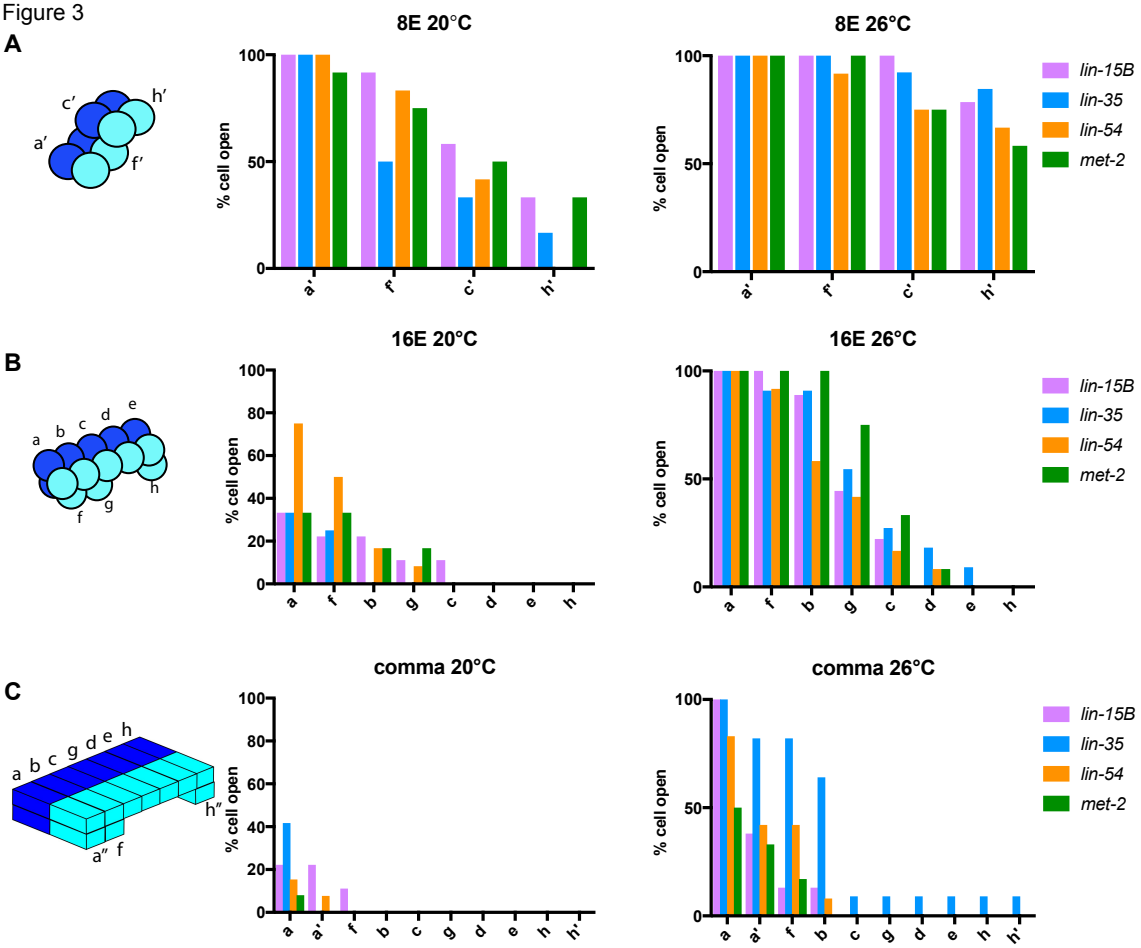

Figure 3.3: In synMuv B mutants anterior intestinal cells are more delayed in compaction than posterior intestinal cells. The position of open cells within a single embryo was monitored throughout development at (A) 8E, (B) 16E, and (C) 20E at both 20°C and 26°C. The anterior-to-posterior location of a cell was noted and that cell was recorded as either open or closed. The percent open of each pair of sister cells was plotted to in an anterior-to-posterior directionality.

right pair. The third division when 4E gives rise to 8E is an anterior-posterior division although the cells are slightly displaced in the dorsal-ventral plane (Fig 3.3A, sister cells labeled as a', c', e', f'). The 4th division is also an anterior-posterior division that gives rise to 16E with some cells more dorsal than others (Fig 3B, sister cells labeled as a, b, c, d, e, f, g, h). The sixteen cells subsequently polarize and change shape before there is a final round of cell division in which only the most anterior pair of sister cells (a) divide in a dorsal-ventral direction, and the most posterior pair of sister cells (h) divide in an anterior-posterior direction leading to the final arrangement of cells within the nucleus (Fig 3.3C, sister cells labeled a, a'', b, c, d, e, f, g, h, h''). We found that there was a clear pattern in the anterior-posterior location of cells with open arrays in an embryo. At 8E when mutants have varying numbers of cells open at 20°C and 26°C, we found that the anterior pair of sister cells maintained open arrays more often in all four genotypes, while the most posterior cells most often had closed arrays (Fig 3.3). For example, at 20°C, when *lin-15B* mutants have a range of 2/8 to 8/8 cells open, the a' sister cells were open 100% of the time. The following pair of sister cells, f', had the next highest percentage of open cells (90%). The more posterior sister cells, c', have a decreasing number of open cells (60%), and the two most posterior sister cells, h', have the lowest percentage of open cells (30%) (Fig. 3.3A). This pattern of open arrays being more often in the anterior and less often in the posterior was observed in all four mutants, at 8E, 16E, and comma stages, at both 20°C and 26°C (Fig 3.3). Overall if an embryo had any intestinal cells with an open array, they were

always the cells found at the anterior section of the intestine (Fig 3.3). This suggests that as development proceeds and chromatin compaction is achieved, cells close in a posterior to anterior direction. This pattern seems to be independent of proliferative state, as there is a final cell division at both anterior and posterior positions to give rise to 20E (Figure 3.3C a and a'', h and h'')

synMuv B proteins regulate compaction of endogenous germline gene loci

To determine if chromatin compaction is also altered at endogenous loci in synMuv B mutants, we performed fluorescent *in-situ* hybridization (FISH). Pairs of red and green probes ~100kb apart were created to flank endogenous loci to determine the chromosomal level of compaction at those loci (Yuzyuk et al*.,* 2009). All loci assessed were located in central regions of autosomes that are generally euchromatic to control for autosomal location. For controls we used probes that flank the *pha-4* gene that should be open and expressed in the intestine, and probes that flank the *myo-3* gene that should be closed and not expressed in the intestine (Ardizzi and Epstein, 1987; Horner et al., 1998). We investigated three synMuv B regulated loci *ekl-1*, *coh-3*, and C05C10.7. All three synMuv B target genes are germline genes that are ectopically upregulated in synMuv B mutants, and whose expression is downregulated upon rescue of high temperature larval arrest (Petrella et al*.,* 2011). Intestinal cells were imaged in 3-D stacks at the 8E, 16E, and comma stage, and we calculated the level of chromatin compaction of the loci based on the 3-D distance between the centroid of each probe (Yuzyuk et al*.,* 2009).

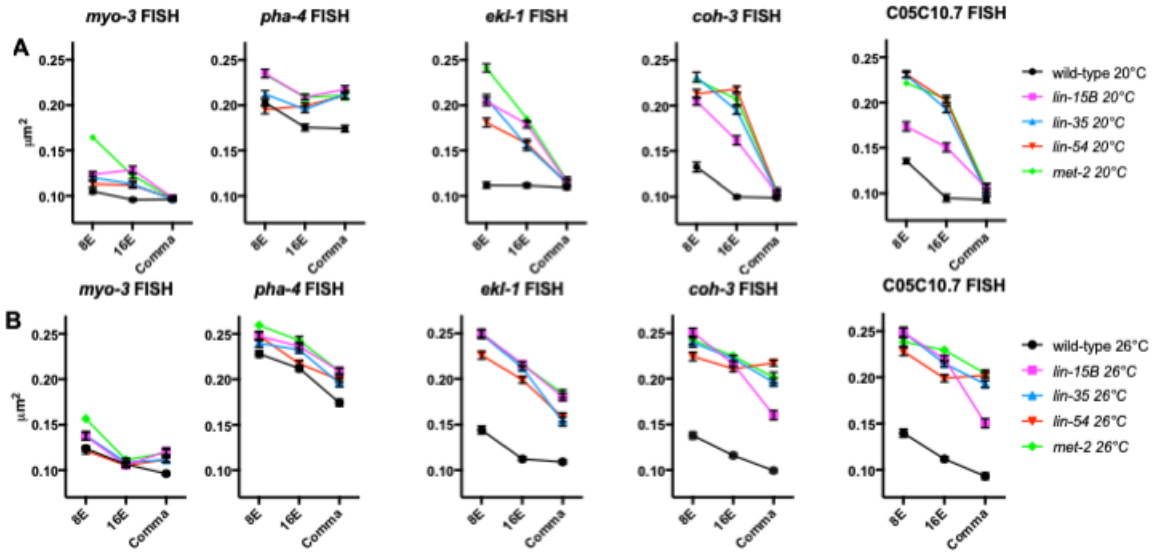

Figure 3.4 Fluorescent *in-situ* hybridization of synMuv B regulated loci reveals more open chromatin in synMuv B mutants. 8E, 16E, and comma stage wild-type, *lin-15B, lin-35, lin-54,* and *met-2* embryos at (A) 20°C and (B) 26°C were labeled with 568-5-dUTP (red) and Alexa Fluor 488 (green) probes 50kb upstream and 50kb downstream of *myo-3, pha-4, ekl-1, coh-3* and C05C10.7. Plots represent the distribution of 3-D-distances between centroids (μm^2). See also Figure 3.5

To understand how compaction of endogenous loci changes with respect to expression status in the intestine and temperature, we looked across developmental time and at different temperatures in mutants and wild-type. We found that, as predicted, the non-expressed *myo-3* control locus was more compact than the expressed *pha-4* control locus in all genotypes at both temperatures in all embryonic stages (Fig. 3.4A and B, Fig. 3.5). The *myo-3* locus demonstrated compaction reminiscent of compaction of extra-chromosomal arrays, which are also not expressed (Fig. 3.4A and B, Fig. 3.5). In wild-type at 20°C *myo-3* is completely compacted by the 8E stage (Fig. 3.4A and B, Fig. 3.5). However, in wild-type at 26°C, there was a significant difference in the level of compaction of the *myo-3* locus between the 8E and 16E stages, representing a delay in compaction timing compared to 20°C (Fig. 3.4A and B, Fig. 3.5A). synMuv B mutants resembled wild-type embryos at the *myo-3* locus at all stages and temperatures. Together, although there may be slight delays in chromatin compaction of a non-expressed locus at elevated temperatures, cellular mechanisms can overcome these delays by late embryogenesis.

We next analyzed the three synMuv B target genes (*ekl-1, coh-3, C05C10.7),* which have higher expression in mutants than wild-type and higher expression at 26°C within mutants. In wild-type, all three of these loci showed similar patterns to the *myo-3* locus with all three loci reaching maximal compaction between the 8E or 16E stage at both temperatures (Fig. 3.4A and B, Fig. 3.5A). Thus, in wild-type at both 20°C and 26°C the synMuv B target loci showed a pattern of compaction like a non-expressed locus. However, in

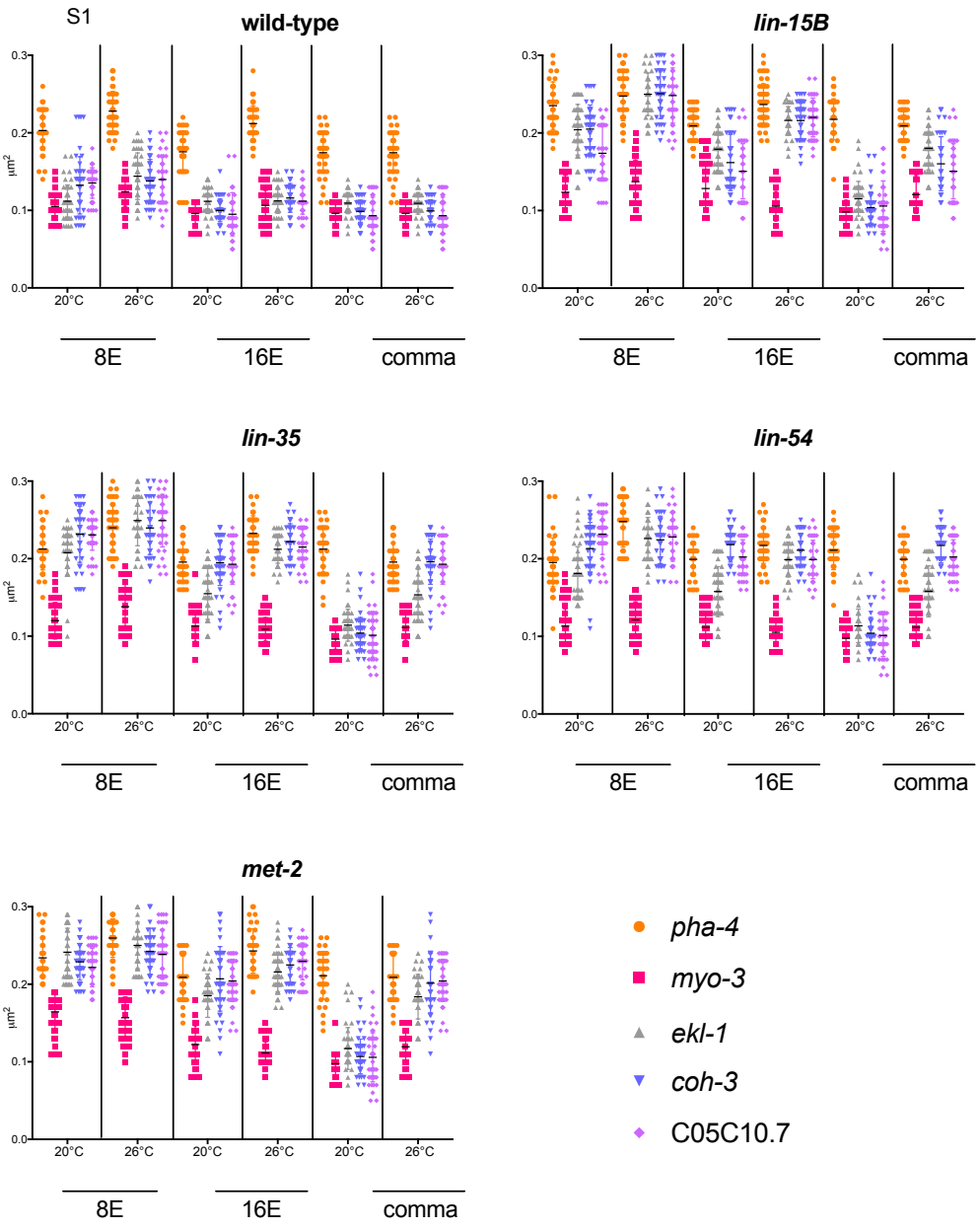

Figure 3.5: Fluorescent *in-situ* hybridization of synMuv B regulated loci reveals more open chromatin in synMuv B mutants at higher temperatures. Wild-type (A), *lin-15B* (B), *lin-35* (D), *lin-54* (D), and *met-2* (E) embryos at 20°C and 26°C at 8E, 16E and comma stage were labeled with 568-5-dUTP (red) and Alexa Fluor 488 (green) probes 50kb upstream and 50kb downstream of *myo-3, pha-4, ekl-1, coh-3* and C05C10.7. Each dot represents the 3-D-distances between centroids (µm^2) of one intestinal cell.

synMuv B mutants the three target genes showed two different patterns of developmental compaction depending on the temperature being assayed. In synMuv B mutants at 20°C at the 8E stage the *ekl-1, coh-3*, and C05C10.7 loci were all less compacted than the same locus in wild-type (Fig. 3.4A). However, in synMuv B mutants at 20°C by comma stage all three loci were equally compacted compared to the same locus in wild-type (Fig. 3.4A). Thus, at 20°C the three synMuv B regulated loci showed a delay in compaction but by late embryogenesis they were as compact as in wild-type. In synMuv B mutants at 26°C the three synMuv B target loci were more open than the same locus in wild-type at all developmental stages (Fig. 3.4B). In *lin-35, lin-54,* and *met-2* mutants, both the *coh-3* and C05C10.7 were as open as the *pha-4* locus in the same genotype (Fig. 3.4B, Fig 3.5C, D, E). Thus, synMuv B target loci demonstrate a level of chromatin compaction similar to highly expressed genes late into development, but only at 26°C. The open chromatin around synMuv B targets into later developmental time periods at high temperature may leave these genes vulnerable to the ectopic mis-expression that underlies the synMuv B mutant HTA phenotype. This suggests that synMuv B proteins establish a closed chromatin environment at genes they regulate in order to repress their fate.

Discussion

Chromatin compaction during development is necessary to achieve proper gene expression and differentiation. Previous studies have identified that H3K9 methylation is essential for chromatin compaction and organization (Ahringer and

Gasser, 2017; Towbin et al., 2012). Although methylation of H3K9 is necessary, the pathways and proteins needed to establish tissue specific chromatin compaction patterns remain unclear. In this study we show that synMuv B proteins are necessary for timely chromatin compaction during development. Loss of any of these proteins: the DREAM complex DNA binding protein LIN-54, the pocket protein that helps maintain the DREAM complex LIN-35, LIN-15B, or the H3K9me1/2 methyltransferase, MET-2, causes impaired chromatin compaction and ectopic germline gene expression in early development. This suggests that binding of LIN-15B, the DREAM complex, and methylation of H3K9 are each necessary for proper gene repression at germline gene loci in somatic tissue. Loss of any one of these proteins causes ectopic expression of germline genes and improper organismal development during temperature stress.

Chromatin is found in a generally unorganized and open state early in development (Politz et al*.,* 2013; Yuzyuk et al., 2009). As development proceeds and differentiation occurs, chromatin becomes compacted and organized in a tissue specific manner (Mutlu et al., 2018; Politz et al., 2013; Yuzyuk et al., 2009). Organization of chromatin within the nucleus precedes upregulation of zygotic gene expression and is important for correct cell fate decisions (Gaertner et al., 2012; Politz et al., 2013; Yuzyuk et al., 2009). Poised Pol II accumulates at promoters in a stage specific, but not tissue specific manner (Gaertner et al., 2012). This means that when gene expression is upregulated at the maternal-to-zygotic switch, it occurs in a tissue-independent manner (Gaertner et al., 2012). Establishment of tissue specific repression, including establishment of repressive

chromatin, must occur before global gene expression is upregulated in order to achieve proper cell fate (Gaertner et al*.,* 2012; Poliltz et al., 2013; Yuzyuk et al., 2009). We hypothesize that repression by synMuv B may be a tissue specific mechanism to establish repressive chromatin environments before the maternal-to-zygotic switch. Loss of these proteins causes global changes in chromatin compaction into the developmental time of the maternal-to-zygotic switch, especially at high temperature, leaving their target loci vulnerable to expression when zygotic gene expression is upregulated.

Other studies have also shown that mutants in chromatin regulators, including *met-2* mutants and Polycomb Repressive Complex (PRC-2) mutants that catalyze H3K27 methylation, have delays in developmental chromatin compaction (Mutlu et al., 2018, Yuzyuk et al., 2009). Like these studies, we observe compaction of chromatin at later stages in synMuv B mutants. This suggests that there are other, possibly redundant, direct or indirect mechanisms that can compensate for loss of these proteins and ensure that chromatin is compacted. Compensation by these mechanisms “buffers” the system enough to ensure proper development at normal conditions. For example, embryos lacking all H3K9 methylation compact their chromatin later in development but develop normally at 20°C (Mutlu et al., 2018, Towbin et al., 2011). Visible phenotypes in these mutants are absent until the organism is stressed. Prior to this study, chromatin compaction at high temperature had not been observed in *C. elegans.* Here, we show that temperature stress prolongs chromatin compaction into later developmental stages. It is possible that chromatin compaction is temperature

sensitive and the organism is not able to compensate for chromatin compaction in a timely manner. Delayed chromatin compaction into developmental time important for cell fate decisions may underlie the increased ectopic expression we observe in synMuv B mutants at 26°C compared to 20°C.

Methylation of H3K9 is imperative to achieve chromatin compaction at the right time and place during development. Loss of MET-2 causes loss of ~80% of H3K9me1/2 across the genome (Towbin et al., 2012; Zeller et al., 2016). Previous studies have shown that *met-2* mutants ectopically express germline genes (Andersen and Horvitz*,* 2007, Towbin et al*.,* 2012). In this study we show that *met-2* mutants phenocopy *lin-15B, lin-54,* and *lin-35* mutants in all chromatin compaction assays. Interestingly, the DREAM complex binds only ~1400 and LIN-15B binds to ~2100 locations throughout the genome, primarily on autosomes (Rechtsteiner et al., 2019). Loss of LIN-15B or DREAM binding, at relatively few places throughout the genome, causes the same phenotypes as losing ~80% of H3K9me1/2. One explanation for this similarity is that LIN-15B and the DREAM complex may be tissue specific regulators of H3K9 methylation at synMuv B regulated loci and this modification may be important for repression of germline genes in somatic tissue. Another explanation is loss of individual mechanisms that contribute to closed chromatin, broad H3K9me2 or DREAM complex/LIN-15B regulation at specific loci, each lead to an increased temperature sensitivity of compact chromatin formation globally. Therefore, the similarity in phenotype is secondary consequence to general changes in chromatin compaction at many loci across the genome. Further analysis of the

interaction of the DREAM complex/LIN-15B with MET-2 and H3K9me2 are needed to distinguish these possibilities.

Ectopic germline gene expression is increased in synMuv B mutants at 26°C compared to 20°C (Petrella et al*.,* 2011). Before this study, the underlying mechanisms for this temperature sensitive phenotype have remained unclear. Here, we show that chromatin compaction is temperature sensitive, even in wild-type backgrounds, and may contribute to this phenotype. Chromatin has been shown to be respondent to changes in temperatures. Previous studies have reported that *Arabidopsis thaliana* can change chromatin dynamics to modify gene expression in response to changes in temperature (Zografos and Sung, 2012). In addition to being temperature respondent, chromatin is also temperature sensitive. Early studies in *Drosophila* revealed that high temperature causes incomplete heterochromatin formation (Hartmann-Goldstein, 1967). This is the first study to investigate the role of temperature stress on chromatin compaction in a developmental context. Here we reveal that chromatin compaction in early development is especially vulnerable to the temperature sensitive nature of chromatin. Chromatin compaction is developmentally delayed when worms experience high temperatures for small amounts of time. Causing further stress to this system by loss of synMuv B proteins results in more drastic delays in chromatin compaction. Loss of these proteins not only cause changes in chromatin compaction at specific loci that they regulate, but also globally. Thus, small changes in local chromatin domains throughout the genome, plus

temperature stress, can indirectly change the chromatin landscape at a global level within the nucleus.

We found that delayed chromatin compaction in synMuv B mutants demonstrated an anterior-to-posterior pattern within intestinal cells. The anterior cells of the intestine were the last to adopt closed chromatin. Because there is both a final anterior and posterior division to form the *C. elegans* intestine, we do not think that the open chromatin is correlated to the number of cell divisions the sister cells have yet to complete. The *C. elegans* intestine is patterned anteriorly to posteriorly by Wnt signaling proteins (Fukushige et al., 1996; Lin et al., 1998; Schroeder and McGhee, 1998). During intestinal cell divisions, Wnt signaling associated transcription factors localize to the most anterior cells of the intestine at each division (Schroeder and McGhee, 1998). It is possible that anteriorly localized transcriptional factors are able to ectopically bind and express uncompacted germline genes in the anterior intestine leading to high temperature arrest.

In this study, we have determined that synMuv B proteins are needed for timely chromatin compaction throughout development at high temperature. Loss of chromatin compaction during critical developmental time periods in which germline genes are globally upregulated during the maternal-to-zygotic switch may underlie the developmental arrest phenotype of synMuv B mutants. It is important to understand how germline genes are repressed in somatic tissue as many somatic cancers that are highly proliferative and metastatic show upregulation of germline genes (Gure et al., 2005; Maine et al., 2016; Xu et al.,

2014). Like *C. elegans*, mammals also repress germline gene expression during embryogenesis in somatic cells and recent work has indicated that this repression is dependent on H3K9me2 (Dixon et al., 2012; Ebata et al., 2017). Given that the DREAM complex is completely conserved between worms and mammals (Litovchick et al., 2007), its role in establishment of developmental repressive chromatin at germline genes may also be conserved. Further studies of synMuv B regulation will provide evidence of how organisms establish and maintain chromatin structure and gene expression states to ensure vitality.

CHAPTER 4: THE CRITICAL DEVELOPMENTAL TIME PERIOD FOR HIGH TEMPERATURE LARVAL ARREST IN SYNMUV B MUTANTS IS MID-TO-LATE EMBRYOGENESIS

Background

The *C. elegans* embryo is a powerful developmental model, as the timing and orientation of every cell division, migration, and apoptotic event has been documented, and the exact lineal and physical relationship of each cell to another is known. Developmental studies of the *C. elegans* embryo has been largely studied at 20°C (Sulston et al., 1983). The E blastomere gives rise to the entire intestinal lineage and arises at approximately 35 minutes after first cleavage (Leung et al., 1999). The intestinal lineage is represented in Figure 1.7 with its relationship to developmental time and embryo appearance at 20°C. The first division of the E blastomere that creates 2E occurs at approximately 100-120 minutes after first cleavage. 4E occurs at 120-180 minutes and 8E occurs between 180-240 minutes. 16E occurs between 240-480 minutes until a final division gives rise to 20E (Sulston et al., 1983). Time after first cleavage and/or the number of intestinal cells are common measurement of developmental time in the *C. elegans* embryo. Although development has not been largely studied at elevated temperatures, it is well known that increased temperature decreases cell division time and thus developmental time in *C. elegans* (Begasse et al., 2015; Wood et al., 1980).

The rapid cell divisions that occur during early *C. elegans* development take place in the absence of zygotic transcription. Maternally loaded proteins and

mRNAs are sufficient to direct development prior to gastrulation. Zygotic gene expression is largely upregulated in the intestinal lineage between the 8E-16E stage (McGhee et al., 2007). Zygotic gene expression at this developmental time, gives identity to the intestine as these transcripts are largely intestinal specific and continue to be expressed in the intestine through L1 (McGhee et al., 2007). It is thought that tissue specific mechanisms for gene regulation must be in place at the onset of upregulation of zygotic gene expression (Levin et al., 2012; Robertson et al., 2015; Spencer et al., 2011). Establishment of tissue specific repression, including establishment of repressive chromatin, must occur before zygotic gene expression is upregulated in order to achieve proper cell fate (Gaertner et al*.,* 2012; Poliltz et al., 2013; Yuzyuk et al., 2009). Work done in *Drosophila* found poised Pol II accumulates at promoters in a stage specific, but not tissue specific manner (Gaertner et al., 2012). This suggests that when gene expression is upregulated at the maternal-to-zygotic switch, it occurs in a tissue-independent manner (Gaertner et al., 2012). This calls for tissue specific modes of transcriptional repression before global activation of Pol II. Although proper timing of tissue specific repression mechanisms is important for proper development, many of the tissue specific regulators remain unknown.

Establishment of heterochromatin occurs early in the *C. elegans* embryo. Prior to the maternal to zygotic switch, nuclei viewed by transmission electron microscopy transition from homogeneous, light speckling in the nucleoplasm to nuclei with electron-dense puncta (Mutlu et al., 2018). Accumulation of these electron-dense domains continues to increase until developmental time when

zygotic gene expression is upregulated (Mutlu et al., 2018). These electron dense regions of heterochromatin begin to form at the 2E stage, increase in number until the 8E stage, and then increase in size from 16E stage on (Mutlu et al., 2018). These regions of heterochromatin are enriched for H3K9 methylation and their formation is dependent on the H3K9 di-methyltransferase, MET-2. Nuclear accumulation of MET-2 from the cytoplasm determines the onset of H3K9 di-methylation (Mutlu et al., 2018). Loss of *met-2* causes delays in the onset of heterochromatin formation (Mutlu et al., 2018). *met-2* mutants do not form electron-dense domains of heterochromatin until 16E, and these domains are less dense and smaller in size compared to domains in wild-type nuclei (Mutlu et al., 2018). Regulation and direction of H3K9me2 via MET-2 to specific regions of the genome during this developmental time remain unknown.

synMuv B proteins, including MET-2, are important for proper gene repression in somatic tissue. Loss of LIN-15B, members of the DREAM complex LIN-54 and LIN-35, or MET-2 cause ectopic germline gene expression in the somatic intestine (Andersen and Horvitz*,* 2007; Petrella et al*.,* 2011; Wang et al., 2005; Wu et al*.,* 2012). Ectopic expression of germline P-granule proteins in synMuv B mutants can be visualized by immunostaining against P-granule component protein PGL-1. Anti-PGL-1 staining reveals that synMuv B proteins have some ectopic somatic expression at 20°C, but this ectopic expression is exacerbated at 26°C (Petrella et al., 2011). Ectopic germline gene expression in the somatic intestine causes synMuv B mutants to arrest as larvae at 26°C. This HTA phenotype is at least in part due to loss of intestinal fate that results in

starvation (Petrella et al., 2011). A previous study identified the broad developmental window associated with high temperature larval arrest in *lin-15B* and *lin-35* mutants occurs during late embryogenesis to early L1 and is irreversible (Petrella et al., 2011).

In work described in this chapter, we determined the developmental time periods of the intestinal lineage and its divisions from 8E to L1 in wild-type and synMuv B mutants at both 20°C and 26°C. We showed that synMuv B mutants have a slower development than wild-type at both 20°C and 26°C. We also determined the specific developmental time window important for high temperature larval arrest in synMuv B mutants. We determined that mid-to-late embryogenesis is the critical period for high temperature arrest and that it is irreversible. We found that elevated ectopic PGL-1 staining persists even upon downshift of embryos from 26°C to 20°C after the critical time developmental time period for arrest. This suggests that high temperature exposure during mid-to-late embryogenesis in synMuv B mutants causes upregulation of ectopic germline gene expression programs in somatic tissue that is irreversible and leads to developmental defects.

Results

synMuv B mutants have delayed development compared to wild-type embryos

synMuv B mutants have developmental delays in chromatin compaction, especially at high temperature. To determine if synMuv B mutants have delays in chromatin compaction due to changes in the overall rate of embryonic

development, we observed the time to each intestinal division at 20°C and 26°C for wild-type, *lin-15B,* and *lin-54* mutants. Previous studies have shown that developmental speed increases at elevated temperatures. We looked at cell-division time in conjunction with absolute time during development to determine if increased developmental speeds could explain the delay in chromatin compaction we see at high temperature. Absolute time starts at fertilization and is constant throughout development. Many biological processes take a certain amount of absolute time to occur throughout development. Contrastingly, many biological processes that occur in development are correlated to the number of cell divisions. Although cell division and absolute timers are often in sync, cell division timers are not constant throughout development. Developmental speed increases at high temperature and thus cell-division timers would occur earlier in absolute time at 26°C compared to 20°C.

To perform these timing experiments, 2 cell embryos expressing a fluorescent intestinal cell marker were dissected from gravid adults, plated at 20°C or 26°C, and observed throughout development. The time in minutes were recorded for each individual embryo as they reached 8E, 16E, comma, pretzel, and L1 stages. Although it has been shown that developmental speed increases at elevated temperatures, the developmental timing of the intestinal lineage has not been described at 26°C (Begasse et al., 2015, Wood et al., 1980). Like previously published data (citation), we found that the time to 8E in wild-type embryos was on average 3.9 hours at 20°C and 3.09 hours at 26°C (Figure 4.1). The decreased developmental time in wild-type embryos was observed at all

stages, as embryos plated at 26°C reach each division approximately an hour before embryos plated at 20°C. On average, wild-type embryos reached the 16E stage at 5.8 hours at 20°C and 5 hours at 26°C (Figure 3.1). They reached comma stage, determined by both number of intestinal cells and the shape of the embryo into a comma, at 8 hours at 20°C and 7 hours at 26°C. Finally, they reached pretzel stage at 9.8 hours at 20°C and 8.9 hours at 26°C before hatching into L1 larvae at 11.5 hours at 20°C and 10.7 hours at 26°C (Figure 3.1). Because we saw an increased speed of development at 26°C, it is possible that faster cell-divisions at high temperature occur at early absolute times in development, and thus chromatin compaction has not had enough absolute time to be completed.

If loss of synchrony between absolute time and cell division time explains the delayed chromatin compaction phenotype in synMuv B mutants, we would expect development to be even faster in these mutants as they have exacerbated delays in chromatin compaction compared to wild-type. However, instead synMuv B mutants were slow to each intestinal division when compared to wild-type embryos (figure 4.1). On average, *lin-15B* mutants reach 8E at 4.5 hours at 20°C and 3.6 hours at 26°C, 35 minutes behind wild-type at 20°C and 30 minutes behind wild-type at 26°C (Figure 4.1, Table 4.1). The trend is similar for *lin-54* mutants at each stage and temperature (Figure 4.1, Table 4.1). At 16E, *lin-15B* mutants are delayed 24 minutes at 20°C and 45 minutes at 26°C as they reached this stage at 6.2 hours at 20°C and 5.7 hours at 26°C (Figure 4.1, Table

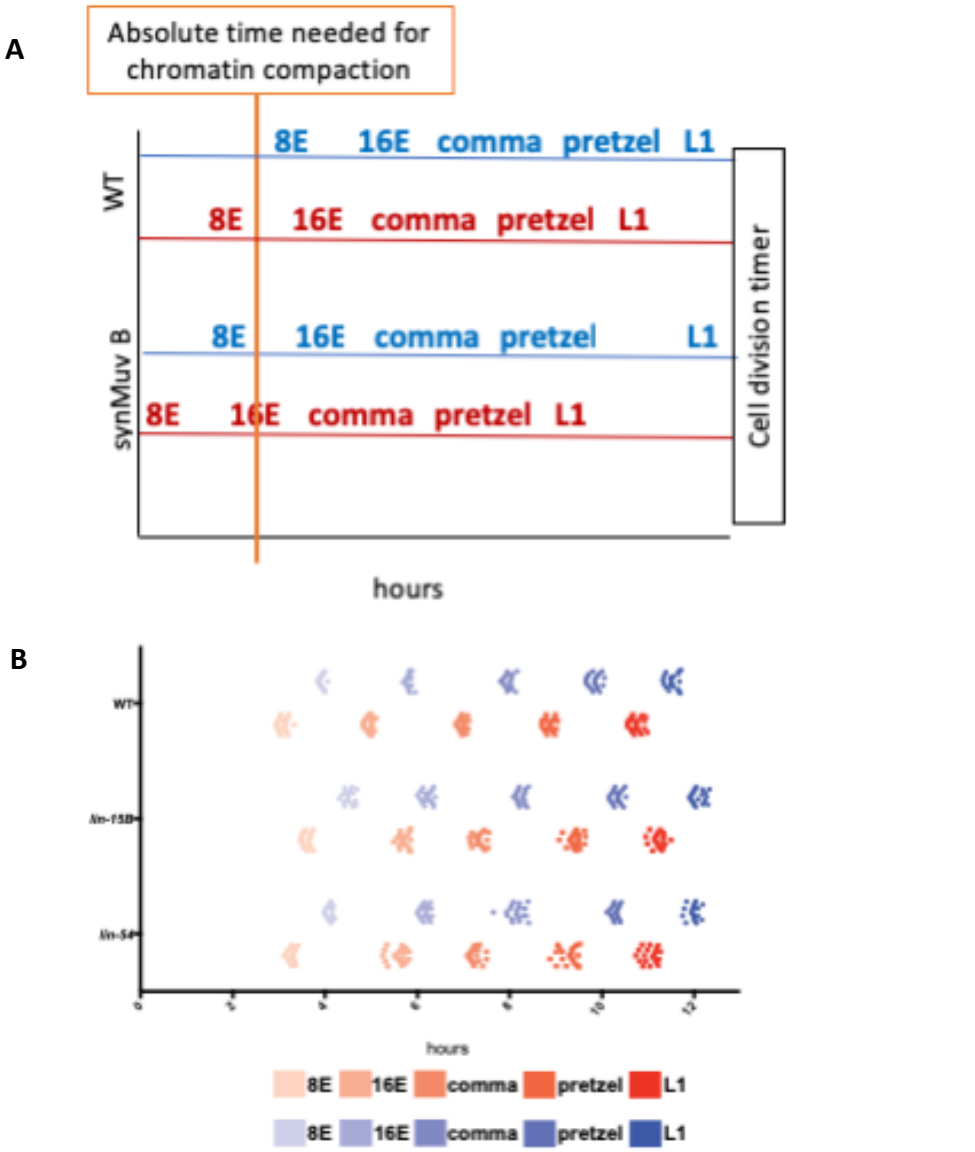

Figure 4.1: synMuv B mutants have delayed developmental timing compared to wild-type embryos A.) a model to explain the delay in chromatin compaction with regards to developmental time. B.)wild-type, *lin-15B,* and *lin-54* L4 P0 hermaphrodites were placed at 20°C or 26°C overnight. The next day, F1 two cell embryos were dissected, plated, and returned to the same temperature. The time to each intestinal stage for 8E, 16, comma, pretzel, and L1 was observed at recorded for each temperature. Each point represents an individual embryo (n=20 embryos/stage and strain and temperature)

4.1). *lin-15B* mutants reached comma stage at 8.2 hours at 20°C and 7.3 hours at 26°C. Finally, pretzel stage was reached at 10.3 hours in *lin-15B* mutants at 20°C and 9.4 hours at 26°C. *lin-15B* mutants hatch into L1 larvae at 12 hours at 20°C and 11.2 hours at 26°C, about 34 minutes delayed at 20°C and 29 minutes delayed at 26°C (figure 4.1). Although synMuv B mutants showed a delay in developmental time, this delay does not increase throughout intestinal development, as they do not spend significantly more time at each intestinal stage. The developmental delay observed by synMuv B mutants stays relatively constant throughout the intestinal lineage. Thus, loss of chromatin compaction in synMuv B mutants does not seem to be explained by a timer mechanism.

16E through comma stage is the critical developmental time-period for larval high temperature arrest in synMuv B mutants

synMuv B mutants arrest at the L1 larval stage, which is at least in part due to ectopic expression of germline genes (Petrella et al*.,* 2011). To determine if the developmental time-period important for the HTA phenotype is consistent with embryonic stages in which we see prolonged open chromatin, we performed temperature shift experiments on *lin-15B, lin-35, lin-54,* and *met-2* mutants. Previous studies determined that the temperature-sensitive period for HTA is in a broad developmental range during embryogenesis and early larval development (Petrella et al*.,* 2011). Since we are seeing distinct differences in chromatin compaction at different stages of embryonic development, we set out to determine a more precise time-period during embryogenesis crucial for HTA.

Table 4.1 Minutes of developmental time at each intestinal stage

	wild-type		***lin-15B***		***lin-54***	
	20°C	**26°C**	**20°C**	**26°C**	**20°C**	**26°C**
2 cell - 8E	236	185	271	215	246	197
8E - 16E	113	112	102	127	126	137
16E - comma	130	121	122	98	119	100
comma - pretzel	111	113	124	124	128	121
pretzel - L1	101	113	106	108	101	106

To perform HTA experiments, 4-cell embryos expressing a fluorescent intestinal cell marker were dissected from gravid adults and downshifted or upshifted at 4E, 8E, 16E, comma, pretzel and L1 developmental stages. Pretzel stage was included as an easily distinguishable later developmental stage to tease apart differences seen in worms shifted at comma and L1. Wild-type embryos were also dissected and shifted at all stages and never arrested (data not shown). All mutant embryos upshifted to 26°C from 20°C at 4E or 8E arrested at the L1 stage (Fig. 4.2). When upshifted at 16E all mutant genotypes except *lin-15B* showed a slightly fewer arrested animals than at earlier stages (Fig. 4.2). A smaller number of embryos upshifted at comma and pretzel stages arrested (Fig. 4.2). Finally, embryos upshifted at the larval L1 stage did not arrest (Fig. 4.2 A, B, C, D). Together, embryos shifted early in development arrested whereas embryos shifted in mid-to-late embryogenesis sometimes arrested, suggesting the likely critical time period for HTA to be after 16E. To complement this experiment, we also performed downshift experiments to define the developmental window crucial for HTA. Embryos downshifted from 26°C to 20°C at 4E did not arrest and about half of embryos downshifted at 8E arrested (Fig. 4.2). Strikingly, most embryos downshifted at 16E and comma arrested (Fig. 4.2). And downshifting at pretzel and L1 stages caused 100% arrest at the larval L1 stage (Fig. 4.2). These data combined suggest 16E through comma is likely to be the most crucial temperature sensitive time-period for HTA. However, upshifting after or downshifting before this time-period can still cause some animals to undergo HTA. Additionally, in chapter 3 we observed chromatin compaction

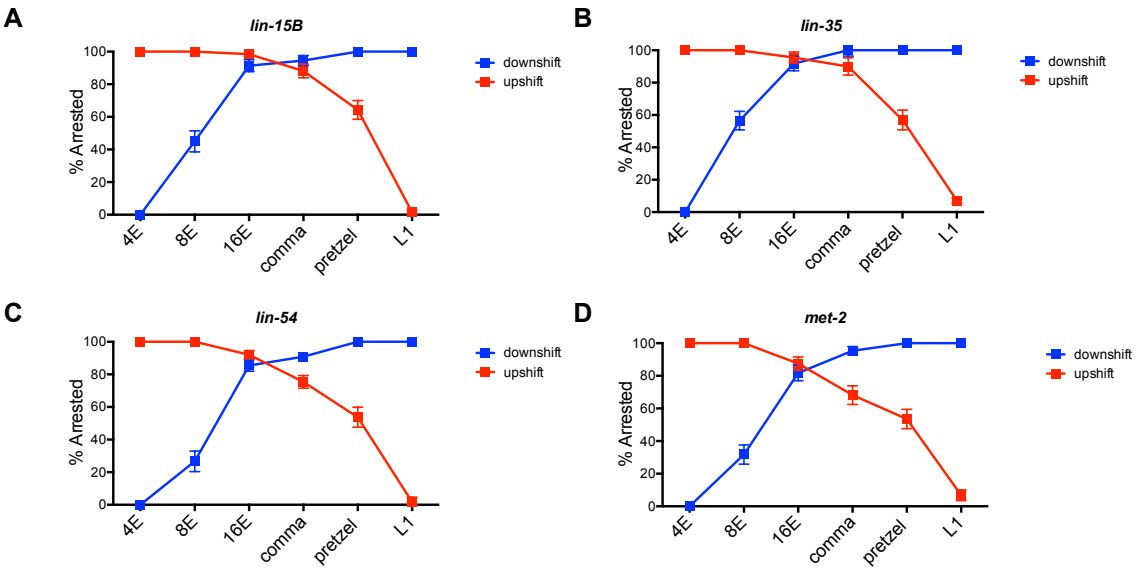

Figure 4.2: 16E through comma stage of embryogenesis is the temperature sensitive time period crucial for larval HTA. *lin-15B* (A)*, lin-35* (B), *lin-54* (C)*,* and *met-2* (D) L4 P0 hermaphrodites were placed at 20°C for upshift or 26°C for downshift experiments. F1 two cell embryos were dissected from P0s, and upshifted (red) or downshifted (blue) at 4E, 8E, 16E, comma, pretzel or L1 and scored for L1 larval arrest (n=60-78/point).

occurs on a cell-by-cell basis and that embryos have both “open” and “closed” cells. Together, these data suggest a buffering in the system that may represent stochastic chromatin compaction, varying amounts of ectopic gene expression, and a leaky arrest phenotype.

synMuv B mutant embryos downshifted to low temperature continue to ectopically express PGL-1

Downshift from 26°C to 20°C at pretzel and L1 stages resulted in 100% larval arrest (Fig. 4.2), suggesting that the ectopic gene expression programs leading to HTA are activated and irreversible. Although it was previously reported that HTA was irreversible upon downshifting, whether germline genes continued to be ectopically expressed after downshift was not assessed (Petrella et al*.,* 2011). We set out to determine if the germline gene *pgl-1* continues to be ectopically expressed after downshift by using strains with the endogenous *pgl-1* locus tagged with GFP (Andralojc et al., 2017). *pgl-1* is a synMuv B regulated germline gene that has been used to show ectopic germline gene expression in synMuv B mutants (Petrella et al., 2011, Wang et al., 2005, Wu et al., 2012). *lin-15B* and *lin-54* mutant embryos were downshifted at 8E, 16E, and comma stage and imaged at the L1 stage to determine the level of ectopic PGL-1 expression. We found that downshifted embryos resembled embryos that were not downshifted and kept at 26°C at all stages (Fig. 4.3, Fig 4.4). There was no difference in the maximum fluorescent intensity when comparing downshifted embryos to those that remained at 26°C (Fig. 4.3, Fig 4.4) There was a

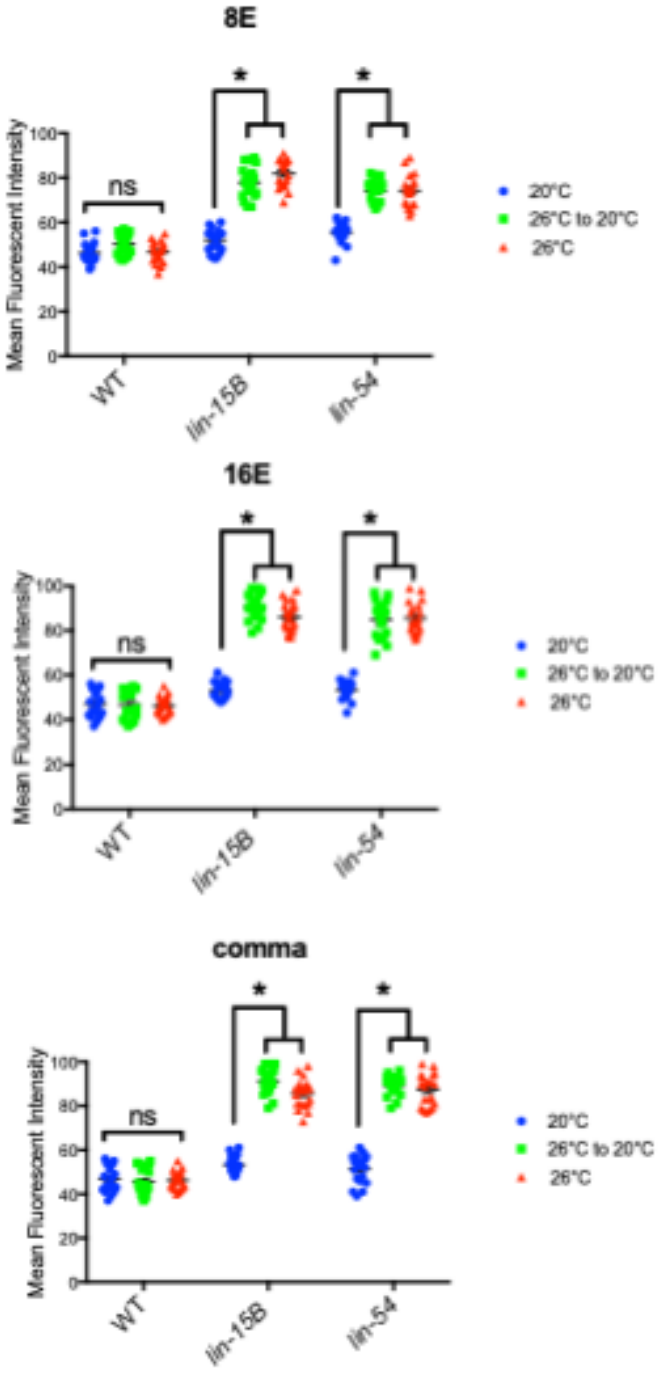

Figure 4.3 synMuv B mutant embryos downshifted to low temperature have increased PGL-1 staining at the L1 stage compared to wild-type. Mean Fluorescent Intensity of PGL-1 expression was determined for L1 wild-type, *lin-15B,* and *lin-54* embryos that were downshifted at 8E (A), 16E (B), comma (C) (n=20 L1/stage and strain and temperature). A 2-way ANOVA was used to determine significance between samples ($p<0.01$).

significant difference when comparing shifted embryos and those kept at 26°C to mutant embryos raised at 20°C (Fig. 4.3, Fig. 4.4). synMuv B mutants also show greater ectopic PGL-1 expression when compared to wild-type at the same stage and temperature, including 20°C (Fig. 4.3, Fig. 4.4). This suggests that the ectopic gene expression program that leads to HTA is activated in early embryogenesis and remains ectopically activated even upon relief of the stress.

Discussion

Proper transcription throughout embryogenesis is crucial for the proper development of an organism and this process is highly regulated by many mechanisms. Previous studies have identified synMuv B proteins as a group of transcriptional repressors important in the soma to germline fate decision during development (Andersen and Horvitz*,* 2007; Petrella et al*.,* 2011; Wang et al., 2005; Wu et al*.,* 2012). Although synMuv B proteins are necessary for proper development, especially at high temperature, the critical time of their repression had not previously been fully elucidated. In this chapter we show that synMuv B mutants have delayed developmental timing compared to wild-type embryos at both 20°C and 26°C. synMuv B mutants have a delay in developmental time to each intestinal stage compared to wild-type. This delay in developmental timing stays relatively constant throughout development. The time that synMuv B mutants remain at each intestinal stage is relatively similar or comparable to that seen in wild-type embryos. Interestingly, *lin-15B* and *lin-54* mutants spend a shorter amount of time in the 16E – comma stage than wild-type embryos.

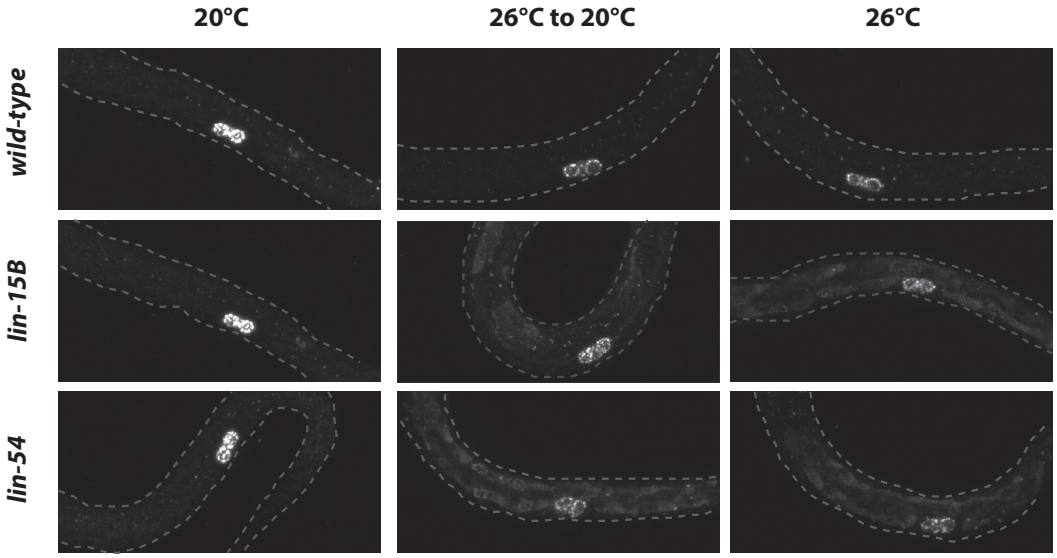

Figure 4.4 synMuv B mutant embryos downshifted to low temperature at 16E ectopically express PGL-1. Wild-type, *lin-15B* mutant, and *lin-54* mutant embryos carrying a PGL-1:GFP transgene were placed at 26°C or 20°C in 1XM9 drops. Embryos were either kept at 26°C, downshifted to 20°C at 16E, or maintained at 20°C, and allowed to arrest at the L1 stage. L1 worms were fixed and imaged in Z-stack using confocal microscopy. Panels represent maximum projection of PGL-1:GFP. Asterisks mark primordial germ cells.

We observed a delay in chromatin compaction in wild-type embryos at 26°C (Chapter 3). It is possible that chromatin compaction during development is the result of a “timer” mechanism. There are two types of developmental timers: absolute timers and cell-division timers. Absolute time starts at fertilization and is constant throughout development. Many biological process take a certain amount of absolute time to occur throughout development. It is possible that there is an amount of absolute time needed during development for MET-2 and H3K9me2 to accumulated in the nucleus. Contrastingly, many biological processes that occur in development are correlated to the number of cell divisions. Although cell division and absolute timers are often in sync, cell division timers are not constant throughout development. Developmental speed increases at high temperature and thus cell-division timers would occur earlier in absolute time at 26°C compared to 20°C. It is possible that the delay in chromatin compaction we observe in synMuv B mutants, especially at high temperature, is due to a loss of synchrony in these timers. If chromatin compaction requires a certain amount of absolute time, and at 26°C, when developmental speed increases, embryos would have open chromatin in to later cell division stages (figure 4.1A). Interestingly, our wild-type data can fit this model. Wild-type embryos at 26°C reach the 8E stage on average 51 minutes before wild-type embryos at 20°C. If chromatin compaction was on an absolute developmental timer, the embryos at 26°C would be further along in developmental cell divisions by the absolute time developmental chromatin compaction was achieved. This could explain why we

see significantly more open chromatin in wild-type embryos at 26°C compared to 20°C at the 8E stage.

Although the developmental timer hypothesis could explain the delay in chromatin compaction we see in wild-type embryos at 26°C, it does not seem to fit our synMuv B mutant data. Because synMuv B mutants have drastically delayed chromatin compaction into later developmental stages as counted by cell-divisions compared to wild-type, especially at high temperature, we would expect their cell division development to be faster than wild-type, especially at 26°C. However,, we see that synMuv B mutants, on average, reach 8E 30-35 minutes slower than wild-type embryos at both 20°C and 26°C. This suggests that the delay in chromatin compaction observed in synMuv B mutants is not due to a loss of synchrony in absolute time with cell-division time. Instead, we hypothesize that synMuv B proteins regulate timely chromatin compaction independent of an absolute timing mechanism, and that loss of these proteins causes delays in the formation heterochromatic domains during development.

We also determined that the embryonic stages in which we see prolonged open chromatin coincide with the developmental time-period important for the HTA phenotype displayed by synMuv B mutants. We found the developmental window for high temperature arrest is likely between 16E and comma stage, although shifting embryos directly before or after this window does cause some arrest. This developmental time coincides with the stages we see open chromatin in synMuv B mutants at 26°C but not 20°C. We hypothesize that the temperature sensitive arrest phenotype we observe in synMuv B mutants is at least due in

part to open chromatin during this critical developmental time at 26°C but not 20°C. The spectrum of cells with both open and closed chromatin at various stages of development could potentially explain why we see some arrest at both sides of the critical time period. This “leaky” arrest phenotype observed before 16E and after comma stage could be explained by the variation in chromatin compaction we observe in synMuv B mutants and may cause varying amounts of ectopic gene expression that leads to arrest.

Interestingly, this critical time period of HTA coincides with an upregulation of zygotic gene expression in the somatic intestine. Tissue specific forms of transcriptional regulation, including organization of chromatin, are established prior to upregulation of the zygotic genome (Gaertner et al., 2012; Politz et al., 2013; Yuzyuk et al., 2009). Poised Pol II accumulates at promoters in a stage specific, but not a tissue specific manner, and loss of tissue specific mechanisms to negatively regulate Pol II result in unwanted gene expression (Gaertner et al., 2012). We hypothesize that repression by synMuv B may be a tissue specific mechanism to establish repressive chromatin environments before the maternal-to-zygotic switch. Loss of these proteins causes global changes in chromatin compaction into the developmental time of the maternal-to-zygotic switch, especially at high temperature, leaving their target loci more open and with a greater chance to be bound and expressed when zygotic gene expression is upregulated. Here we show that once upregulated, somatic misexpression of germline genes is irreversible upon downshift. This suggests that ectopic gene expression programs turned on in synMuv B mutants are occurring in each cell

and mutants are unable to recover proper gene expression upon downshift. It is important to note that we stained against PGL-1 protein and it's possible that this protein is stable through development and not degraded and that misexpression has stopped upon downshift. In order to distinguish this, smFISH targeting PGL-1, which would label the mRNAs, will be applied to embryos upon downshift.

CHAPTER 5: LIN-15B WORKS IN SERIES WITH MET-2 AND THE DREAM COMPLEX TO REPRESS GERMLINE GENES

Background

Repression of germline genes in somatic tissue is important for proper cell fate decisions, development and somatic cell maintenance. Loss of regulator mechanisms that repress germline genes can lead to developmental defects and are a characteristic of aggressive highly replicative and metastatic cancers (Al-Amin et al., 2016; Janic et al., 2010; Petrella et al., 2011; Whitehurst, 2014). Repression of germline genes represents an interesting challenge in the developing embryo as the zygote is the product of two germline cells. Therefore, the epigenetic state of the zygote has to be completely erased so that the single cell can give rise to all tissue types (Furuhashi et al., 2010; Kreher et al., 2018; Tabuchi et al., 2018). Also, many germline enriched genes are found in the euchromatic chromosome centers (Rechtsteiner et al., 2019). Loci specific mechanisms must be properly employed to establish repressive environments at germline gene loci in somatic tissue without disrupting expression of flanking genes.

A subset of synMuv B proteins, including members of the DREAM complex, LIN-15B, and HPL-2 associate at germline gene promoters in somatic tissue to repress their expression. (Wang *et al*. 2005; Fay and Yochem 2007). Members of the DREAM complex include members of the conserved repressive Muv B core (LIN-54, LIN-37, LIN-52, LIN-53 and LIN-9), the conserved E2F/DP complex (EFL-1 and DPL-1), and the pocket protein (LIN-35) (Harrison et al., 2006). Loss of these proteins causes ectopic germline gene expression and high temperature

larval arrest at 26˚C (Petrella et al., 2011). Mutants of *lin-15B*, *hpl-2,* and *met-2* also ectopically express germline genes and show larval arrest at 26˚C (Petrella et al., 2011). Much like DREAM complex members, *lin-15B* mutants also show changes in regulation of somatic RNAi and cause transgene silencing in the soma but LIN-15B has not shown to biochemically be associated with DREAM (Wang et al. 2005; Wu et al. 2012). Mutations in DREAM complex members, LIN-15B, HPL-2 and MET-2 all result in ectopic expression of germline genes in soma, but the way these different proteins function in parallel to repress germline genes in the somatic tissues of wild-type animals is not understood.

Although LIN-15B has overlapping binding sites in the genome as DREAM complex members and demonstrate the same phenotypes as seen in DREAM complex mutants, recent data suggests LIN-15B may be a separate entity to the DREAM complex (Rechsteiner et al., 2019). Although there is binding overlap of LIN-15B with DREAM complex, LIN-15B also binds to genes devoid of DREAM and has putative DNA binding activity (Rechsteiner et al., 2019, Wormbase). Interestingly, enrichment of H3K9me2 at germline gene promoters is lost in *lin-15B* mutants whereas, promoter enriched H3K9me2 is lost to a much lesser extent in DREAM complex mutants. This suggests that LIN-15B is necessary for establishment or maintenance of H3K9me2 at synMuv B regulated germline genes.

H3K9 is mono and di-methylated by the histone methyltransferase MET-2. Loss of H3K9me2 in *met-2* mutants causes ectopic germline gene expression similar to DREAM and *lin-15B* mutants, suggesting di-methylation of H3K9 is an

important repressive mechanism at synMuv B regulated loci (Andersen and Horvitz, 2007). H3K9 is further tri-methylated by the methyltransferase SET-25 (Towbin et al., 2012). H3K9me2 and H3K9me3 are differentially located throughout the genome in *C. elegans* and SET-25 has not been shown to be linked to synMuv B regulated processes (McMurchy et al., 2017). Furthermore, methylated histones can be demethylated in order to erase the histone modifications. Although there are not many studies to date exploring demethylase activity in *C. elegans*, the predicted H3K9 demethylase is JMJD-1.1. How H3K9 methylation at synMuv B regulated germline genes is established or maintained has not previously been studied.

In this chapter, we sought out to genetically analyze what proteins are involved in the repression of germline genes in somatic tissue. We determined that complete loss of H3K9me2 phenocopies loss of LIN-15B and DREAM complex members at germline gene promoters. We also determined that MET-2 mediated H3K9me2, but not SET-25 mediated H3K9me3 is necessary for germline gene repression. Loss of LIN-15B in addition to loss of all H3K9me2 does not enhance the HTA phenotype, suggesting LIN-15B and MET-2 work in series to repress germline gene expression. Loss of LIN-15B and the demethylase JMJD-1.1 combined does not rescue the HTA phenotype, suggesting that blocking of demethylase activity is not the mechanism in which LIN-15B maintains H3K9me2 at germline gene promoters. Furthermore, loss of LIN-15B and other DREAM complex members does not enhance the HTA phenotype, suggesting that LIN-15B and DREAM complex proteins are also

working in series to repress germline gene expression. Lastly, we found putative DNA motifs at LIN-15B associated promoters to which LIN-15B could potentially bind. Together, this supports a model where LIN-15B binds to germline gene promoters in somatic tissue, promotes H3K9me2 by MET-2 and DREAM complex binding at these loci in order to repress their fate.

Results

Global loss of H3K9me2 leads to phenotypes similar to *lin-15B* and DREAM complex mutants

To determine if di-methylation of H3K9 at germline gene promoters is necessary for phenotypes associated with loss of synMuv B proteins, we analyzed mutants that lack histone methyltransferase activity responsible for H3K9 methylation. MET-2 is responsible for methylation of H3K9me1/2 and SET-25 catalyzes H3K9me3. Loss of MET-2 and SET-25 leads to a global loss of all H3K9 methylation (Garrigues et al., 2015; Towbin et al., 2012). We analyzed mutants that lack these methyltransferases for the HTA phenotype and ectopic expression of the germline protein PGL-1. If loss of H3K9 methylation is associated with ectopic germline gene expression and the HTA phenotype, we would expect that *met-2* and *set*-25 mutants would show these phenotypes. *set-25* single mutants, which lose H3K9me3, showed neither an HTA phenotype nor ectopic PGL-1 expression. (Figure 5.1 A and B). Therefore, H3K9me3 is not necessary for repression of germline genes in the soma. In contrast, *met-2* single mutants, which lose 80-90% of H3K9me2 and ~70% of H3K9me3 (Towbin

Figure 5

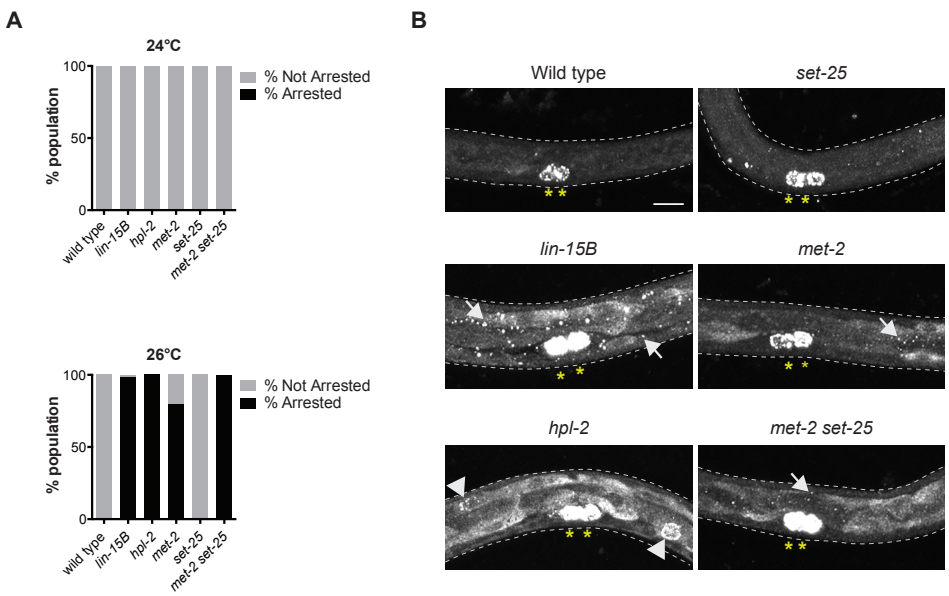

Figure 5.1: Complete loss of H3K9me2 during development phenocopies synMuv B mutants. (A) The percentage of F1 animals that arrested before the L4 larval stage was assessed for all genotypes indicated after parent hermaphrodites were upshifted from 20°C to 24°C or 26°C. (B) Assessment of ectopic expression of PGL-1 in L1 animals at 26°C. Yellow asterisks indicate the two primordial germ cells in which PGL-1 is solely expressed in wild type. Arrowheads indicate ectopic perinuclear punctate PGL-1 in intestinal cells. Arrows indicate ectopic punctate PGL-1 that is not perinuclear. Scale bar: 10μm.

et al. 2012), displayed ~80% larval arrest around the L3 stage at 26˚C, but no larval arrest at 24˚C (Figure 5.1 A). Thus, *met-2* mutants show an HTA phenotype similar to but weaker than *lin-15B* mutants (Figure 5.1 A). We also observed ectopic expression of PGL-1 in *met-2* mutants at 26˚C similar to *lin-15B* mutants, with the PGL-1 protein being primarily cytoplasmic and diffuse in intestinal cells (Figure 5.1 B). To test if the remaining 10-20% of H3K9me2 catalyzed by SET-25 in *met-2* mutants (Towbin *et al.* 2012) partially represses germline gene expression in somatic cells, we analyzed *met-2 set-25* double mutants, which have been shown to completely lack H3K9 methylation during embryonic stages (Towbin *et al.* 2012; Garrigues *et al.* 2015). Consistent with residual SET-25-mediated H3K9me2 serving a role in repression of germline genes in somatic cells, *met-2 set-25* double mutants showed significantly enhanced larval arrest at 26˚C when compared to *met-2* single mutants (Figure 5.1 A). Similar to *lin-15B* and other synMuv B mutants, *met-2 set-25* double mutants did not show increased larval arrest at 24˚C. Ectopic PGL-1 in *met-2 set-25* double mutants at 26˚C was similar to that seen in *met-2* single mutants (Figure 5.1 B). Altogether, our results show that a global loss of H3K9me2 phenocopies both the HTA and ectopic germline gene expression seen in synMuv B mutants.

One of the known proteins that binds to methylated H3K9 to create a repressive chromatin environment is HP1 (Garrigues et al., 2015). In *C. elegans* there are two HP1 homologs, HPL-1 and HPL-2. *hpl-2* is a synMuv B gene and mutants display a variety of phenotypes including HTA and ectopic germline

gene expression in the soma (Figure 5.1) (Couteau *et al.* 2002*;* Petrella *et al.* 2011), while *hpl-1* mutants generally lack observable phenotypes (Schott *et al.* 2006). When genes with H3K9me2 promoter peaks are compared to genes bound by HPL-2, we found that genes with a H3K9me2 promoter peak that is lost in *lin-15B* mutants are the same genes enriched for promoter-bound HPL-2 (Rechtsteiner et al. 2019). This suggests that HPL-2 binding may contribute to regulation of germline genes that are repressed in somatic cells through an H3K9me2 promoter peak. However, we noted differences in the pattern of PGL-1 accumulation in the soma of *hpl-2* mutants compared to either *lin-15B* or *met-2 set-25* mutants. 75% (15/20) of *hpl-2* mutant L1s displayed intestinal PGL-1 staining that was perinuclear and punctate, reminiscent of PGL-1 staining in the germline (Figure 5.1C) (Petrella et al. 2011; Wu et al. 2012). In contrast, none of the *lin-15B, met-2,* or *met-2 set-25* mutants analyzed (n=9-20) displayed that pattern of intestinal staining (Figure 5.1C), unlike the previously published analysis of *met-2* (Wu *et al.* 2012). This suggests that the HTA phenotype and ectopic PGL-1 expression in *met-2* and *lin-15B* mutants is not explained by disruption of HPL-2 binding. These differences in the pattern of ectopic PGL-1 suggest that loss of H3K9me2 either at a subset of genes in *lin-15B* mutants or globally in *met-2 set-25* mutants is not equivalent to loss of HPL-2*.*

LIN-15B and MET-2 work in series to repress germline gene expression in somatic tissue

Because promoter enriched H3K9me2 at germline genes is lost in *lin-15B* mutants and loss of germline gene accumulated H3K9me2 phenocopies LIN-15B

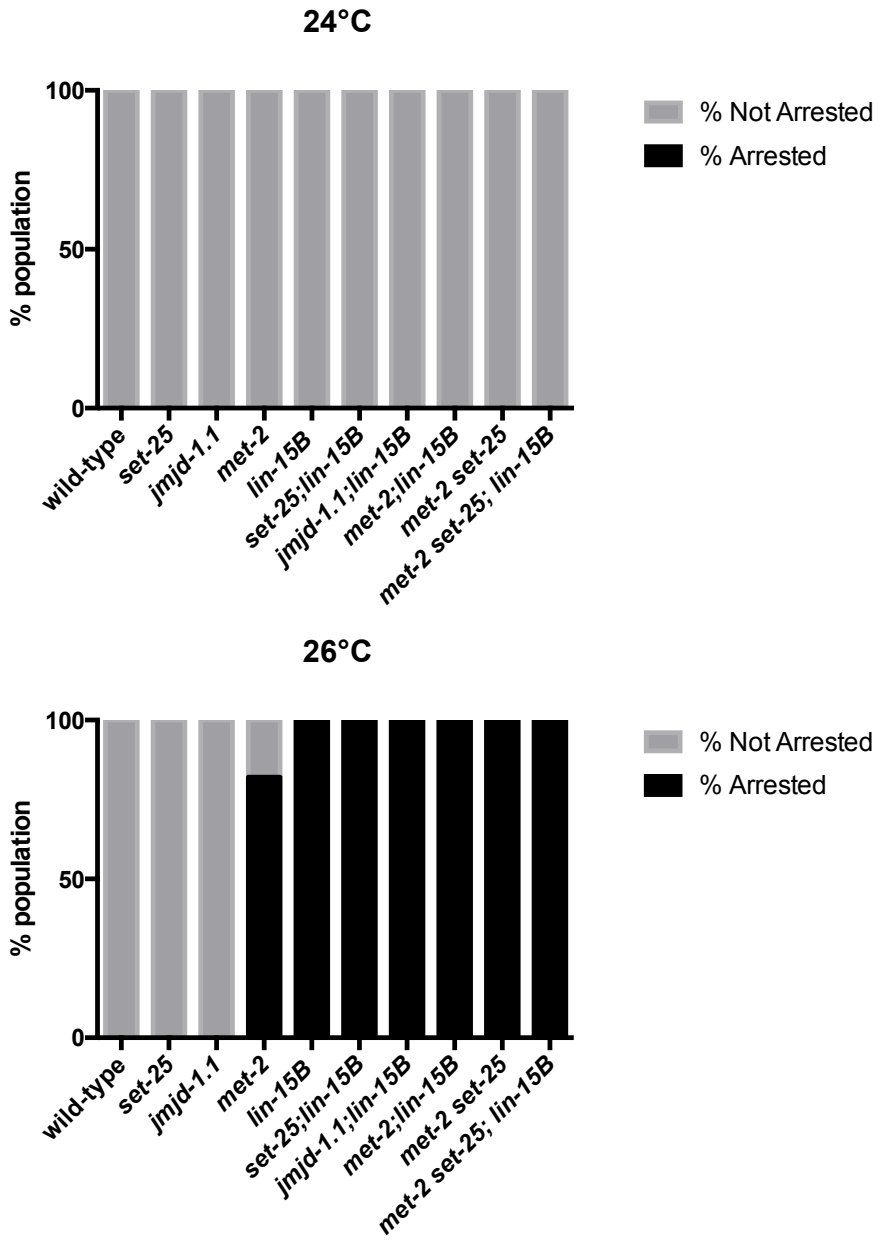

Figure 5.2: Additional loss of H3K9 methyltransferases or the H3K9 demethylase in *lin-15B* mutants does not rescue or enhance the HTA phenotype. The percentage of F1 animals that arrested before the L4 larval stage was assessed for all genotypes indicated after parent hermaphrodites were upshifted from 20°C to (A) 24°C or (B) 26°C.

mutants, we set out to determine how LIN-15B promotes H3K9me2 at these promoters. We analyzed compound mutants of *lin-15B* and H3K9 regulators for the HTA phenotype to genetically dissect these regulatory pathways. If loss of H3K9 methyltransferases in addition to loss of *lin-15B* enhances the HTA phenotype, we would conclude that these proteins work in parallel pathways to repress germline gene expression. In contrast, we found that although both *met-2* and *lin-15B* single mutants arrest at 26°C, *met-2;lin-15B* double mutants do not arrest at 24°C (Figure 5.2). Thus, the HTA phenotype is not enhanced and we conclude that LIN-15B and MET-2 work in series to repress germline gene expression. *met-2* mutants lose only ~80% of H3K9me2, but *met-2 set-25* double mutants lose 100% of H3K9me2, to ensure that complete loss of H3K9me2 in addition to loss of *lin-15B* did not enhance the HTA phenotype, we tested a *met-2 set-25;lin-15B* triple mutant (Towbin et al., 2012). Much like *met-2;lin-15B* double mutants *met-2 set-25;lin-15B* triple mutants arrest at 26°C but do not enhance the HTA phenotype at 24°C (Figure 5.2).

To determine if LIN-15B maintains H3K9me2 at germline gene promoters by blocking demethylase activity, we analyzed *jmjd-1.1;lin-15B* double mutants for the HTA phenotype. If LIN-15B blocks demethylase activity, we would expect that additional loss of JMJD-1.1 would rescue the HTA phenotype in *lin-15B* mutants. In contrast, *jmjd-1.1;lin-15B* double mutants arrest at 26°C (Figure 5.2). Loss of both *jmjd-1.1* and *lin-15B* did not enhance the HTA phenotype at 24°C (Figure 5.2). This suggests that LIN-15B does not block *jmjd-1.1* activity in order to promote H3K9me2 at germline gene promoters.

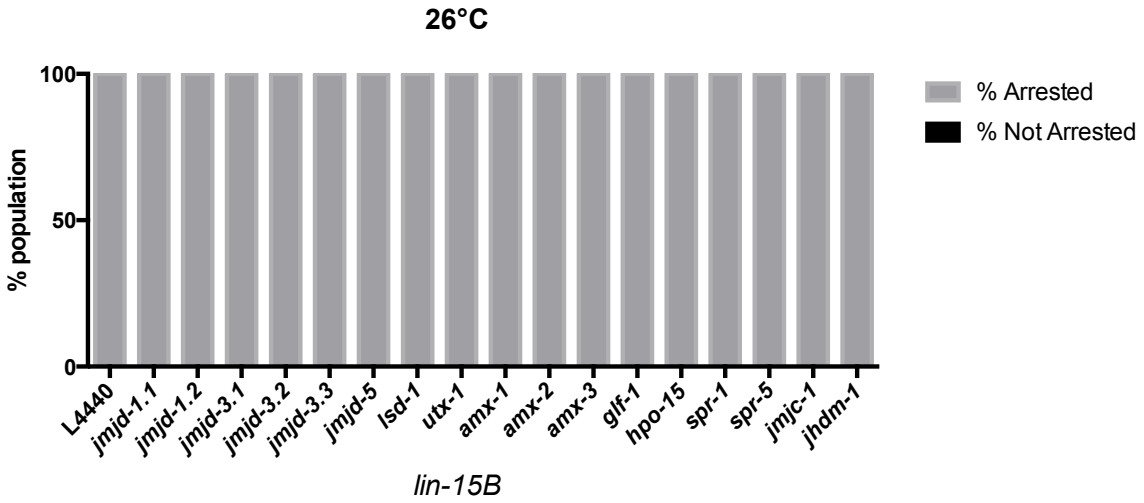

Figure 5.3: RNAi knockdown of known *C. elegans* demethylases in a *lin-15B* mutant background does not rescue the HTA phenotype. L4 *lin-15B* mutant parents were transferred to empty vector or gene-specific RNAi bacteria at 26°C. The percentage of F1 animals that arrested before the L4 larval stage was assessed.

Because little is known about histone demethylases in *C. elegans*, we performed an RNAi screen against all known *C. elegans* histone demethylases in a *lin-15B* background. We analyzed the HTA phenotype of *lin-15B* mutants with knockdown of 17 different histone demethylases (*jmjd-1.1, jmjd-1.2, jmjd-3.1, jmjd-3.2, jmjd-3.3, jmjd-5, lsd-1, utx-1, amx-1, amx-2, amx-3, glf-1, hpo-15, spr-1, spr-5, jmjc-1,*and *jhdm-1)* (Figure 5.3). Knockdown of single demethylases did not rescue the HTA phenotype in a *lin-15B* mutant background (Figure 5.3). Although there is the potential for redundancy, and RNAi does not completely knock down the gene, this preliminary screen showed no rescue of the phenotype and suggests that loss of H3K9me2 at germline gene promoters in *lin-15B* mutants is not due to demethylase activity. LIN-15B does not work in a genetic pathway with JMJD-1.1 or any other putative histone demethylase to repress germline genes in somatic tissue.

LIN-15B and the DREAM complex work in the same pathway to repress germline gene expression in somatic tissue.

It has previously been suggested that LIN-15B is associated with the DREAM complex. Consistent with their model, *lin-15B* mutants show phenotypes similar to DREAM complex mutants, such as HTA and ectopic PGL-1 expression, but LIN-15B has not been biochemically shown to associate with the DREAM complex. Because *lin-15B* mutants show distinct differences in promoter enriched H3K9me2 compared to DREAM complex mutants, we set out to determine if DREAM complex *lin-15B* double mutants can enhance the HTA

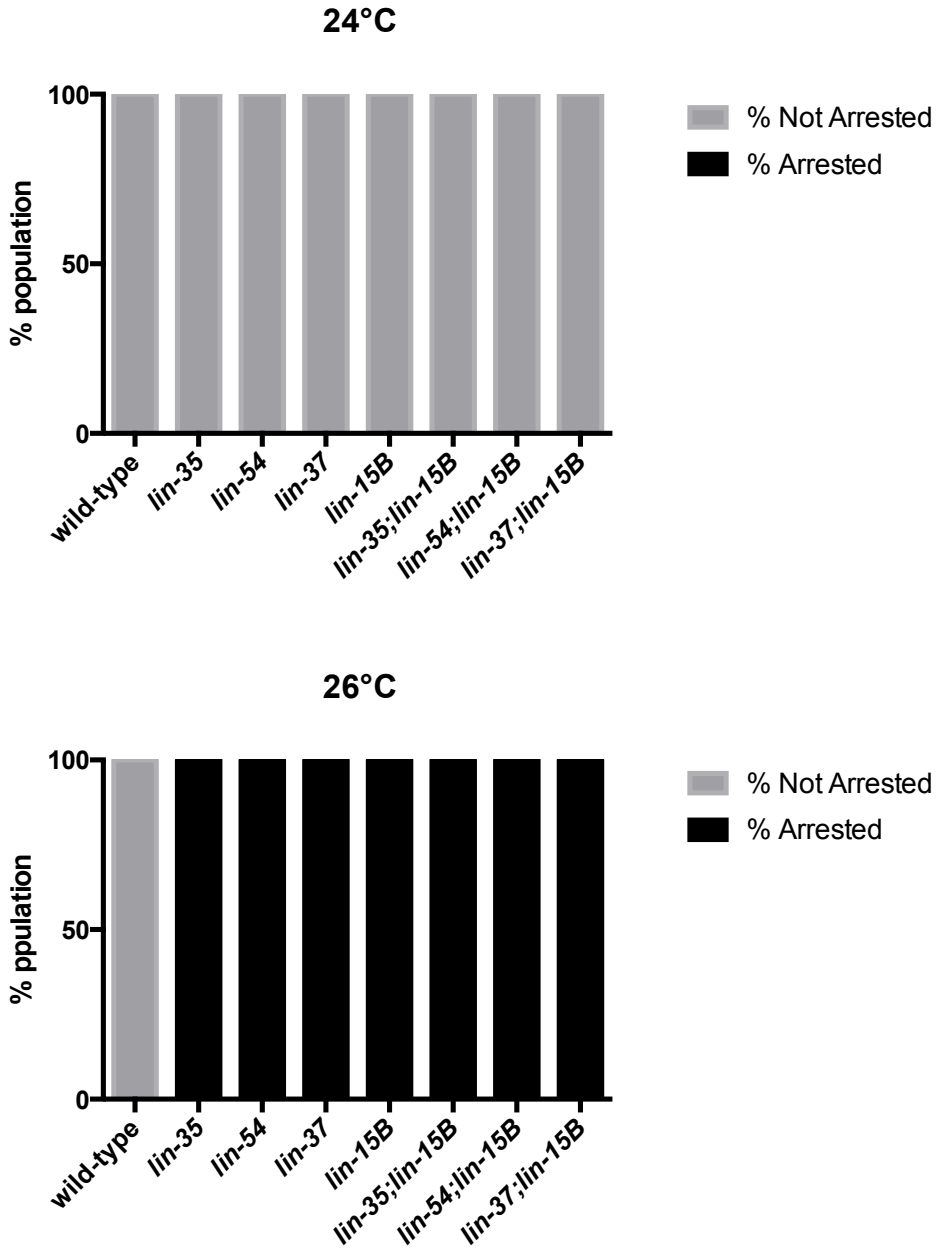

Figure 5.4: Loss of DREAM components in *lin-15B* mutants does not enhance the HTA phenotype. The percentage of F1 animals that arrested before the L4 larval stage was assessed for all genotypes indicated after parent hermaphrodites were upshifted from 20°C to (A) 24°C or (B) 26°C.

phenotype. As previously reported, *lin-35, lin-37, lin-54* and *lin-15B* single mutants all arrest at the L1 stage (Figure 5.4) (Petrella et al., 2011). *lin-35;lin-15B, lin-37;lin-15B and lin-54;lin-15B* double mutants arrest at 26°C, but not at 24°C (Figure 5.4). Because DREAM complex *lin-15B* double mutants do not enhance the HTA phenotype at 24°C , we conclude that LIN-15B and the DREAM complex work in series to repress germline genes in somatic tissue.

LIN-15B associated promoters are enriched for conserved THAP binding sites and AT rich sequences

LIN-15B has putative DNA binding domains including a THAP domain and AT hooks (Wormbase). THAP-Zinc finger binding proteins are highly conserved through mammals and recognize the DNA Sequence AGTACGGGCAA. The GGCA core is essential for recognition by the THAP domain and a T or G four basepairs upstream is also strictly required (Clouaire et al., 2005). AT hooks are DNA-binding motifs that can bind to the minor grove of Adenine and Thymine rich DNA (Singh et al., 2006). To determine if there were conserved sequences that could be recognized by LIN-15B's THAP or AT hook domain at LIN-15B enriched promoters, we used a computer program, MEME-ChIP, to identify putative LIN-15B binding motifs. A data set that included genes bound by LIN-15B in embryos, LIN-35 in embryos, LIN-54 in embryos and had enrichment of H3K9me2 at promoters in L1s was used (Rechtsteiner et al., 2019). 177 promoters that were bound by LIN-15B, LIN-35, LIN-54 and H3K9me2 were identified and 500bp upstream of the TSS were inserted into the motif finding

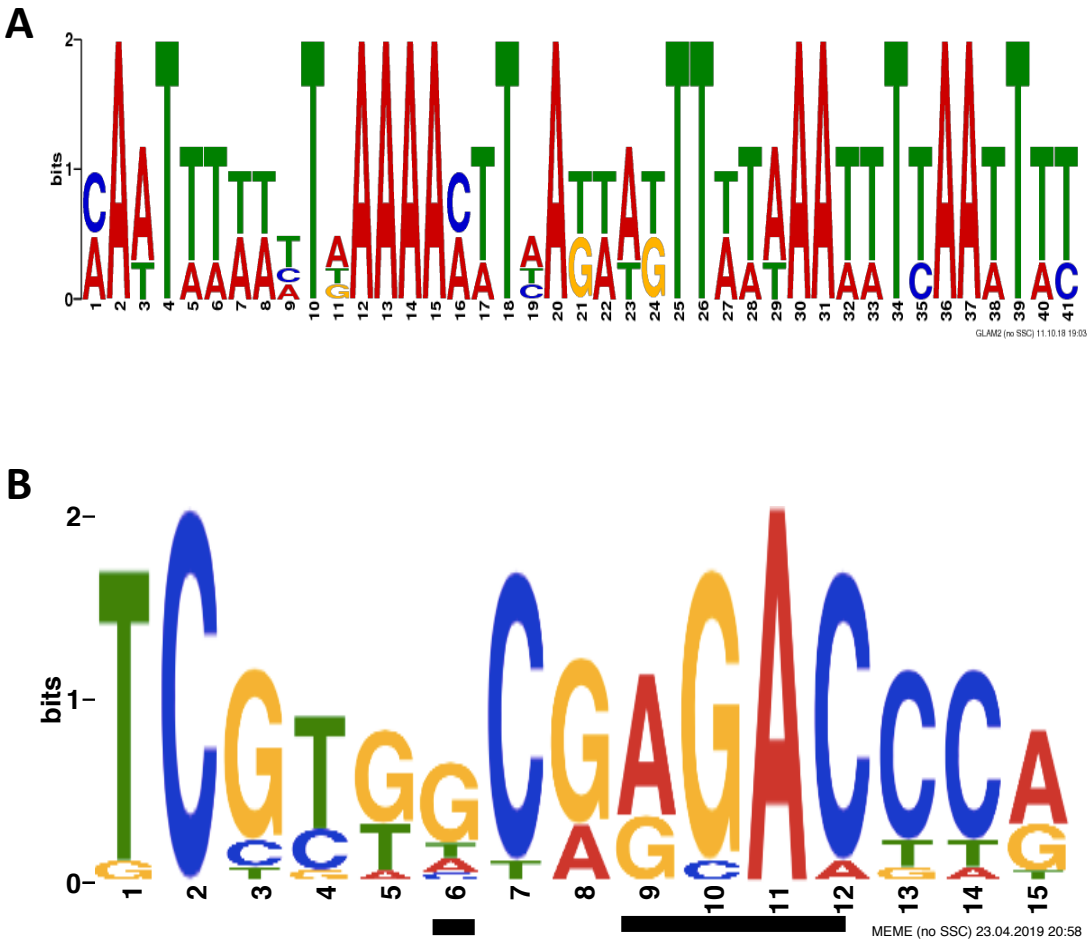

Figure 5.5: LIN-15B associated promoters are enriched for AT rich sequences and contain putative THAP binding sites. An overrepresented motif at LIN-15B bound promoters as predicted by MEME-ChIP.

software. We found that some LIN-15B bound promoters were enriched for the THAP binding sequences and all were AT rich (Figure 5.5). It is possible that LIN-15B binds to germline genes independent of DREAM complex and further studies of LIN-15B's binding capability are needed to determine this.

Discussion

Proper repression of germline gene expression throughout development is important to achieve proper cell fate. Our data, along with other recent work, strongly implicates deposition of H3K9me2 at the proper time in development as necessary to create repressive chromatin in differentiating somatic cells. In *C. elegans* H3K9me2 and H3K9me3 levels are very low in the nuclei of early stage embryos and only start to accumulate when cells are transitioning from early embryogenesis to mid-embryogenesis at about the 50-100 cell stage (Mutlu et al. 2018). The onset of heterochromatin in embryos is at least in part due to the nuclear import of H3K9me1/2 methyltransferase MET-2. Nuclear import of MET-2 and the onset of heterochromatin just precedes the stage in development when zygotic transcription is globally upregulated (Spencer et al. 2011; Levin et al. 2012; Robertson and Lin 2015; Mutlu et al. 2018). At this time in development, clear regions of compact chromatin can be viewed within the nucleus. (Mutlu *et al.* 2018). Loss of nuclear import of MET-2 causes delays in chromatin compaction into later development stages (Mutlu et al., 2018). We also report that *met-2* mutants have a delay in chromatin compaction until later developmental stages, especially at high temperature. This suggests a role in

which synMuv B proteins regulate timing of chromatin compaction during embryogenesis. We found that, like *met-2* mutants, global formation of compact chromatin is delayed*, lin-15B*, *lin-54* and *lin-35* mutants, especially at high temperature. Loss of these proteins at high temperature cause delays in chromatin into developmental time periods when zygotic gene expression is upregulated and ectopic expression of germline genes in somatic tissue occurs in mutants. This suggests that developmental chromatin compaction likely plays a role in lineage-specific gene repression and is proposed to be driven at least in part by H3K9 methylation and synMuv B proteins.

In this chapter we show that loss of H3K9me2, either through loss of the MET-2 and SET-25 histone methyltransferases that catalyze the modification or through loss of proper localization of H3K9me2 to germline genes in *lin-15B* mutants, leads to misexpression of germline-specific genes in somatic cells. Loss of H3K9me2 at germline gene promoters in *lin-15B* mutants shows the same phenotypes: arrested development and loss of cell fate, as global loss of H3K9me2 in *met-2 set-25* mutants. Global loss of H3K9me2 phenocopies loss of LIN-15B at germline specific promoters. We set out to determine if double mutants in this pathway would enhance the HTA phenotype at lower temperatures. Other synMuv B mutants in the repressive NuRD, *let-418* and *mep-1* show enhanced ectopic PGL-1 expression and arrest during larval development at 20°C. Because *lin-15B* single mutants only arrest at 26°C, we tested *lin-15B* compound mutants at 24°C for larval arrest and enhancement of the HTA phenotype. Because we didn't see enhancement of the HTA phenotype

at 24°C, we concluded that that LIN-15B and MET-2 work in series with the DREAM complex to repress germline genes in somatic tissue. Because *lin-15B* mutants lose H3K9me2 at synMuv B regulated germline genes, we hypothesize that specific localization of H3K9me2 to germline gene promoters facilitated by LIN-15B is an important aspect of establishing the chromatin landscape of germline genes to prevent their expression in somatic lineages throughout development.

Because LIN-15B has similar binding sites to that of members of the DREAM complex and phenocopies DREAM complex mutants, it was previously proposed that LIN-15B is a member of the DREAM complex (Wu *et al.* 2012). Our data indicate that, although LIN-15B works in series with the DREAM complex to bind to and represses germline genes, its molecular function at those genes is potentially distinct. LIN-15B has putative DNA binding capability through its THAP or AT hook domains. It is possible that LIN-15B independently localizes to similar targets as the DREAM complex. Here we show that LIN-15B bound promoters are enriched for AT rich sequences and at least some contain the THAP recognized core sequence. Further studies, such as yeast 2 hybrid assays must be carried out to determine if LIN-15B has DNA binding capabilities.

Interestingly, recent work from the Seydoux lab has shown that the downregulation of LIN-15B protein in the germline is important for germline development (Lee et al., 2017). Maternally loaded LIN-15B must be removed from the primordial germ cells (PGCs) during development, while DREAM members such as LIN-35 and LIN-54 are not (Lee et al., 2017). This, together

with our data, suggests that LIN-15B may be first to bind germline gene promoters to repress their fate and thus must be removed from the PGCs in order to avoid repression of germline genes in germline tissue. If LIN-15B helps establish H3K9me2 at germline gene promoters in somatic tissue, its downregulation would be important in the germline where expression is necessary for proper germline fate.

Accumulation of multiple regulators to germline gene promoters is crucial for their proper repression. In *C. elegans*, the DREAM complex, LIN-15B, MET-2, and HPL-2 all accumulate at germline genes to ensure their repression in somatic tissue (Rechtsteiner et al., 2019). Loss of these proteins cause arrest of development at high temperature (Petrella et al., 2011). How each of these proteins work together to repress germline genes in somatic tissue remains unknown. The establishment of H3K9me2 by LIN-15B may be one of the steps necessary for proper repression. In order to determine this, further studies to determine how LIN-15B may recruit MET-2 and members of DREAM complex to germline gene promoters will need to be carried out.

CHAPTER 6: DISCUSSION

Tissue specific establishment of repressive chromatin is imperative for proper gene expression, development, and cell fate maintenance

Proper deployment of the genome throughout development is crucial for correct cell fate decisions. Organization of chromatin into repressed and active domains during development is necessary to achieve proper gene expression and differentiation. During early development, chromatin is found in a generally unorganized and open state (Politz et al*.,* 2013; Yuzyuk et al., 2009). As development proceeds and differentiation occurs, chromatin becomes compacted and organized in a tissue specific manner (Mutlu et al., 2018; Politz et al., 2013; Yuzyuk et al., 2009). It is imperative that chromatin compaction and organization precedes upregulation of zygotic gene expression in order for proper gene expression and correct cell fate decisions (Gaertner et al., 2012; Politz et al., 2013; Yuzyuk et al., 2009). Recent work has shown that poised Pol II accumulates at promoters in a stage specific, but not tissue specific manner (Gaertner et al., 2012). This suggests that the maternal-to-zygotic switch occurs in a tissue-independent, but time specific manner (Gaertner et al., 2012). Establishment of tissue specific repression, including establishment of repressive chromatin, must occur before global gene expression is upregulated in order to achieve proper cell fate (Gaertner et al*.,* 2012; Poliltz et al., 2013; Yuzyuk et al., 2009). We hypothesize that repression by synMuv B proteins may be a tissue specific mechanism to establish repressive chromatin environments before the maternal-to-zygotic switch. In this work, we determined that the loss of these proteins causes global changes in chromatin compaction into the developmental

time of the maternal-to-zygotic switch, especially at high temperature, leaving their target loci available to expression when zygotic gene expression is upregulated

synMuv B proteins are important for proper transcriptional repression during development

We determined that a subset of synMuv B proteins are necessary for timely chromatin compaction during development. This subset of synMuv B proteins represent members of the conserved DREAM complex, LIN-15B and the H3K9me2 methyltransferase MET-2. Previous work determined that the DREAM complex, LIN-15B, and MET-2 are important for the soma-germline fate decision (Andersen et al., 2007; Petrella et al., 2011). The DREAM complex, LIN-15B, and MET-2 associated H3K9me2 at promoters of germline genes and repress their expression (Garrigues et al., 2015; Goetsch et al., 2017; Rechtsteiner et al., 2018; Tabuchi et al., 2011). *lin-35, lin-15B, lin-54,* and *met-2* mutants ectopically express germline genes in somatic tissue. Enhanced ectopic expression of germline genes, specifically in the somatic intestine, causes synMuv B mutants to arrest at the L1 larval stage (HTA) (Petrella et al., 2011). This data suggests that each of these proteins work together to repress germline gene expression in the soma, especially at high temperature, to achieve proper development.

Recent studies have begun to tease apart the different roles of members of the DREAM complex at synMuv B target genes (Goetsch et al., 2017). Recently, it was found that the pocket protein, LIN-35, mediates the assembly and accumulation of the E2F/DP complex (EFL-1 and DPL-2) and the repressive

MuvB core (LIN-54, LIN-37, LIN-52, LIN-53, and LIN-9) at synMuv B regulated genes. Loss of *lin-35* resulted in diminished DREAM assembly and binding across the genome (Goetsch et al., 2017). In this study, we set out to determine the role of the DREAM complex, LIN-15B and MET-2 at germline gene promoters in somatic tissue.

synMuv B proteins have delayed chromatin compaction, especially at high temperature

We hypothesize that the DREAM complex and LIN-15B regulate gene expression at the chromatin level for many different reasons. First, *met-2* mutants also ectopically express germline genes and arrest at high temperature (Rechtsteiner et al., 2018). This suggests a mechanism for H3K9me2 in the repression of germline genes in the soma. Secondly, the H3K9me2 associated protein HPL-2 is also a synMuv B protein that when lost, leads to the ectopic expression of germline genes in the somatic intestine and arrest at the L1 stage (Petrella et al., 2011*).* Furthermore, the HTA phenotype can be rescued in synMuv B mutants by subsequent knockdown of other chromatin modifiers, including *mes-4* (Petrella et al., 2011). In order to determine if loss of DREAM complex members and LIN-15B affect chromatin organization and compaction, we looked at global and loci specific chromatin compaction in *lin-15B, lin-35, lin-54* and *met-2* mutants. Here, we determine that loss of DREAM complex members *lin-35* and *lin-54,* phenocopy loss of *lin-15B* and *met-2* in all chromatin compaction assays. Loss of any of these regulators at germline gene promoters causes impaired chromatin compaction into later stage developmental time

periods and ectopic germline gene expression in early development, especially at high temperature. This suggests that binding of LIN-15B, the DREAM complex, and methylation of H3K9 are each necessary for proper chromatin compaction and gene repression at germline gene loci in somatic tissue.

Delayed chromatin compaction observed in synMuv B mutants concurs with the developmental time critical for the HTA phenotype

We wanted to determine if prolonged open chromatin into later developmental stages concurred with the developmental time critical for the HTA phenotype observed in synMuv B mutants. Indeed, we determined that the embryonic stages in which we see prolonged open chromatin coincide with the developmental time-period that is likely important for the HTA phenotype displayed by synMuv B mutants. We found the developmental window for high temperature arrest is between 16E and comma stage. This developmental time coincides with the stages we see open chromatin in synMuv B mutants at 26°C but not 20°C. We hypothesize that the temperature sensitive arrest phenotype we observe in synMuv B mutants is at least part due to open chromatin during this critical developmental time at 26°C but not 20°C.

The critical time period for HTA coincides with the upregulation of zygotic gene expression.

Interestingly, we found that the critical time period of HTA coincides with an upregulation of zygotic gene expression in the somatic intestine. Tissue specific forms of transcriptional regulation, including organization of chromatin, are established prior to upregulation of the zygotic genome (Gaertner et al.,

2012; Politz et al., 2013; Yuzyuk et al., 2009). Poised Pol II accumulates at promoters in a stage specific, but not tissue specific manner. Loss of tissue specific mechanisms to negatively regulate Pol II result in ectopic gene expression (Gaertner et al., 2012). We hypothesize that repression by synMuv B may be a tissue specific mechanism to establish repressive chromatin environments before the maternal-to- zygotic switch. Loss of these proteins causes global changes in chromatin compaction into the developmental time of the maternal-to-zygotic switch, especially at high temperature, leaving their target loci vulnerable to expression when zygotic gene expression is upregulated. Here we show that once upregulated, somatic misexpression of germline genes is irreversible upon downshift. This suggests that ectopic gene expression programs turned on in synMuv B mutants are global and mutants are unable to recover proper gene expression upon downshift.

We also found that delayed chromatin compaction in synMuv B mutants demonstrated an anterior-to-posterior pattern within intestinal cells. The anterior cells of the intestine were the last to adopt closed chromatin, a pattern independent of replication capacity, as there is a both final anterior and posterior division to form the *C. elegans* intestine (McGhee, 2007). This delay in chromatin compaction occurs at time periods when global zygotic gene expression is upregulated. Interestingly the *C. elegans* intestine is one of the first tissues to turn on zygotic expression. Zygotic expression of signaling molecules can be seen as early as the 1E stage (McGhee, 2007). Some of these signaling molecules are Wnt signaling proteins and they pattern the *C. elegans* intestine in

an anterior to posterior direction (Fukushige et al, 1996; Lin et al, 1998; Schroeder and McGhee, 1998). Wnt signaling associated transcription factors are localized to the most anterior cells of the intestine at each division (Schroeder and McGhee, 1998). It is possible that anteriorly loaded transcriptional factors are able to ectopically bind and express accessible uncompacted germline genes in the anterior intestine leading to high temperature arrest.

Delayed chromatin compaction in synMuv B mutants does not seem to be explained by a developmental timer of chromatin compaction.

Chromatin compaction may be the result of a developmental timer during embryogenesis. Developmental timers are often represented as an absolute timer or a cell division timer. Absolute timers start at fertilization and are constant throughout development. Cell division timers are associated with the number of cells during development and is not always consistent with absolute time as developmental speed and cell division rate can increase or decrease at different conditions. Certain biological processes need an amount of absolute time to occur, whereas, other biological processes occur based on in response to the number of cell divisions. It is possible that chromatin compaction during development needs a certain amount of absolute time to occur. It is possible that the delay in chromatin compaction we see at high temperature is an artifact of increased developmental speeds up at 26°C. Because cell divisions occur faster at 26°C, embryos reach later cell division time in absolute time. If this were the case, chromatin compaction would not be strictly linked to cell-division stage but instead be a consequence of the time needed to established a closed chromatin

environment. Thus, compaction would occur at later cell division developmental stages at high temperature. This hypothesis could explain our wild-type data for chromatin compaction and developmental time. As previously observed, we also determined that development occurs at a faster rate at 26°C. Wild-type embryos at 26°C reach the 8E stage on average 51 minutes before wild-type embryos at 20°C. If chromatin compaction was on an absolute developmental timer, the embryos at 26°C would be further along in cell division development by the time chromatin compaction was achieved. We did observe this in wild-type embryos at 26°C and this could explain why we see significantly more open chromatin in wild-type embryos at 26°C compared to 20°C at the 8E stage.

Although the developmental timer hypothesis could explain the delay in chromatin compaction we see in wild-type embryos at 26°C, it does not seem to fit our synMuv B mutant data. synMuv B mutants have significantly delayed chromatin compaction into 8E at 20°C and into 16E and comma stage at 26°C. If synMuv B mutants have delayed chromatin compaction due to a timer affect, we would expect to see their cell division developmental time occurring even earlier in absolute time compared to wild-type. This was not the case, as synMuv B mutants have delayed development compared to wild-type embryos. synMuv B mutants, on average, reach 8E 30-35 minutes slower than wild-type embryos at both 20°C and 26°C. Thus, we do not think that delayed chromatin compaction observed in synMuv B mutants is due to a developmental timer affect. We hypothesize that synMuv B mutants establish timely chromatin compaction in a cell and loci specific manner during development.

Developmentally regulated H3K9me2 is important for repressive chromatin formation.

Numerous studies have identified that H3K9 methylation is essential for chromatin compaction and organization (Ahringer and Gasser, 2017; Towbin et al., 2012). The onset of compacted chromatin in development is coupled to nuclear localization of the H3K9me2 methyltransferase, MET-2 (Mutlu et al., 2018). Nuclear accumulation of MET-2 establishes H3K9me2 prior to upregulation of zygotic gene expression that occurs at the ~50-100 cell stage (Mutlu et al., 2018). At this stage, the formation of dense heterochromatic domains can be visualized by transmission electron microscopy (Mutlu et al., 2018). It is thought that MET-2 associated H3K9me2 establishes repressive environments before the onset of zygotic gene expression (Spencer *et al.* 2011; Levin *et al.* 2012; Robertson and Lin 2015; Mutlu *et al.* 2018). Although methylation of H3K9 is necessary for proper gene repression and chromatin compaction, the pathways and proteins needed to establish areas of compaction in a tissue specific way remain unclear.

In addition to MET-2 mediated H3K9me2 establishment, we show a role for synMuv B proteins in the timing of chromatin compaction during embryogenesis. Much like *met-2* mutants, the formation of compact chromatin is delayed in *lin-15B*, *lin-35* and *lin-54* mutants (Mutlu et al., 2018). Global loss of H3K9me2 in *met-2* mutants phenocopy DREAM and *lin-15B* mutants in all chromatin compaction, HTA, and ectopic PGL-1 expression assays. This suggests that chromatin compaction and repression of germline genes is driven

by H3K9 methylation and is crucial for proper gene expression and development, especially at high temperature.

H3K9me2 is enriched at synMuv B regulated promoters

Although H3K9me2 is predominantly found at repeat rich regions of autosomal arms, recent studies have discovered H3K9me2 enrichment at promoters (Rechtsteiner et al., 2018; Zeller et al., 2016; Liu *et al*. 2011; Garrigues *et al*. 2015; Evans *et al.* 2016; Ahringer and Gasser 2018). Specifically, work from our lab has shown H3K9me2 is enriched at synMuv B regulated germline genes found in euchromatic regions of the genome (Rechtsteiner et al., 2018). Promoter enrichment of H3K9me2 in autosomal centers provides a new regulatory role for H3K9me2. Interestingly, the localization of H3K9me2 to germline gene promoters at synMuv B targets is disrupted strongly in *lin-15B* mutants and weakly in DREAM complex mutants (Rechtsteiner et al., 2018). It is important to note that canonical repeat associated H3K9me2 is not disrupted in *lin-15B* mutants (Rechtsteiner et al., 2018). This data suggests that loss of proper localization of H3K9me2 to germline gene promoters in *lin-15B* mutants, leads to misexpression of germline-specific genes in somatic cells. We hypothesize that specific localization of H3K9me2 to germline gene promoters facilitated by LIN-15B is an important aspect of resetting the chromatin landscape of germline genes to prevent their expression in somatic lineages.

LIN-15B has similar binding sites across the genome to that of DREAM complex members. Furthermore, *lin-15B* mutants ectopically express germline genes, show high temperature larval arrest, and have enhanced RNAi like DREAM complex mutants (Petrella et al., 2011; Wang et al., 2005; Wu et al., 2012). Due to this phenotypic evidence, LIN-15B has previously been thought to be a member of the DREAM complex (Wu et al. 2012). Our data indicate that, although LIN-15B binds to and represses many of the same genes as the DREAM complex, its molecular function at those genes is potentially distinct. LIN-15B has putative DNA binding capability through its THAP or AT hook domains. If LIN-15B can bind DNA, it can independently localize to similar targets as the DREAM complex. In this work, we show that LIN-15B bound promoters are enriched for AT rich sequences and the THAP recognized core sequence of TNNGGCA.. In order to determine the capacity of LIN-15B to bind DNA, further studies such as yeast 2 hybrid or gel-shift assays must be completed.

Loss of H3K9me2 leads to phenotypes similar to *lin-15B* mutants.

To determine if LIN-15B mediates H3K9me2 at germline gene promoters, we characterized H3K9me2 regulators for *lin-15B* mutants phenotypes. We show that global loss of H3K9me2 through loss of the *met-2* and *set-25* histone methyltransferases phenocopies loss of promoter localized H3K9me2 to germline genes in *lin-15B* mutants. Both *met-2* single mutants and *met-2 set-25* double mutants ectopically express germline genes in the somatic intestine and arrest at 26°C. *hpl-2* mutants also arrest at high temperature and ectopically express

germline genes in the somatic intestine. Interestingly, ectopic PGL-1 staining is perinuclear in *hpl-2* mutants, but diffuse in *lin-15B* and *met-2* mutants. Because *met-2* mutants phenocopy *lin-15B* mutants, we conclude that global loss of H3K9me2 causes similar phenotypes to that observed in *lin-15B* mutants. This supports a role for LIN-15B mediated H3K9me2 localization at synMuv B regulated promoters.

Additionally, recent work from the Seydoux lab has implicated the loss of LIN-15B protein in the germline is important for germline development (Lee *et al.* 2017). Maternally provided LIN-15B is normally removed from the primordial germ cells (PGCs), while DREAM components are not (Lee *et al.* 2017). If LIN-15B mediates H3K9me2 at germline gene promoters, loss of LIN-15B from the PGCs may protect essential germline genes from being H3K9 methylated and repressed in those cells. This supports a model in which LIN-15B is the first to bind germline gene promoters and directs methylation of H3K9me2 and binding of the repressive DREAM complex. How the different synMuv B complexes work together to fully repress germline-specific genes in somatic cells is still an open question. The establishment of H3K9me2 may be an initiating step in germline gene repression or may be one part of a series of redundant steps necessary to repress germline genes.

LIN-15B, MET-2 and the DREAM complex work in series to repress germline genes in somatic tissue

To determine if LIN-15B and MET-2 work in series to repress germline genes by H3K9me2, we created *met-2; lin-15B* double mutants and scored them

for HTA. Because additional loss of *met-2* and *lin-15B* did not enhance the HTA phenotype at 24°C, we conclude that MET-2 and LIN-15B work in series within the same pathway to repress germline genes in the soma. We carried out similar experiments with *lin-35;lin-15B, lin-37;lin-15B* and *lin-54;lin-15B* double mutants and also did not observe enhancement of the HTA phenotype. Thus, based on this assay, we genetically determined that LIN-15B and MET-2 work in series with the DREAM complex to repress germline genes in somatic tissues.

Accumulation of multiple regulators to germline gene promoters is crucial for their proper repression. In *C. elegans*, the DREAM complex, LIN-15B, H3K9me2 and HPL-2 all accumulate at germline genes to ensure their repression in somatic tissue (Rechtsteiner et al., 2018). Loss of these proteins cause repercussions for development (Petrella et al., 2011). It is possible that although these factors all co-localize to the same target genes, they may have separate and additive functions at these promoters to achieve repression that was not observed in this assay. It is possible that there are additive effects of subsequent loss of these genes that did not cause enhancement of the HTA phenotype at 24°C. Although some synMuv B mutants due arrest at lower temperatures, 20°C, due to ectopic germline gene expression (*let-418* and *mep-1)*, it is possible that small additive effects in compound mutants would not cause a drastic enough increase in ectopic germline gene expression to cause an enhancement of HTA at lower temperatures. Further studies must be completed in order to the specific roles of each protein and how they work together to achieve proper gene repression. . The establishment of H3K9me2 by LIN-15B

may be one of the steps necessary for proper repression. In order to determine this, further studies to determine how LIN-15B may recruit MET-2 and members of DREAM complex to germline gene promoters will need to be carried out. ChIP-qPCR in DREAM and *lin-15B* mutants backgrounds should be performed to determine if DREAM complex can bind in the absence of *lin-15B* and vice-versa.

synMuv B mutants and chromatin are temperature sensitive

The experiments performed here were all done with a high temperature condition at the end of the temperature range where laboratory experiments are routinely done. This raises the question of whether these temperature stresses reflect levels that these organisms would experience under more natural conditions. Work in the last 10-15 years has greatly expanded our understanding of the ecology of naturally occurring *C. elegans* populations (Schulenburg and Félix, 2017). Unlike what was previously thought, it is now known that the reproductive lifespan of *C. elegans* occurs at the soil surface, often within rotting plant vegetation (Félix and Duveau, 2012; Frézal and Félix, 2015; Kiontke et al., 2011). In our temperature shift experiments, a window of 6-8 hours within embryogenesis at 26°C elicited a severe chromatin delay in developing embryos, even in wild-type. Given the short time period needed, it seems likely, that there are circumstances where *C. elegans* embryos in natural habitats would experience the temperatures tested here. Thus, having mechanisms that regulate chromatin compaction during development at these temperatures is necessary for species survival.

Furthermore, almost all of the phenotypes displayed by synMuv B mutants are temperature sensitive. The multivulval phenotype for which they were named is enhanced at elevated temperatures of 25°C. Ectopic germline gene expression is also enhanced in synMuv B mutants at 26°C compared to 20°C. Finally, the high temperature arrest phenotype causes L1 arrest at 26°C but not 24°C or 20°C. Although temperature underlies many of these phenotypes, before this study, the underlying mechanisms for this temperature sensitive phenotype have remained unclear. *lin-35, lin-15B,* and *met-2* mutants are null alleles that result in no protein at all temperatures and *lin-54* mutants, although not nulls, lose 80% of DREAM complex binding at all temperatures (Petrella et al., 2011; Tabuchi et al., 2011). Here, we show that chromatin compaction is temperature sensitive, even in wild-type backgrounds, and may contribute to this phenotype.

Chromatin has previously been shown to be temperature sensitive. reactive to changes in temperatures. Early studies in *Drosophila* revealed that high temperature causes incomplete heterochromatin formation (Hartmann-Goldstein, 1967). In addition to being temperature sensitive, chromatin is also temperature respondent. Previous studies have reported that plants can change chromatin dynamics to modify gene expression in response to changes in temperature (Zografos and Sung, 2012). This is the first study to investigate the role of temperature stress on chromatin compaction in a developmental context. Here we reveal that chromatin compaction in early development is especially vulnerable to the temperature sensitive nature of chromatin. Chromatin compaction is developmentally delayed when worms experience high

temperatures for small amounts of time. Causing further stress to this system by loss of synMuv B proteins results in more drastic delays in chromatin compaction. Loss of these proteins not only cause changes in chromatin compaction at specific loci that they regulate, but also globally. Thus, small changes in local chromatin domains throughout the genome, plus temperature stress, can indirectly change the chromatin landscape at a global level within the nucleus.

H3K9me2 mediated repression of germline genes is important for organismal survival and disease prevention

Although the DREAM complex, LIN-15B and promoter enriched H3K9me2 are only found to regulate a subset of germline-promoting genes, loss of this repression is detrimental to the organism. Organisms defective in this regulation cannot thrive in when faced with moderate temperature stress. Recent work in *Drosophila* has revealed the importance of H3K9 methylation in repression of a subset of coding genes to maintain proper cell fate. In the *Drosophila* ovary, loss of H3K9me3 leads to up-regulation of testis-specific transcripts and changes the fate of ovarian germ cells, leading to sterility (Smolko *et al.* 2018). As described in *C. elegans,* prior investigations of H3K9 methylation loss in *Drosophila* had focused primarily on up-regulation of repetitive elements (Guo et al., 2015; Rangan et al., 2011; Wang et al., 2011; Zeller et al., 2016). However, it is clear that H3K9me2/3 loss leading to up-regulation of small sets of coding genes in a tissue-specific manner can have profound effects on cell fate and function. As more studies investigate the roles of H3K9me2/3 in repression of coding genes, it

seems likely that new pathways will be uncovered that are necessary to create different patterns of H3K9me2/3 in different tissues for maintenance of proper cell fate.

Ectopic expression of germline genes in somatic tissue leads to a variety of adverse consequences in diverse animal species. These include L1 starvation and reduced apoptosis during development in *C. elegans* synMuv B mutants, tumor formation in *Drosophila l(3)mbt* mutants, and poor outcomes in human tumors that express germline genes (Janic *et al.* 2010; Petrella *et al.* 2011; Whitehurst 2014; Al-Amin *et al.* 2016). Thus, there is a need across species to repress germline gene expression in the soma to facilitate proper development and somatic function. Our data suggest that repression of germline genes during development in somatic tissues through H3K9me2 may be a conserved mechanism. As in *C. elegans* embryonic somatic cells, mammalian ES cells also repress expression of germline genes (Blaschke *et al.* 2013). Mouse ES cells have been shown to lose repression of germline genes when H3K9me2 marking of those genes is compromised by either Vitamin C treatment or knock-down of Max (myc-associate factor X) (Blaschke *et al.* 2013; Maeda *et al.* 2013; Sekinaka *et al.* 2016; Ebata *et al.* 2017). The conservation of H3K9me2 on germline genes and its role in repressing those genes in developing somatic lineages may represent a conserved regulatory role for H3K9me2. Both *C. elegans* and *Drosophila* repress germline genes in the soma through complexes known to interact with chromatin (Janic *et al.* 2010; Petrella *et al.* 2011; Wu *et al.* 2012), it will be interesting to investigate if ectopic expression of germline genes in human

somatic tumors is due to loss of these conserved complexes. Finally, not all germline genes, but only a specific subset, are ectopically expressed in these models. Why only certain germline genes are vulnerable to misexpression, if those genes are the same across species, and which cellular processes are disrupted as a result of germline gene misexpression singularly or as a group, are open questions. Further investigation could have broad implications for understanding conserved basic chromatin mechanisms and therapeutic targets for cancer treatment.

Altogether, in this study, we uncover that synMuv B proteins are needed for chromatin compaction throughout development, especially at high temperature. Loss of chromatin compaction during developmental time periods in which germline genes are globally upregulated during the maternal-to-zygotic switch may underlie the developmental arrest phenotype of synMuv B mutants. It is important to understand how germline genes are repressed in somatic tissue as many somatic cancers that are highly proliferative and metastatic show upregulation of germline genes (Gure et al., 2005; Maine et al., 2016; Xu et al., 2014). Like *C. elegans*, mammals also repress germline gene expression during embryogenesis in somatic cells and recent work has indicated that this repression is dependent on H3K9me2 (Ebata, et. al., 2017; Lian, et. al., 2018). Given that the DREAM complex is completely conserved between worms and mammals (Litovchick, et al., 2007), its role in establishment of developmental repressive chromatin at germline genes may also be conserved.

A model for synMuv B germline gene regulation

We propose a model (Figure 6.1) in which LIN-15B is the first to bind germline gene promoters in somatic tissue through it's putative THAP or AT hook domain. Binding of LiN-15B promoters di-methylation of H3K9 by the methyltransferase MET-2 at these promoters. H3K9me2 and LIN-15B binding promotes and stabilizes binding of the repressive DREAM complex in order to repress germline fates in somatic tissue. All of this occurs prior to the 8E stage in wild-type embryos, preceding the maternal to zygotic switch. As zygotic gene expression is globally upregulated, promoter localization of LIN-15B, DREAM and H3K9me2 ensures germline gene repression in somatic tissues.

We predict that LIN-15B binds to germline gene promoters first to establish a repressive chromatin environment at these loci. Loss of *lin-15B* causes loss of H3K9me2 at synMuv B regulated germline gene promoters

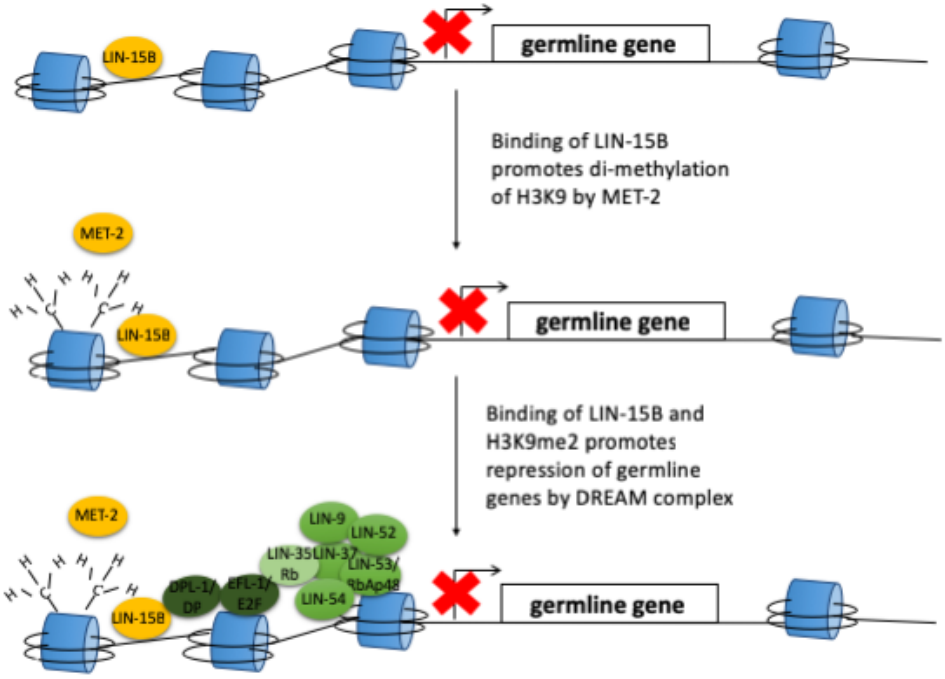

Figure 6.1 A Model for synMuv B germline gene repression. LIN-15B binds germline gene promoters in soma through its putative DNA binding domain and promotes H3K9me2 by MET-2. This stabilizes biding of the repressive DREAM complex in order to repress germline gene expression in somatic tissue.

(Figure 6.2). Loss of LIN-15B and H3K9me2 at these promoters likely destabilizes binding of the repressive DREAM complex (Figure 6.2). This results in a loss of a repressive environment at these loci and causes small amounts of ectopic expression of germline genes in somatic tissue at 20°C (Figure 6.2). We discovered that chromatin compaction is temperature sensitive, and exposure to 26°C causes loss of chromatin compaction even in wild type. Loss of the repressive environment established by LIN-15B, MET-2, and DREAM complex, in addition to loss of chromatin compaction at 26°C, results in increased ectopic expression of germline genes in somatic tissues (Figure 6.2). Loss of the repressive chromatin environment in *lin-15B, met-2,* or DREAM complex mutants has detrimental impacts to development. Loss of these factors causes prolonged open chromatin into developmental time periods in which global upregulation of zygotic gene expression occurs. Without LIN-15B, MET-2, or the DREAM complex, the tissue-specific mechanism for germline gene repression is not established and these loci are available to be bound and ectopically expressed, especially at high temperature (Figure 6.2). Further studies will need to be preformed in order to determine if LIN-15B recruits or promotes H3K9me2 and DREAM complex binding at germline gene promoters, Future studies of synMuv B regulation will provide evidence of how organisms establish and maintain chromatin structure and gene expression states, especially during times of stress, to ensure vitality.

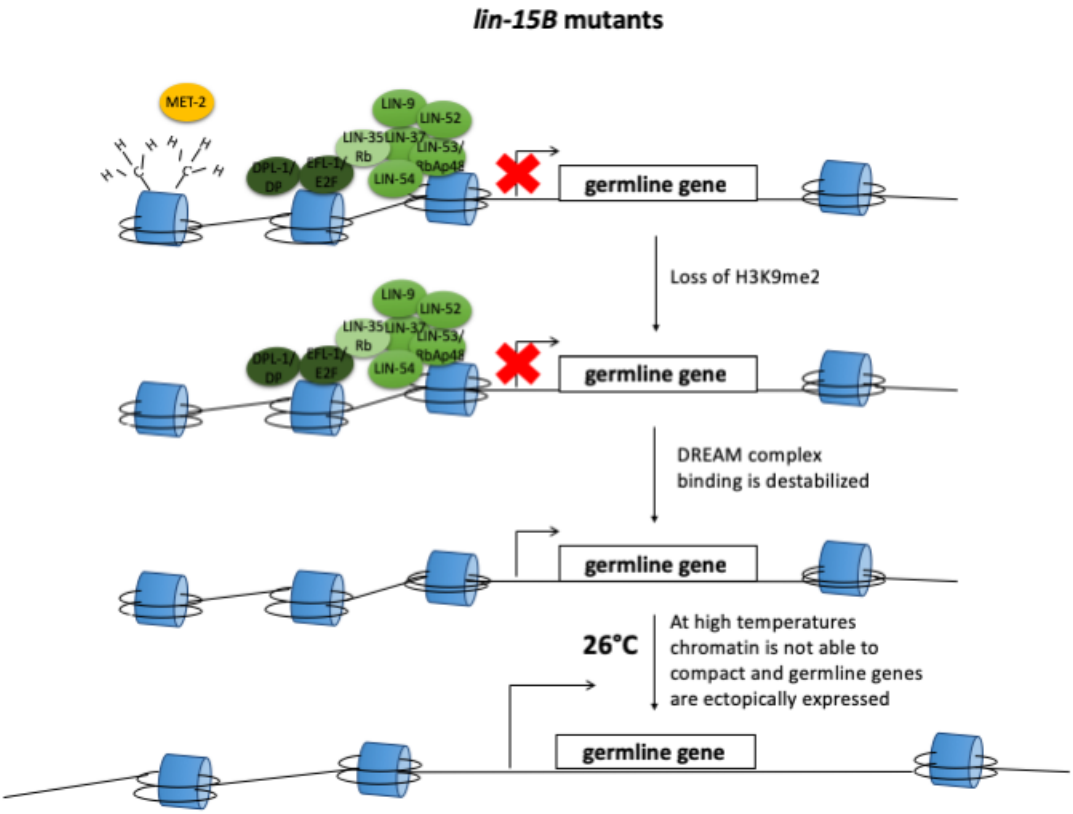

Figure 6.2 A model for loss of LIN-15B at germline gene promoters. *lin-15B* mutants lose H3K9me2 enrichment at germline gene promoters in somatic tissue.Loss of LIN-15B and H3K9me2 destabilizes DREAM complex binding at germline gene promoters. Loss of the repressive chromatin environment at these promoters in addition to loss of chromatin compaction at hight temperature leads to increased ectopic germline gene expression at high temperature.

BIBLIOGRAPHY

Ahringer, J., and Gasser, S.M. (2018). Repressive Chromatin in Caenorhabditis elegans: Establishment, Composition, and Function. Genetics *208*, 491–511.

Al-Amin, M., Min, H., Shim, Y.-H., and Kawasaki, I. (2016). Somatically expressed germ-granule components, PGL-1 and PGL-3, repress programmed cell death in C. elegans. Sci. Rep. *6*, 33884.

Albertson, D.G., and Thomson, J.N. (1982). The kinetochores of Caenorhabditis elegans. Chromosoma *86*, 409–428.

Andersen, E.C., and Horvitz, H.R. (2007). Two C. elegans histone methyltransferases repress lin-3 EGF transcription to inhibit vulval development. Dev. Camb. Engl. *134*, 2991–2999.

Andralojc, K.M., Campbell, A.C., Kelly, A.L., Terrey, M., Tanner, P.C., Gans, I.M., Senter-Zapata, M.J., Khokhar, E.S., and Updike, D.L. (2017). ELLI-1, a novel germline protein, modulates RNAi activity and P-granule accumulation in Caenorhabditis elegans. PLoS Genet. *13*, e1006611.

Ardizzi, J.P., and Epstein, H.F. (1987). Immunochemical localization of myosin heavy chain isoforms and paramyosin in developmentally and structurally diverse muscle cell types of the nematode Caenorhabditis elegans. J. Cell Biol. *105*, 2763–2770.

Bannister, A.J., and Kouzarides, T. (2011). Regulation of chromatin by histone modifications. Cell Res. *21*, 381–395.

Baugh, L.R., Hill, A.A., Claggett, J.M., Hill-Harfe, K., Wen, J.C., Slonim, D.K., Brown, E.L., and Hunter, C.P. (2005). The homeodomain protein PAL-1 specifies a lineage-specific regulatory network in the C. elegans embryo. Dev. Camb. Engl. *132*, 1843–1854.

Begasse, M.L., Leaver, M., Vazquez, F., Grill, S.W., and Hyman, A.A. (2015). Temperature Dependence of Cell Division Timing Accounts for a Shift in the Thermal Limits of C. elegans and C. briggsae. Cell Rep. *10*, 647–653.

Brasher, S.V., Smith, B.O., Fogh, R.H., Nietlispach, D., Thiru, A., Nielsen, P.R., Broadhurst, R.W., Ball, L.J., Murzina, N.V., and Laue, E.D. (2000). The structure of mouse HP1 suggests a unique mode of single peptide recognition by the shadow chromo domain dimer. EMBO J. *19*, 1587–1597.

Carrozza, M.J., Li, B., Florens, L., Suganuma, T., Swanson, S.K., Lee, K.K., Shia, W.-J., Anderson, S., Yates, J., Washburn, M.P., et al. (2005). Histone H3 methylation by Set2

directs deacetylation of coding regions by Rpd3S to suppress spurious intragenic transcription. Cell *123*, 581–592.

Clark, R.F., and Elgin, S.C. (1992). Heterochromatin protein 1, a known suppressor of position-effect variegation, is highly conserved in Drosophila. Nucleic Acids Res. *20*, 6067–6074.

Clouaire, T., Roussigne, M., Ecochard, V., Mathe, C., Amalric, F., and Girard, J.-P. (2005). The THAP domain of THAP1 is a large C2CH module with zinc-dependent sequence-specific DNA-binding activity. Proc. Natl. Acad. Sci. U. S. A. *102*, 6907–6912.

Corona, D.F.V., Clapier, C.R., Becker, P.B., and Tamkun, J.W. (2002). Modulation of ISWI function by site-specific histone acetylation. EMBO Rep. *3*, 242–247.

Couteau, F., Guerry, F., Muller, F., and Palladino, F. (2002). A heterochromatin protein 1 homologue in Caenorhabditis elegans acts in germline and vulval development. EMBO Rep. *3*, 235–241.

Dal Santo, P., Logan, M.A., Chisholm, A.D., and Jorgensen, E.M. (1999). The inositol trisphosphate receptor regulates a 50-second behavioral rhythm in C. elegans. Cell *98*, 757–767.

Deuring, R., Fanti, L., Armstrong, J.A., Sarte, M., Papoulas, O., Prestel, M., Daubresse, G., Verardo, M., Moseley, S.L., Berloco, M., et al. (2000). The ISWI chromatin-remodeling protein is required for gene expression and the maintenance of higher order chromatin structure in vivo. Mol. Cell *5*, 355–365.

Dixon, J.R., Selvaraj, S., Yue, F., Kim, A., Li, Y., Shen, Y., Hu, M., Liu, J.S., and Ren, B. (2012). Topological domains in mammalian genomes identified by analysis of chromatin interactions. Nature *485*, 376–380.

Ebata, K.T., Mesh, K., Liu, S., Bilenky, M., Fekete, A., Acker, M.G., Hirst, M., Garcia, B.A., and Ramalho-Santos, M. (2017). Vitamin C induces specific demethylation of H3K9me2 in mouse embryonic stem cells via Kdm3a/b. Epigenetics Chromatin *10*, 36.

Elgin, S.C.R., and Reuter, G. (2013). Position-effect variegation, heterochromatin formation, and gene silencing in Drosophila. Cold Spring Harb. Perspect. Biol. *5*, a017780.

Fay, D.S., and Yochem, J. (2007). The SynMuv genes of Caenorhabditis elegans in vulval development and beyond. Dev. Biol. *306*, 1–9.

Félix, M.-A., and Duveau, F. (2012). Population dynamics and habitat sharing of natural populations of Caenorhabditis elegans and C. briggsae. BMC Biol. *10*, 59.

Frézal, L., and Félix, M.-A. (2015). C. elegans outside the Petri dish. ELife *4*.

Fukushige, T., and Krause, M. (2005). The myogenic potency of HLH-1 reveals wide-spread developmental plasticity in early C. elegans embryos. Dev. Camb. Engl. *132*, 1795–1805.

Fukushige, T., Schroeder, D.F., Allen, F.L., Goszczynski, B., and McGhee, J.D. (1996). Modulation of gene expression in the embryonic digestive tract of C. elegans. Dev. Biol. *178*, 276–288.

Fukushige, T., Hawkins, M.G., and McGhee, J.D. (1998). The GATA-factor elt-2 is essential for formation of the Caenorhabditis elegans intestine. Dev. Biol. *198*, 286–302.

Furuhashi, H., Takasaki, T., Rechtsteiner, A., Li, T., Kimura, H., Checchi, P.M., Strome, S., and Kelly, W.G. (2010). Trans-generational epigenetic regulation of C. elegans primordial germ cells. Epigenetics Chromatin *3*, 15.

Gaertner, B., Johnston, J., Chen, K., Wallaschek, N., Paulson, A., Garruss, A.S., Gaudenz, K., De Kumar, B., Krumlauf, R., and Zeitlinger, J. (2012). Poised RNA polymerase II changes over developmental time and prepares genes for future expression. Cell Rep. *2*, 1670–1683.

Garrigues, J.M., Sidoli, S., Garcia, B.A., and Strome, S. (2015). Defining heterochromatin in C. elegans through genome-wide analysis of the heterochromatin protein 1 homolog HPL-2. Genome Res. *25*, 76–88.

Gilleard, J.S., and McGhee, J.D. (2001). Activation of hypodermal differentiation in the Caenorhabditis elegans embryo by GATA transcription factors ELT-1 and ELT-3. Mol. Cell. Biol. *21*, 2533–2544.

Goetsch, P.D., Garrigues, J.M., and Strome, S. (2017). Loss of the Caenorhabditis elegans pocket protein LIN-35 reveals MuvB's innate function as the repressor of DREAM target genes. PLoS Genet. *13*, e1007088.

Gonzalez-Sandoval, A., Towbin, B.D., Kalck, V., Cabianca, D.S., Gaidatzis, D., Hauer, M.H., Geng, L., Wang, L., Yang, T., Wang, X., et al. (2015). Perinuclear Anchoring of H3K9-Methylated Chromatin Stabilizes Induced Cell Fate in C. elegans Embryos. Cell *163*, 1333–1347.

Greer, E.L., Beese-Sims, S.E., Brookes, E., Spadafora, R., Zhu, Y., Rothbart, S.B., Aristizábal-Corrales, D., Chen, S., Badeaux, A.I., Jin, Q., et al. (2014). A histone methylation network regulates transgenerational epigenetic memory in C. elegans. Cell Rep. *7*, 113–126.

Guiley, K.Z., Liban, T.J., Felthousen, J.G., Ramanan, P., Litovchick, L., and Rubin, S.M. (2015). Structural mechanisms of DREAM complex assembly and regulation. Genes Dev. *29*, 961–974.

Guo, Y., Yang, B., Li, Y., Xu, X., and Maine, E.M. (2015). Enrichment of H3K9me2 on Unsynapsed Chromatin in Caenorhabditis elegans Does Not Target de Novo Sites. G3 Bethesda Md *5*, 1865–1878.

Gure, A.O., Chua, R., Williamson, B., Gonen, M., Ferrera, C.A., Gnjatic, S., Ritter, G., Simpson, A.J.G., Chen, Y.-T., Old, L.J., et al. (2005). Cancer-testis genes are coordinately expressed and are markers of poor outcome in non-small cell lung cancer. Clin. Cancer Res. Off. J. Am. Assoc. Cancer Res. *11*, 8055–8062.

Harrison, M.M., Ceol, C.J., Lu, X., and Horvitz, H.R. (2006). Some C. elegans class B synthetic multivulva proteins encode a conserved LIN-35 Rb-containing complex distinct from a NuRD-like complex. Proc. Natl. Acad. Sci. U. S. A. *103*, 16782–16787.

Hartmann-Goldstein, I.J. (1967). On the relationship between heterochromatization and variegation in Drosophila, with special reference to temperature-sensitive periods. Genet. Res. *10*, 143–159.

Hillier, L.W., Reinke, V., Green, P., Hirst, M., Marra, M.A., and Waterston, R.H. (2009). Massively parallel sequencing of the polyadenylated transcriptome of C. elegans. Genome Res. *19*, 657–666.

Horner, M.A., Quintin, S., Domeier, M.E., Kimble, J., Labouesse, M., and Mango, S.E. (1998). pha-4, an HNF-3 homolog, specifies pharyngeal organ identity in Caenorhabditis elegans. Genes Dev. *12*, 1947–1952.

Hubley, R., Finn, R.D., Clements, J., Eddy, S.R., Jones, T.A., Bao, W., Smit, A.F.A., and Wheeler, T.J. (2016). The Dfam database of repetitive DNA families. Nucleic Acids Res. *44*, D81–D89.

Ikegami, K., Egelhofer, T.A., Strome, S., and Lieb, J.D. (2010). Caenorhabditis elegans chromosome arms are anchored to the nuclear membrane via discontinuous association with LEM-2. Genome Biol. *11*, R120.

Janic, A., Mendizabal, L., Llamazares, S., Rossell, D., and Gonzalez, C. (2010). Ectopic expression of germline genes drives malignant brain tumor growth in Drosophila. Science *330*, 1824–1827.

Jenuwein, T., and Allis, C.D. (2001). Translating the histone code. Science *293*, 1074–1080.

Ji, N., and van Oudenaarden, A. (2012). Single molecule fluorescent in situ hybridization (smFISH) of C. elegans worms and embryos. WormBook Online Rev. C Elegans Biol. 1–16.

Kiontke, K.C., Félix, M.-A., Ailion, M., Rockman, M.V., Braendle, C., Pénigault, J.-B., and Fitch, D.H.A. (2011). A phylogeny and molecular barcodes for Caenorhabditis, with numerous new species from rotting fruits. BMC Evol. Biol. *11*, 339.

Koester-Eiserfunke, N., and Fischle, W. (2011). H3K9me2/3 binding of the MBT domain protein LIN-61 is essential for Caenorhabditis elegans vulva development. PLoS Genet. *7*, e1002017.

Kornberg, R.D. (1974). Chromatin structure: a repeating unit of histones and DNA. Science *184*, 868–871.

Kreher, J., Takasaki, T., Cockrum, C., Sidoli, S., Garcia, B.A., Jensen, O.N., and Strome, S. (2018). Distinct Roles of Two Histone Methyltransferases in Transmitting H3K36me3-Based Epigenetic Memory Across Generations in Caenorhabditis elegans. Genetics *210*, 969–982.

Lachner, M., O'Carroll, D., Rea, S., Mechtler, K., and Jenuwein, T. (2001). Methylation of histone H3 lysine 9 creates a binding site for HP1 proteins. Nature *410*, 116–120.

Lee, C.-Y.S., Lu, T., and Seydoux, G. (2017). Nanos promotes epigenetic reprograming of the germline by down-regulation of the THAP transcription factor LIN-15B. ELife *6*.

Lee, C.-Y.S., Lu, T., and Seydoux, G. Nanos promotes epigenetic reprograming of the germline by down-regulation of the THAP transcription factor LIN-15B. ELife *6*.

Leung, B., Hermann, G.J., and Priess, J.R. (1999). Organogenesis of the Caenorhabditis elegans intestine. Dev. Biol. *216*, 114–134.

Levin, M., Hashimshony, T., Wagner, F., and Yanai, I. (2012). Developmental milestones punctuate gene expression in the Caenorhabditis embryo. Dev. Cell *22*, 1101–1108.

Lin, R., Hill, R.J., and Priess, J.R. (1998). POP-1 and anterior-posterior fate decisions in C. elegans embryos. Cell *92*, 229–239.

Litovchick, L., Sadasivam, S., Florens, L., Zhu, X., Swanson, S.K., Velmurugan, S., Chen, R., Washburn, M.P., Liu, X.S., and DeCaprio, J.A. (2007). Evolutionarily conserved multisubunit RBL2/p130 and E2F4 protein complex represses human cell cycle-dependent genes in quiescence. Mol. Cell *26*, 539–551.

Liu, T., Rechtsteiner, A., Egelhofer, T.A., Vielle, A., Latorre, I., Cheung, M.-S., Ercan, S., Ikegami, K., Jensen, M., Kolasinska-Zwierz, P., et al. (2011). Broad chromosomal domains of histone modification patterns in C. elegans. Genome Res. *21*, 227–236.

Maddox, P.S., Oegema, K., Desai, A., and Cheeseman, I.M. (2004). "Holo"er than thou: chromosome segregation and kinetochore function in C. elegans. Chromosome Res. Int. J. Mol. Supramol. Evol. Asp. Chromosome Biol. *12*, 641–653.

Maine, E.A., Westcott, J.M., Prechtl, A.M., Dang, T.T., Whitehurst, A.W., and Pearson, G.W. (2016). The cancer-testis antigens SPANX-A/C/D and CTAG2 promote breast cancer invasion. Oncotarget *7*, 14708–14726.

McGhee, J.D. (2007). The C. elegans intestine. WormBook Online Rev. C Elegans Biol. 1–36.

McGhee, J.D., Sleumer, M.C., Bilenky, M., Wong, K., McKay, S.J., Goszczynski, B., Tian, H., Krich, N.D., Khattra, J., Holt, R.A., et al. (2007). The ELT-2 GATA-factor and the global regulation of transcription in the C. elegans intestine. Dev. Biol. *302*, 627–645.

McMurchy, A.N., Stempor, P., Gaarenstroom, T., Wysolmerski, B., Dong, Y., Aussianikava, D., Appert, A., Huang, N., Kolasinska-Zwierz, P., Sapetschnig, A., et al. (2017). Correction: A team of heterochromatin factors collaborates with small RNA pathways to combat repetitive elements and germline stress. ELife *6*.

Mutlu, B., Chen, H.-M., Moresco, J.J., Orelo, B.D., Yang, B., Gaspar, J.M., Keppler-Ross, S., Yates, J.R., Hall, D.H., Maine, E.M., et al. (2018). Regulated nuclear accumulation of a histone methyltransferase times the onset of heterochromatin formation in C. elegans embryos. Sci. Adv. *4*, eaat6224.

Nakayama, J., Rice, J.C., Strahl, B.D., Allis, C.D., and Grewal, S.I. (2001). Role of histone H3 lysine 9 methylation in epigenetic control of heterochromatin assembly. Science *292*, 110–113.

Nielsen, P.R., Nietlispach, D., Mott, H.R., Callaghan, J., Bannister, A., Kouzarides, T., Murzin, A.G., Murzina, N.V., and Laue, E.D. (2002). Structure of the HP1 chromodomain bound to histone H3 methylated at lysine 9. Nature *416*, 103–107.

Nora, E.P., Lajoie, B.R., Schulz, E.G., Giorgetti, L., Okamoto, I., Servant, N., Piolot, T., van Berkum, N.L., Meisig, J., Sedat, J., et al. (2012). Spatial partitioning of the regulatory landscape of the X-inactivation centre. Nature *485*, 381–385.

Olins, A.L., and Olins, D.E. (1974). Spheroid chromatin units (v bodies). Science *183*, 330–332.

Perino, M., and Veenstra, G.J.C. (2016). Chromatin Control of Developmental Dynamics and Plasticity. Dev. Cell *38*, 610–620.

Petrella, L.N., Wang, W., Spike, C.A., Rechtsteiner, A., Reinke, V., and Strome, S. (2011). synMuv B proteins antagonize germline fate in the intestine and ensure C. elegans survival. Dev. Camb. Engl. *138*, 1069–1079.

Politz, J.C.R., Scalzo, D., and Groudine, M. (2013). Something silent this way forms: the functional organization of the repressive nuclear compartment. Annu. Rev. Cell Dev. Biol. *29*, 241–270.

Priess, J.R. (2005). Notch signaling in the C. elegans embryo. WormBook Online Rev. C Elegans Biol. 1–16.

Priess, J.R., and Thomson, J.N. (1987). Cellular interactions in early C. elegans embryos. Cell *48*, 241–250.

Rangan, P., Malone, C.D., Navarro, C., Newbold, S.P., Hayes, P.S., Sachidanandam, R., Hannon, G.J., and Lehmann, R. (2011). piRNA production requires heterochromatin formation in Drosophila. Curr. Biol. CB *21*, 1373–1379.

Rechtsteiner, A., Costello, M.E., Egelhofer, T.A., Garrigues, J.M., Strome, S., and Petrella, L. (2018). LIN-15B promotes enrichment of H3K9me2 on the promoters of a subset of germline genes that are repressed in somatic cells in C. elegans. BioRxiv 497438.

Rechtsteiner, A., Costello, M.E., Egelhofer, T.A., Garrigues, J.M., Strome, S., and Petrella, L.N. (2019). Repression of Germline Genes in *Caenorhabditis elegans* Somatic Tissues by H3K9 Dimethylation of Their Promoters. Genetics genetics.301878.2018.

Robertson, S., and Lin, R. (2015). The Maternal-to-Zygotic Transition in C. elegans. Curr. Top. Dev. Biol. *113*, 1–42.

Schroeder, D.F., and McGhee, J.D. (1998). Anterior-posterior patterning within the Caenorhabditis elegans endoderm. Dev. Camb. Engl. *125*, 4877–4887.

Schulenburg, H., and Félix, M.-A. (2017). The Natural Biotic Environment of Caenorhabditis elegans. Genetics *206*, 55–86.

Simon, J.A., and Kingston, R.E. (2013). Occupying chromatin: Polycomb mechanisms for getting to genomic targets, stopping transcriptional traffic, and staying put. Mol. Cell *49*, 808–824.

Singh, M., D'Silva, L., and Holak, T.A. (2006). DNA-binding properties of the recombinant high-mobility-group-like AT-hook-containing region from human BRG1 protein. Biol. Chem. *387*, 1469–1478.

Smolko, A.E., Shapiro-Kulnane, L., and Salz, H.K. (2018). The H3K9 methyltransferase SETDB1 maintains female identity in Drosophila germ cells. Nat. Commun. *9*, 4155.

Spencer, W.C., Zeller, G., Watson, J.D., Henz, S.R., Watkins, K.L., McWhirter, R.D., Petersen, S., Sreedharan, V.T., Widmer, C., Jo, J., et al. (2011). A spatial and temporal map of C. elegans gene expression. Genome Res. *21*, 325–341.

Sulston, J.E., Schierenberg, E., White, J.G., and Thomson, J.N. (1983). The embryonic cell lineage of the nematode Caenorhabditis elegans. Dev. Biol. *100*, 64–119.

Tabuchi, T.M., Deplancke, B., Osato, N., Zhu, L.J., Barrasa, M.I., Harrison, M.M., Horvitz, H.R., Walhout, A.J.M., and Hagstrom, K.A. (2011). Chromosome-biased binding and gene regulation by the Caenorhabditis elegans DRM complex. PLoS Genet. *7*, e1002074.

Tabuchi, T.M., Rechtsteiner, A., Jeffers, T.E., Egelhofer, T.A., Murphy, C.T., and Strome, S. (2018). Caenorhabditis elegans sperm carry a histone-based epigenetic memory of both spermatogenesis and oogenesis. Nat. Commun. *9*, 4310.

Takahashi, Y., Rayman, J.B., and Dynlacht, B.D. (2000). Analysis of promoter binding by the E2F and pRB families in vivo: distinct E2F proteins mediate activation and repression. Genes Dev. *14*, 804–816.

Towbin, B.D., González-Aguilera, C., Sack, R., Gaidatzis, D., Kalck, V., Meister, P., Askjaer, P., and Gasser, S.M. (2012). Step-wise methylation of histone H3K9 positions heterochromatin at the nuclear periphery. Cell *150*, 934–947.

Wang, D., Kennedy, S., Conte, D., Kim, J.K., Gabel, H.W., Kamath, R.S., Mello, C.C., and Ruvkun, G. (2005). Somatic misexpression of germline P granules and enhanced RNA interference in retinoblastoma pathway mutants. Nature *436*, 593–597.

Wang, J., Jia, S.T., and Jia, S. (2016). New Insights into the Regulation of Heterochromatin. Trends Genet. TIG *32*, 284–294.

Wang, X., Pan, L., Wang, S., Zhou, J., McDowell, W., Park, J., Haug, J., Staehling, K., Tang, H., and Xie, T. (2011). Histone H3K9 trimethylase Eggless controls germline stem cell maintenance and differentiation. PLoS Genet. *7*, e1002426.

Whitehurst, A.W. (2014). Cause and consequence of cancer/testis antigen activation in cancer. Annu. Rev. Pharmacol. Toxicol. *54*, 251–272.

Wood, W.B. (1991). Evidence from reversal of handedness in C. elegans embryos for early cell interactions determining cell fates. Nature *349*, 536–538.

Wood, W.B., Hecht, R., Carr, S., Vanderslice, R., Wolf, N., and Hirsh, D. (1980). Parental effects and phenotypic characterization of mutations that affect early development in Caenorhabditis elegans. Dev. Biol. *74*, 446–469.

Wu, X., Shi, Z., Cui, M., Han, M., and Ruvkun, G. (2012). Repression of germline RNAi pathways in somatic cells by retinoblastoma pathway chromatin complexes. PLoS Genet. *8*, e1002542.

Xu, X., Tang, X., Lu, M., Tang, Q., Zhang, H., Zhu, H., Xu, N., Zhang, D., Xiong, L., Mao, Y., et al. (2014). Overexpression of MAGE-A9 predicts unfavorable outcome in breast cancer. Exp. Mol. Pathol. *97*, 579–584.

Yeates, T.O. (2002). Structures of SET domain proteins: protein lysine methyltransferases make their mark. Cell *111*, 5–7.

Yuzyuk, T., Fakhouri, T.H.I., Kiefer, J., and Mango, S.E. (2009). The Polycomb Complex Protein mes-2/E(z) Promotes the Transition from Developmental Plasticity to Differentiation in C. elegans Embryos. Dev. Cell *16*, 699–710.

Zeller, P., Padeken, J., van Schendel, R., Kalck, V., Tijsterman, M., and Gasser, S.M. (2016). Histone H3K9 methylation is dispensable for Caenorhabditis elegans development but suppresses RNA:DNA hybrid-associated repeat instability. Nat. Genet. *48*, 1385–1395.

Zhu, J., Hill, R.J., Heid, P.J., Fukuyama, M., Sugimoto, A., Priess, J.R., and Rothman, J.H. (1997). end-1 encodes an apparent GATA factor that specifies the endoderm precursor in Caenorhabditis elegans embryos. Genes Dev. *11*, 2883–2896.

Zografos, B.R., and Sung, S. (2012). Vernalization-mediated chromatin changes. J. Exp. Bot. *63*, 4343–4348.